Universitatea *Transilvania* din Braşov

HABILITATION THESIS

Title: Obtaining, characterisation and applications of polymeric materials based on secondary raw materials

Domain: Materials Engineering

Author: Assoc. Prof. Dr. Liana Sanda Balteș

Transilvania University of Brașov, Romania

BRAŞOV, 2017

CONTENT

ACKNOWLEDGEMENT

The research was funded by FP7 Grant 212782, „Magnetic Sorting and Ultrasound Sensor Technologies for Production of High Purity Secondary Polyolefins from Waste", acronym W2Plastics/2009. Period 2008-2013.

The research was also co-financing by the National Research Program for the project „Magnetic Sorting and Ultrasound Sensor Technologies for Production of High Purity Secondary Polyolefins from Waste", 152 EU, Capacități Program, Modul III, 2 PC7, Euratom 011, ANCS. Period 2011-2012.

The research was support by the strategic grant POSDRU/159/1.5/S/137070 (2014) of the Ministry of National Education, Romania, co-financed by the European Social Fund–Investing in People, within the Sectoral Operational Program Human Resources Development 2007–2013.

The research was funded by the Sectorial Operational Programme Human Resources Development (SOP HRD), financed from the European Social Fund and by the Romanian Government under the project number POSDRU/159/1.5/S/134378.

The research work was supported by the Romanian National Authority for Scientific Research and Innovation, CNCS-UEFISCDI, project number PN-II-RU-TE-2014-4-0173.

Also many thanks to OLYMPUS and NAMICON Romania for the professional support and help to develop the applications for the research work.

Kind thanks to the colleagues involved in the W2Plastics consortium, especially to Prof.dr. Peter Rem from Delft University of Technology.

Many thanks to my colleagues, together with whom I obtained and realized the results to be presented.

ABSTRACT

The present habitation thesis represents a synthesis of scientific and academic activity in the field of materials science and engineering for the period between 1998 and 2017, after the public defense in December 4, 1998 of the Ph.D. thesis with title "*Contributions on thermomagnetic heat treatments of tool steels*". The goal of this habilitation thesis is to obtain, characterise and propose new applications of polymeric materials based on secondary raw materials. Research is focused on polyolefins, as they are the highly-used polymers.

In this respect, chapter 1 ***Obtaining of the secondary polymers*** presents the overall framework of the FP7 project *Magnetic Sorting and Ultrasound Sensor Technologies for Production of High Purity Secondary Polyolefins from Waste,* which was the basis for funding an important part of my research activity. It also shows the trends in the field of polymeric waste management in the Brasov area.

Chapter 2 ***Characterization of the polyolefins as secondary raw materials*** presents different methods for polyolefins´ characterisation such as: gravimetric analysis, image analysis, infrared analysis, mechanical analysis, determination of material crystallinity, determination of contact angle, determination of roughness by atomic force microscopy, qualitative determination of water vapours adsorption from the atmosphere, determination of adsorption of water, microbiological tests, measuring of the heat of combustion (calorific value).

Chapter 3 ***Improving the quality of the secondary polyolefins using magnetic density separation*** presents a new equipment and the related technology to separate the polyolefins using a magnetic fluid, because both PP and PE float in water and it is difficult to separate one from the other. This emerging technology is called Magnetic Density Separation (MDS). For industrial implementation, is required a feasibility study, to allow the owners to decide the opportunity of this equipment with increased capacity. The feasibility study provides all data necessary for the investment decision. Separation of plastics waste using MDS technology with magnetic fluid allows different immersion depth for different type of polymers; it is of great importance the determination of the acoustical properties of polymeric materials (longitudinal ultrasounds velocity). The results can also be found.

Chapter 4 ***Application of the secondary polyolefins in composites materials*** presents the possibilities to improve the polyolefin waste using it in composites materials with different types of composition. Polyolefins composite materials domain is very large due to the multiple combination possibilities that have developed over the years. The possibility of replacing in specific applications the virgin polyolefins from composites materials by second raw materials coming from polymeric wastes is of real interest. Glass fibre reinforced polyester composites (GFPCs) are currently used in a plethora of applications such as construction structures, automotive covers, boat hulls, blades for wind turbines and so forth. Thus, studies regarding the influence of UV radiation on the GFPCs structure and properties under prolonged exposure are of outmost importance. Results are available in the chapter. Because the composite materials can be used in applications requiring mechanical friction, this chapter presents determination of static coefficient of friction on flat surfaces. The selection of polymeric composites from waste as materials for sliding components of machines and devices is a very important aim for tribologists as well as tribological behaviour of non-polymer-on-polymer tribosystems. The best tribological combination practically confirmed is steel on polymer; therefore the tests were done with this system.

Chapter 5 ***Polymers moulding*** presents two applications of polymer flow inside mould in order to study the influence of shape on the technological and stress results. Results concerning the study of the influence of shape on the material consumption, part deformation and injection time are presented.

Proposals for further research are based on the two subjects related to materials engineering, especially materials for environmental protection, introduced in the first five chapters: new materials for environmental protection with photocatalytic properties and composite materials from secondary raw materials.

REZUMAT

Prezenta teză de abilitare constituie o sinteză a activității didactice și de cercetare în domeniul Științei și Ingineriei Materialelor din perioada 1998 și până în prezent. Sunt evidențiate cele mai semnificative rezultate obținute după susținerea tezei de doctorat, din 4 decembrie 1998, cu titlul ″Contribuții la tratamentul termomagnetic al oțelurilor pentru scule″. Subiectul prezentei teze de abilitare este de a obține, caracteriza și propune noi aplicații ale materialelor polimerice bazate pe materii prime secundare. Cercetarea este orientată pe poliolefine având în vedere că acestea sunt cele mai des utilizate materialele plastice.

Capitolul 1 denumit ***Obținerea polimerilor secundari***, prezintă desfășurarea generală a proiectului cadru 7 *"Tehnologii de sortare magnetică și senzori cu ultrasunete pentru obținerea de poliolefine secundare de înaltă puritate din deșeuri"* care a stat la baza finanțării unei părți importante din activitatea mea de cercetare. De asemenea sunt prezentate direcțiile în domeniul managementului deșeurilor polimerice din zona Brașov, ca sursă de materii prime secundare.

Capitolul 2 intitulat ***Caracterizarea poliolefinelor ca materii prime secundare***, prezintă diferite metode de caracterizare ca: analiza gravimetrică, analiza de imagine, analiza în infraroșu, teste mecanice, determinarea cristalinității materialelor, determinarea unghiului de contact, determinarea rugozității cu ajutorul microscopiei de forță atomică, determinarea adsorbției de vapori din atmosferă, determinarea adsorbției de apă, teste microbiologice, măsurarea căldurii rezultate în urma arderii.

Capitolul 3 se referă la ***Îmbunătățirea calității poliolefinelor secundare folosind separarea magnetică pe baza densității*** și prezintă un echipament nou și tehnologia aferentă, ca produse ale proiectului FP7 mai sus menționat, care sunt folosite la separarea poliolefinelor utilizând un fluid magnetic, deoarece atât polipropilena cât și polietilena plutesc în apă, ambele având densitatea mai mică de 1 și fiind greu de separat. Această tehnologie este denumită MDS (separarea pe baza densității în câmp magnetic). Pentru implementarea industrială a echipamentului a fost prevăzut un studiu de fezabilitate, care să ofere toate datele necesare pentru luarea deciziei privind investiția viitoare. Separarea plasticelor prin această tehnologie presupune diferite adâncimi de imersie, în funcție de tipul polimerului, fiind de o deosebită importanță determinarea proprietăților acustice ale materialelor analizate (viteza undelor longitudinale). De asemenea, sunt prezentate rezultatele studiului.

Capitolul 4 denumit ***Aplicații ale poliolefinelor secundare în materiale compozite***, prezintă posibilități de îmbunătățire ale deșeurilor poliolefinice prin utilizarea lor în materialele compozite, în diferite combinații. Domeniul materialelor compozite pe bază de poliolefine este foarte vast datorită numeroaselor combinații posibile dezvoltate de-a lungul timpului. Posibilitatea de a înlocui în anumite aplicații fibrele virgine cu poliolefine provenite din deșeuri, este de un real interes. Fibrele de sticlă folosite ca materiale de adaos în componența compozitelor sunt utilizate într-o mulțime de aplicații ca structuri în domeniul construcțiilor, carcase de mașini, carcase de bărci, pale pentru turbinele eoliene, etc. Studiile privind influența razelor UV asupra structurii compozitului cu fibră de sticlă la expunere prelungită sunt de cea mai mare importanță. Acest capitol prezintă determinarea coeficientului static de frecare pe suprafețe plane pentru diferite compoziții de materiale compozite pe bază de polimeri secundari. Având in vedere intensa lor utilizare, testele au fost făcute pentru cuple polimer-metal.

Capitolul 5 ***Injectarea polimerilor*** prezintă două aplicații ale curgerii polimerilor în interiorul matrițelor pentru a studia influența formei piesei asupra tehnologiei și a tensiunilor. Se prezintă rezultatele studiului influenței formei asupra consumului de material, deformării și timpului de injecție.

Planurile de viitor pentru cercetare se bazează pe cele două subiecte legate de ingineria materialelor, în special materialele pentru protecția mediului, prezentate în primele cinci capitole: noi materiale cu proprietăți fotocatalitice pentru protecția mediului și materiale compozite din materii prime secundare.

A. PROFESSIONAL AND SCIENTIFIC ACHIEVEMENTS

Context and motivation

Composite materials based on polymeric materials as secondary raw materials were one of my research main objectives. In the last 27 years my teaching and research activities have been in the field of Materials Engineering.

The teaching subjects of my courses and the practical laboratories and projects that were conducted during this period were focused almost exclusively on disciplines dealing with Materials Science and Engineering, Modern Control Methods, Technologies and Equipment for Waste Recycling, Composites and amorphous materials, Materials defects, Physical metallurgy in Romanian language and Matériaux et traitements thermiques and Évolution des Matériaux in French. Teaching activities have been also performed in English in the frame of Erasmus mobilities at Technical University Delft, the Netherlands.

The research activity has been supported by 3 international research grants as director/responsible. The subject of these grants was related to materials engineering, recycling, and using of solar energy in thin layers.

Research in materials and industrial engineering was also supported by 8 national grants, where I participated as member of the teams.

Applicative research in the field of Materials Engineering and Industrial Processing and Technologies has been materialized in 9 contracts with companies. The subjects of these contracts were technical assistance for development of new products, investigations of nonconformities or failure analysis, assimilation or optimization of processing technologies, improvement of quality assurance, audit for production lines or laboratories, etc.

I was also involved in two Leonardo da Vinci projects with companies and universities from Spain and Germany. The international cooperation has been an important way for career development by mean of research or teaching mobilities, co-organizing of conferences, seminars and summer schools. Relevant collaborations have been established with universities from the Netherlands, France and Spain.

Scientific activity resulted in 30 ISI articles, 9 of them as first author and 1 corresponding author. Among these contributions 14 are articles in ISI Thomson Reuters journals, and 7 have an impact factor greater than 0.5. Another 16 articles are indexed in relevant international databases.

The experience of auditing academic programs has been exercised as member in the 1st Commission for Engineering Sciences of ARACIS (Romanian Agency for Quality Assurance in Higher Education).

Minimum criteria of CNATCDU (Materials Engineering domain, Monitorul Oficial al României, partea I, Nr. 890 bis/27.XII.2012) to support habilitation thesis are accomplished or exceeded.

Minimum criteria		Minimum requested	Accomplished
A1. Teaching & training		40	89.12
A2. Research		300	508.62
A3. Recognition & activity impact		60	188.43
TOTAL (A)		400	786.17
Mandatory minimum terms subcategories		**Minimum requested**	**Accomplished**
A.1.1.1. Books / chapters in engineering books as author (first author)		2(1)	3(2)
A.1.2.1. Didactic textbook		1	2
A.1.2.2. Laboratory guidance / applications		1	3
A.2.1. Articles in ISI Thomson Reuters journals & proceedings		15	30
of which	Articles in ISI Thomson Reuters journals	10	14
	Articles in ISI Thomson Reuters journals min. 0.5 impact factor	5	7
	Articles in ISI Thomson Reuters journals as main author, regardless of the impact factor	5	10
A.2.2 Articles in journals and volumes of scientific events indexed in international databases		5	10
A.2.4 Research grants (obtained by competition)			
A.2.4.1 As director/responsible	International grant	3	3
	National grant		0
A.2.4.2 As member/participant	International grant	-	0
	National grant		8

Scientific sources for the habilitation thesis

The scientific content of the habilitations thesis represents a summary of papers published in journals indexed by ISI or other international databases. Information contained in presentations at some international conferences and included in volumes of proceedings was also used.

[1] Baltes L., Draghici C., Manea C., Ceausescu D., Tierean M., Trends in Selective Collection of the Household Waste, Environmental Engineering and Management Journal, July/August 2009, Vol.8, No. 4, 985-991.

[2] Patachia S., Moldovan A., Tierean M., Baltes L., Composition Determination of the Romanian Municipal Plastics Wastes, The 26th International Conference on Solid Waste Technology and Management, March 27 - 30, 2011, Philadelphia, U.S.A., Journal of Solid Waste Technology and Management, ISSN 1091-8043, 940-951.

[3] Patachia F.S.C., Catana Damian L.N., Tierean M., Baltes L., Microbial Safety of Plastic Materials Obtained from Wastes, Environmental Engineering and Management Journal, 14(2015), 6, 2015, 1303-1312.

[4] Costiuc L., Patachia S., Baltes L., Tierean M., Investigation on Energy Density of Plastic Waste Materials, The 26th International Conference on Solid Waste Technology and Management, March 27 - 30, 2011, Philadelphia, U.S.A., Journal of Solid Waste Technology and Management, 930-939.

[5] Rem P., Di Maio F., Hu B., Houzeaux G., Baltes L., Tierean M., Magnetic fluid equipment for sorting of secondary polyolefins from waste, Environmental Engineering and Management Journal, 12, 2013, 951-958.
[6] Tierean M.H., Baltes L.S., Rem P.C, Foris T. Feasibility study of the production of secondary polyolefins from the plastic wastes using magnetic density separation, Metalurgia International, Special issue vol. XVIII no. 5 (2013), 149-152.
[7] Ursutiu D., Samoila C., Baltes L.S., Tierean M.H., Vekas L., Jinga V., Labview in ultrasound plastic materials measurement, Journal of Optoelectronics and Advanced Materials, Vol. 15, No. 7- 8, July – August 2013, 750 - 754.
[8] Baltes L.S., Tierean M.H., Patachia S., Investigation on the friction coefficient of the composite materials obtained from plastics wastes and cellulosic fibres, Journal of Optoelectronics and Advanced Materials, Vol. 15, No. 7- 8, July - August 2013, 785 - 790.
[9] Balteş L.S., Study concerning part and injection molding die design, Metalurgia International, vol. 16/5, 2011,166-170.
[10] Baltes L., Ţierean M., Influence of the part shape on the polymer flow inside mold an overall strength, Annals of DAAAM for 2009 & Proceedings of the 20th International DAAAM Symposium, ISBN 978-3-901509-70-4, ISSN 1726-9679, pp 553, Editor B. Katalinic, Published by DAAAM International, Vienna, Austria 2009, 1107-1108.
[11] Croitoru C., Patachia S., Papancea A., Baltes L., Tierean M., Glass fibres reinforced polyester composites degradation monitoring by surface analysis, Applied Surface Science, 358, 2015, 518-524.
[12] Croitoru C., Giubega A., Patachia S., Baltes L., Pascu A., Roata I., Tierean M., State of the Art in Calcite and Polyolefins Recycling, Bulletin of the Transilvania University of Braşov, Series I, Vol. 9 (58) No. 1 - 2016, 35-40.

INTRODUCTION

The accelerated growth of the world's population and its extremely rapid mobility have generated local or global imbalances both in food necessary, water, housing, clothing, footwear, medicine, the spread of diseases as well as in the management of material and energy flows, including waste.

Non-renewable natural resources (coal, oil, natural gas, ferrous and non-ferrous ores) or renewable (wood, industrial plants) have become insufficient.

The only solution to meet the material needs of the growing population is to obtain synthetic materials that replace the natural materials and whose production can be adjusted as needed. An assortment of synthetic materials that have taken over all current fields of activity, through the extraordinary ability to adapt their properties to the application requirements are polymeric materials.

Polymers are obtained from petroleum and natural gas by chemical processes. Initially, monomers, small-molecular substances, which exhibit two or more functional groups that can interact, lead to the production of polymers, characterized by big size molecules.

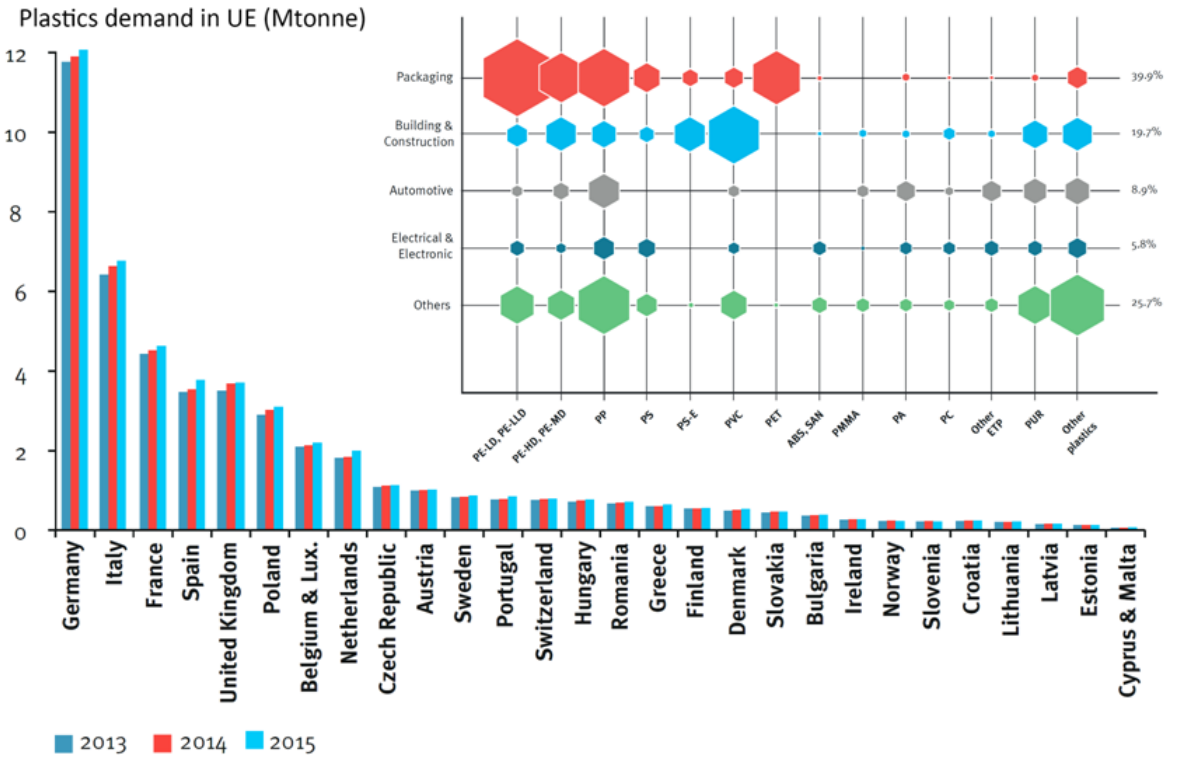

Figure I.1. Plastic materials EU demand per country and Plastics demand by polymer and market segment [1]

Regarding the production and use of synthetic polymers, it has been shown that the use of petroleum as a raw material for the production of polymers is counterbalanced by the reduction of the amount of energy required for the processing and transport of parts made of polymeric materials, compared to the processing and transport of the same goods made of metal. For example, 1.7 million tons of plastic used in Western Europe/year are obtained from the equivalent of 3.25 million tons of oil. However, 12 million tons of oil (which can be used in

energy production) can be saved due to the easier (less energy-consuming) processing of plastics in the manufacture of automotive components, metalworking, and lower transport weight. Energy savings also lead to a reduction in CO_2 emissions of 30 million tonnes per year [2].

From this point of view, the production of synthetic polymers seems sustainable.

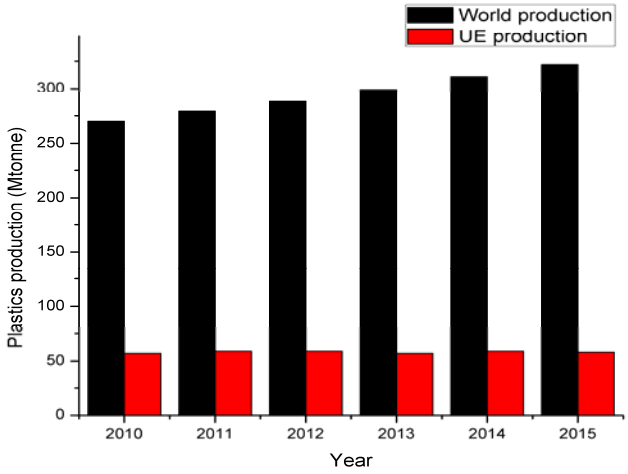

Figure I.2. Plastics production in EU counties and in the world [1]

The EU plastic demand (figure I.1.) includes plastic materials (thermoplastics and polyurethanes) and other plastics (thermosets, adhesives, coatings and sealants). Also the European plastics demand (EU-28+NO/CH) by polymer type up to 2015 are presented in the same figure [1]. It can be seen that the highest UE demand is for polyolefins (PE+PP) used for packaging.

According to the latest data, the production at EU and world level is presented in figure I.2. It can be observed the continuous growth of the wold plastic production despite of the UE stagnation during the period 2010-2015. From figure I.1 it can be remarqued the growth of the plastic demand in all UE countries (total 49 Mtonnes). Correlating the data from these two first figures it can be noted the increase of the UE imports, which determines the UE dependence from the other markets.

As mentioned earlier, petroleum is the raw material for the production of polymers. Since petroleum is a resource that does not regenerate, solutions must be found to preserve it and to reduce the amount of residue resulting from processing. Polymer waste recycling is the solution that protects the environment and reduces the consumption of natural raw materials. Also this solution is convenient for the UE countries because the raw material is a by-product of their own economy and households, not necessary to be imported.

Unfortunately, in 2014 landfilling was still the first option in many EU countries. In general, countries with landfill ban achieve higher recycling rates (figure I.3.). Romania is in the lower part of the left diagram, our landfill rate being greater than 50%.

In 2014, 25.8 million tonnes of post-consumer plastics waste ended up in the official waste streams. 69.2% was recovered through recycling and energy recovery processes while 30.8% still went to landfill.

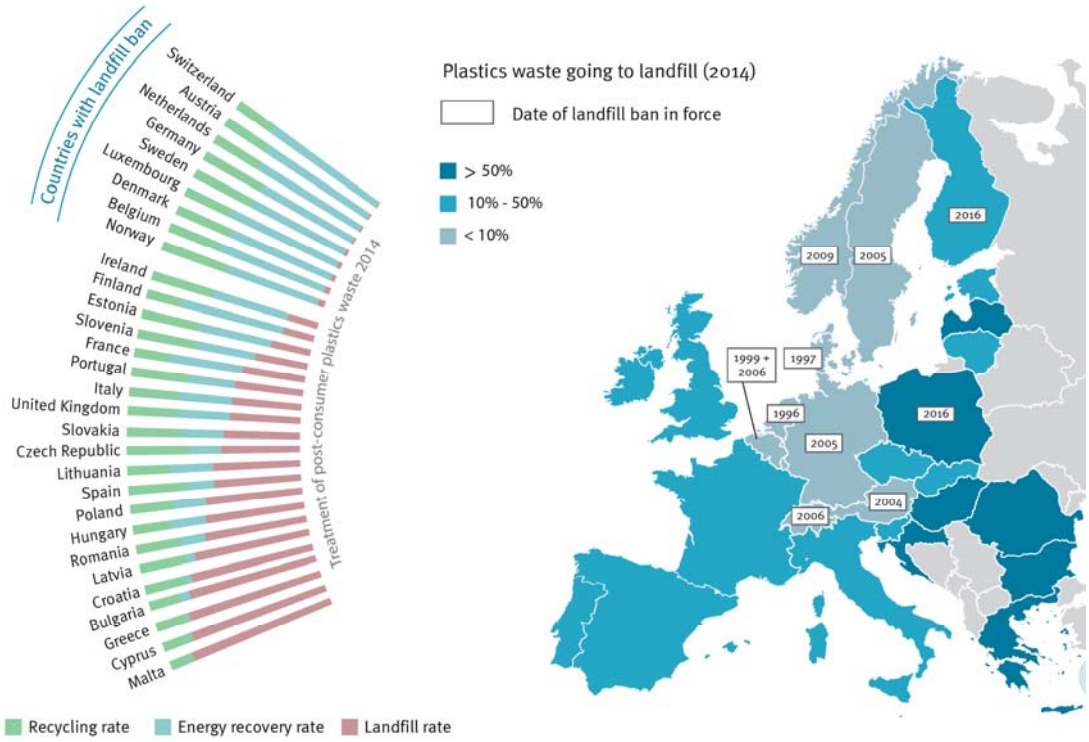

Figure I.3. Plastics waste treatment by country in 2014 [1]

In 2014, 25.8 Mtonnes of post-consumer plastics waste ended up in the official waste streams; 69.2% was recovered through recycling and energy recovery processes while 30.8% still went to landfill (figure I.4.). It should be noted the rising tendency of the recycling and energy recovery curve and the downward trend of landfilling.

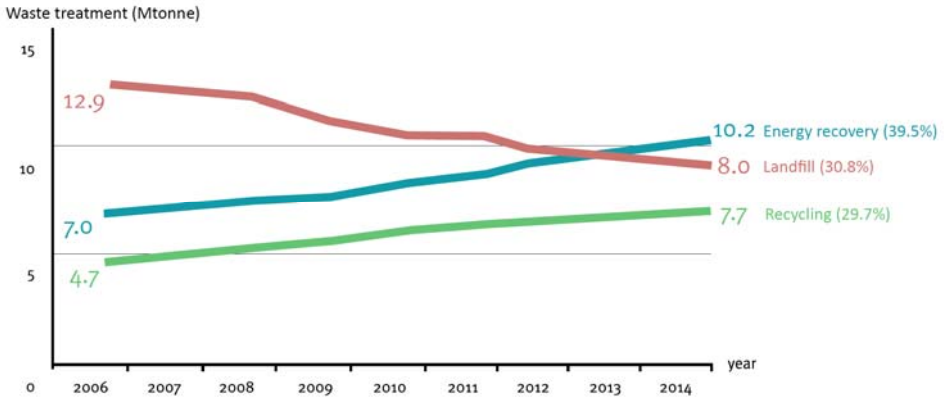

Figure I.4**.** Plastics waste treatment in EU28+2 [1]

As a consequence of these facts, the recycling challenge is zero plastic to landfill until 2025 (figure I.5). This is the possibility of saving 60 million tons of plastic waste, which means 750 million barrels of oil or 37.5 billion USD (Brent crude oil price = 50USD/barrel) [http://www.oil-price.net/].

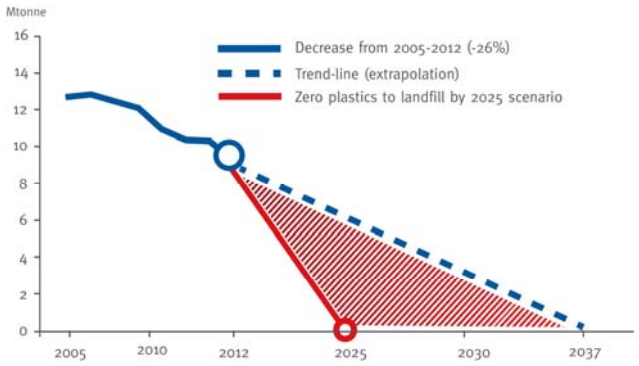

Figure I.5. Zero plastic to landfill until 2025 [3]

All the above presented data supports the idea of polymeric materials recycling and using them as secondary raw materials for new products.

The goal of this habilitation thesis is to obtain, characterise and propose new applications of polymeric materials based on secondary raw materials. Research has focused on polyolefins, as they are the highly-used polymers.

My research activity has been fed into the EU research priorities in the frame of FP7 projects. The proof is the FP7 project *Magnetic Sorting and Ultrasound Sensor Technologies for Production of High Purity Secondary Polyolefins from Waste*, acronym W2PLASTICS, project number 212782, topic: ENV-2007-3.1.3-02: New technologies for waste sorting. Period 2008-2013. The project has supported a consistent part of the achievements in my research activity.

Also the National Research Program supported a part of the founding (*cofinancing)* of the FP7 project with the title *„Magnetic Sorting and Ultrasound Sensor Technologies for Production of High Purity Secondary Polyolefins from Waste”*, 152 EU, Capacități Program, Modul III, 2 PC7, Euratom 011, ANCS, 2011-2012.

One of the main focus areas of the "Climate action, environment, resource efficiency and raw materials Challenge" in Horizon 2020 is waste [154]. In this sense, the main concern is to support the transition towards a more circular economy, where the waste generated in one industry becomes a secondary raw material for another industry.

This transition will generate growth and jobs, while contributing to environmental protection and reducing Europe's dependency on raw material imports.

R&I want to support innovation in the whole production & consumption cycle and across all sectors of economic activity, with the involvement of all societal actors. Furthermore, the research in waste is also supporting different EU initiatives (VOICES, Public-Private Partnerships on sustainable process industries and on bio-based industries) and contributing to the resource efficiency road map.

The major research and action areas covered by the waste priority are: addressing the shift towards a circular economy through industrial symbiosis developing a system approach for the reduction recycling and reuse of food waste encouraging the recycling of raw materials from products and buildings moving towards near-zero waste at European and global level and preparing and promoting innovation procurement for resource efficiency.

Chapter 1

OBTAINING OF THE SECONDARY POLYMERS

1.1. Ways to manage polymer wastes

EU recommends waste management based on three principles:

- ✓ Prevention of waste generation
- ✓ Recycling and reuse
- ✓ Final disposal of waste

The 4 R principle: reduce, reuse, recycle and recover proves its validity.

Taking into account environmental factors, the EU recommends until 2020 (figure I.5.) that all plastic wastes be directed to mechanical, chemical or energy recovery processing plants (table 1.1, figure 1.1.), from which 50% of household waste and 70% of construction and demolition wastes to be recycled or reused. Also, the intensification of recycling processes would help Europe to be less dependent on the import of raw materials.

Table 1.1. Recycling methods of plastics materials [4]

ISO 15270	ASTM D7209 — 06	Methods
Mechanical recycling	Primary recycling	Melting, Pelletizing
	Secondary recycling	Injection moulding of a sandwich structure
Chemical recycling	Tertiary recycling	Pyrolysis, Liquefaction, Gasification
Energy recovery	Quaternary recycling	Incineration

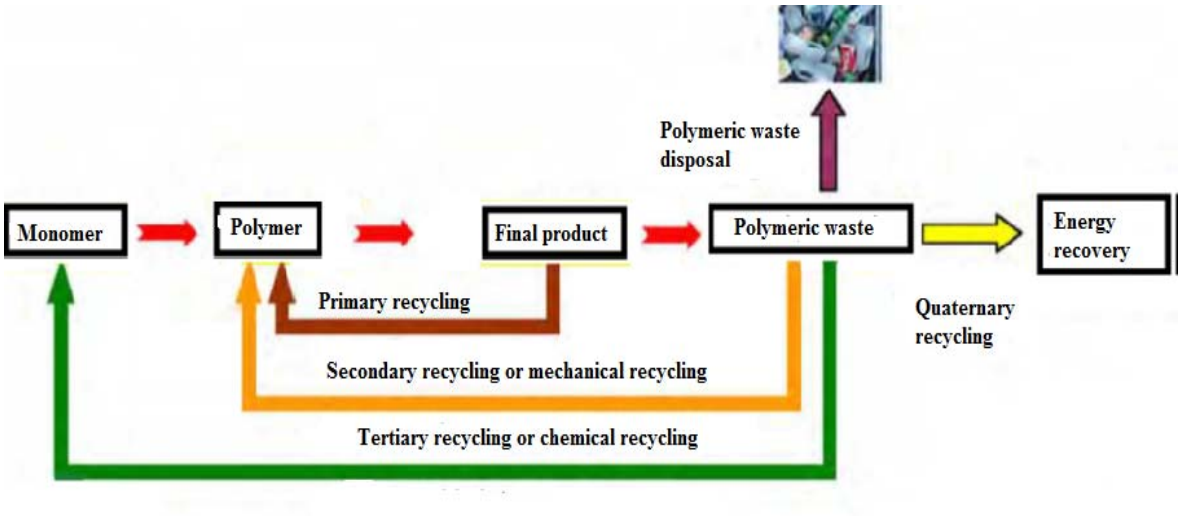

Figure 1.1. The current recycling methods for polymers

➢ **Mechanical (primary) recycling** is the most commonly used technique in the plastics industry in Europe. It recovers the clean, carefully selected waste for the purpose of being reused as new plastic products with physico-chemical and mechanical properties

equivalent to those of the original materials (figure 1.2.). The disadvantages of this method are related to the high costs of collection, sorting and cleaning. Therefore, mechanical recycling is not always economically efficient [5]. There is, however, a wide range of products that can be recycled by this method: transparent or coloured PET and HDPE containers, PVC waste, automotive components, expanded PS, WEEE and so on.

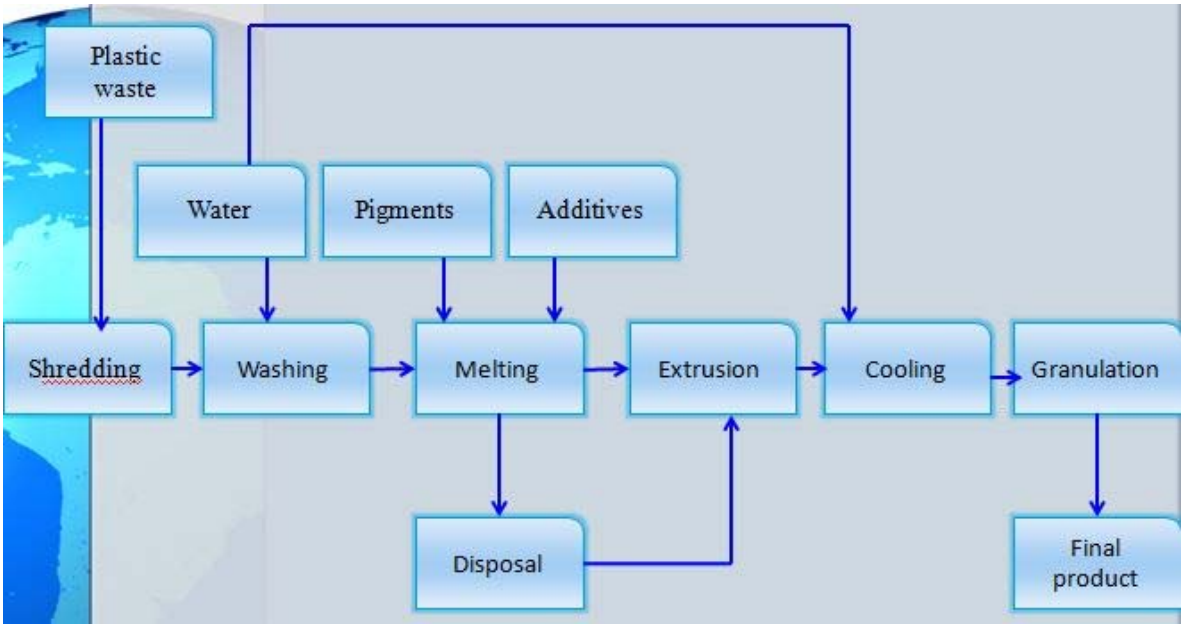

Figure 1.2. Primary recycling

Plastics can be sorted manually (expensive) or automated by identifying the type of plastic with sensors such as FTIR, recognizing the constructive features of plastic bottle, recognizing bottle codes with specialized programmed readers, by differences in density (by means of cyclones or by flotation), by the different wetting capacity. Shredding is done by grinding in special mills. By the washing process the contaminants are removed. Washing is generally done with water and soap. It is a mandatory step being followed by centrifugal drying to remove water or remove the remaining foils or labels. Waste, thus dried, feeds an extruder where plasticizing, homogenization and degassing occur. Then the material is granulated or processed to obtain the final product.

Ambrose et al. [6] mechanically recycled 100% municipal plastic waste, obtaining good quality products. The chemical and thermal properties of these recycled materials were compared with similar products made from virgin plastics.

Dodbiba et al. [7] compared two ways of recycling electrical waste (TVs), mechanical recycling and incineration. The authors concluded that the mechanical recycling is more appropriate from the point of view of environmental standards, since the method of energy recovery through incineration has generated harmful emissions to the environment.

Cavalieri and Padella [8] used a milling process with liquid CO_2 for polymer waste mixtures. A powder material was obtained which was successfully used as a matrix for the production of new composite materials. The materials obtained presented good mechanical properties.

- **Secondary recycling** refers to the use of mixed waste with virgin plastics to produce a sandwich structure, where the recycled material is completely covered by the new material. This recycling method is applied to products for which the impurities or the appearance of the recycled material are not important.

➢ **Tertiary (chemical) recycling** consists of applying classes of advanced recycling methods involving the decomposition of solid polymeric materials into various chemical compounds with low molecular weight that can be used as raw materials for the production of high quality chemicals or plastics. This type of recycling has no restrictions for upcoming applications. These methods involve high temperatures to ensure decomposition of the polymer chain in the absence of air (pyrolysis/figures 1.3., 1.4.), in the presence of hydrogen under pressure (hydrocracking), in the controlled presence of oxygen (gasification/figure 1.5.).

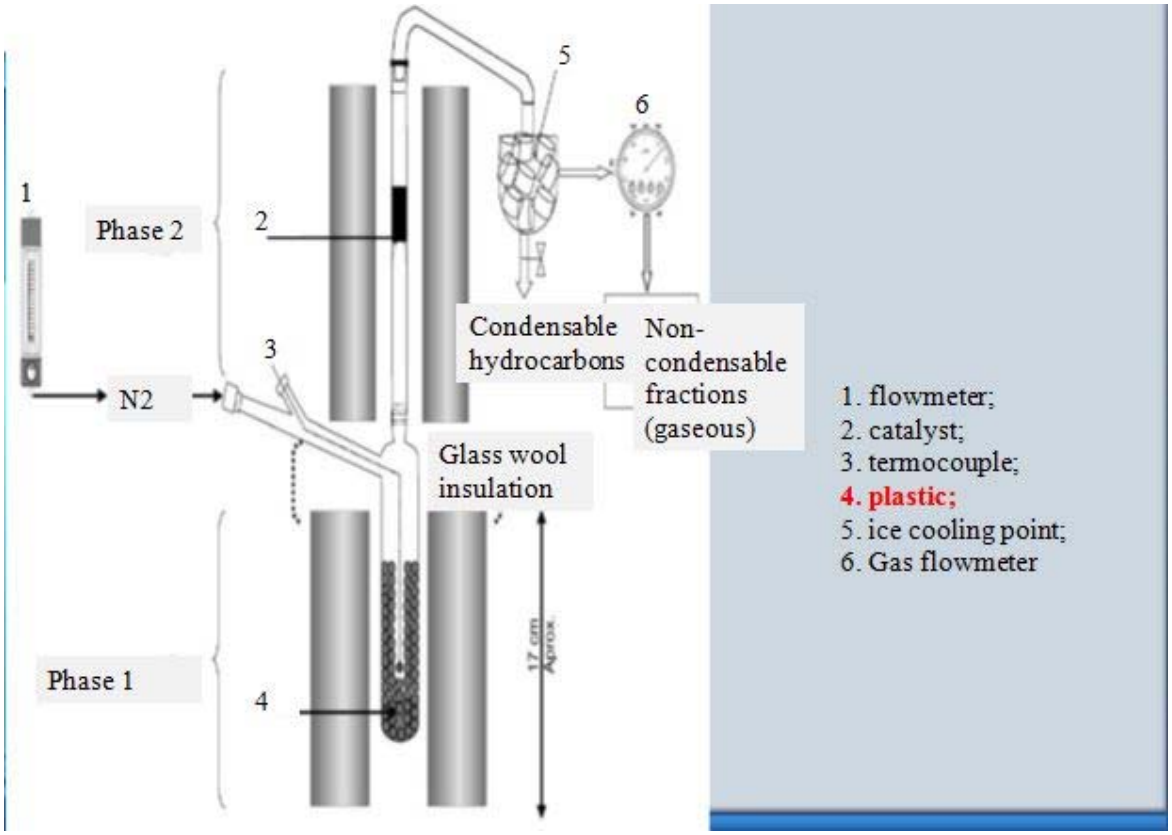

Figure 1.3. Pyrolysis equipment [9]

Chemical recycling is applied with the aim of recovering energy, especially for waste that cannot be mechanically recycled due to excessive contamination, difficulty in separation or due to polymer degradation properties [10].

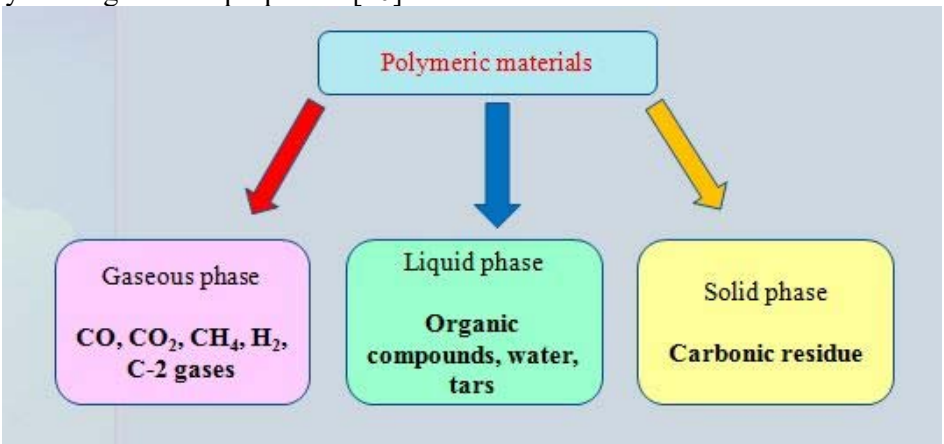

a)

Polymer	Temperature (°C)	Gas (% wt)	Liquid (% wt)	Residues (% wt)
Virgin polymer				
LDPE	450	0.5	46.6	52.9
HDPE	450	0.5	38.5	61
PP	450	6.2	67.3	26.5
Waste				
LDPE	450	8.5	72.1	19.4
HDPE	450	3.3	44.2	52.5
PP	450	15.3	64.7	20

b)

Figure 1.4. Materials resulting from the pyrolysis process (a) and % composition (b) [10], [11]

After the pyrolysis process, a smaller and less toxic volume of gas is obtained compared to the gas emissions from the incineration process.

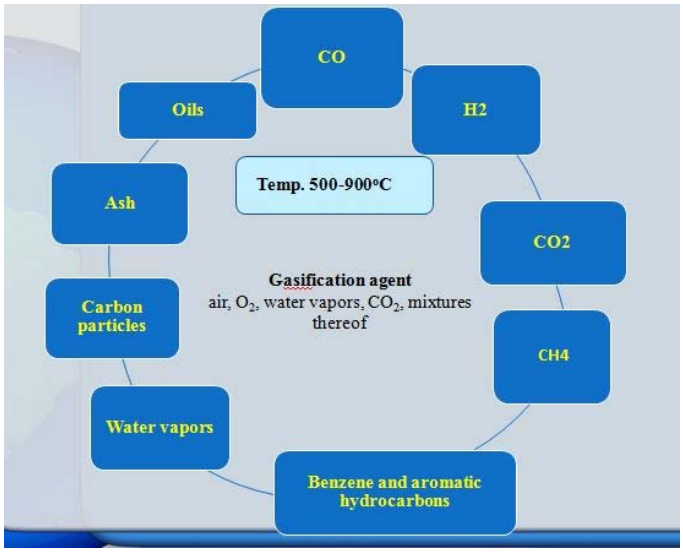

Figure 1.5. Gasification process

Gasification is a conversion technology, more than 200 years old [12], of great interest, especially in the last 10 - 15 years resulting from the need for energy independence given by the increasing of natural gas price. Gasification is a thermo-chemical process of transformation of any carbon-containing material into a gaseous mixture of carbon monoxide (CO), hydrogen (H_2), carbon dioxide (CO_2), methane (CH_4), tar (benzene and other aromatic hydrocarbons), water vapor, carbonaceous particles, ash and oils [13]. The gasification process takes place only at high temperatures (500-900°C), atmospheric pressure or high pressures in the presence of a gasifying agent, such as air, oxygen, water vapour, CO_2, or a mixture thereof. The final composition of the gaseous compounds is dependent on the type of material, the experimental parameters and the gasification agent. During the gasification of organic matter, the following processes are carried out: drying (evaporation of water which represent the humidity of the material), pyrolysis (thermal decomposition in the absence of oxygen), partial combustion (oxidation of carbon resulting from the pyrolysis process) and gasification (reaction of the final carbon with CO_2, H_2 and H_2O to produce combustible gases CO, H_2 and CH_4).

In the frame of FP7 Project Magnetic Sorting and Ultrasound Sensor Technologies for Production of High Purity Secondary Polyolefins from Waste (Transilvania University of Brasov

as Partner), acronym W2Plastics, project number 212782, topic: ENV-2007-3.1.3-02: New technologies for waste sorting, pyrolysis analyses were performed.

- **Quaternary (energy) recycling** is done through incineration and is an effective way of reducing the high volume of waste. Plastic wastes are used as fuels in thermal power plants, replacing conventional fuels, or as a source of energy in cement plants. Incineration is a process of oxidation of combustible materials, mainly with the formation of CO_2 and H_2O. Table 1.2. presents the calorific values for some plastics as compared to classic fuel examples. It is noticed that plastic waste has high calorific value, making it a convenient energy source.

Table 1.2. The value of calorific power for plastics compared to some conventional fuel [14]

Material	Calorific power [MJ/kg]
PE	43.3 - 46.5
PP	46.5
PS	41.9
Kerosen	46.5
Diesel	45.2
Naphtha	42.5
Petroleum	42.3
Household waste	31.8

The disadvantage of incineration of plastics is the emission of toxic gaseous pollutants resulting from their incomplete combustion (eg CO, unreacted or partially oxidized hydrocarbons, chlorinated compounds) or sulphur and nitrogen oxides that have a negative impact on the environment.

Also, heavy metals such as lead and cadmium found in polymers, due to their use as initiators or additives containing them, remain in ash.

Experiments, results and discussions in the frame of the FP7 Project W2Plastics in characterizing polyolefins from this point of view, as secondary polymeric materials, are presented in Chapter 2.

Secondary recycling of polymers responds not only to the quantitative diminution of polymer waste but also to obtaining of new products that generate low emissions comparing to virgin fibres polymeric materials. Aspects concerning the injection moulding of polymers are presented in Chapter 5.

Table 1.3. presents the emission factors for each type of virgin and recycled plastic.

Table 1.3. Emission factors for each type of virgin and recycled plastic [15]

Emisions (kg/Mg)	PET		PE		PP		PS		PVC	
	*P	*R	*P	*R	*P	*R	*P	*R	*P	*R
CO_2	2363	163	2400	163	2100	942	2200	942	2000	942
CH_4	25	0.016	28	0.016	28	0.016	24	0.016	22	0.016
NO_x	9.5	0.081	6.5	0.081	6.4	0.081	6.9	0.081	6.3	0.081
VOC_x	7.2	6.95	7.8	6.95	7.7	6.95	5.9	6.95	5.8	6.95
SO_x	14	-	4.9	-	5.4	0	5.2	0	5.3	-
PM	4.6	-	1.5	-	1.7	0	2.4	0	1.4	-
HCl	0.058	n/a	0.011	n/a	0.011	n/a	0.014	n/a	0.016	n/a
Energy (GJ/Mg)	107.2	46.07	79.76	19.94	76.42	19.87	84.8	11.63	59.8	9.13
* P = virgin fibre; R = recycled										

Despite the significant efforts made to optimize the presented recycling methods, all of these have a number of disadvantages regarding the price or the complexity of the installations,

the difficulty of collecting and selecting the waste, or the impact of recycling technology on the environment.

1.2. Magnetic Sorting and Ultrasound Sensor Technologies for Production of High Purity Secondary Polyolefins from Waste, acronym W2Plastics, project number 212782, topic: ENV-2007-3.1.3-02: New technologies for waste sorting [16]

The efficient large-scale recycling of plastic waste is of increasing interest from an ecological and economical point of view but it represents a goal that has yet to be achieved by the recycling industry. This project aims at a fundamental change of the present status (2007) of plastics recycling by creating a breakthrough technology for the recycling of polyolefins from complex wastes, i.e., wastes such as Waste from Electric and Electronic Equipment (WEEE), household waste and Automotive Shredder Residue (ASR).

Polyolefin's (PP, HDPE, LDPE) are a very important family of polymers, being more than a third of the total plastics consumption in Europe and complex wastes provide the vastest, presently unused potential resource of secondary polyolefin's.

One of the important consequences of switching from post-industrial waste to complex wastes is that process control and quality control become essential technologies to keep track of changes of the input waste, in terms of the amounts of valuable materials, major contaminant (rubber, wood, etc.) concentrations and particle size distribution of the input waste. Process control and quality control are equally vital to guarantee a consistent product quality, since the feed contains large amounts of contaminants and even small hick-ups of the process can deliver significant amounts of these contaminants to product bins and destroy the quality of the stored material. There are several emerging sensor technologies that are promising for the online assessment of the quality of feed and product streams in polyolefin recycling. Ultrasound imaging has the potential to detect impurities in product streams as well as detecting process failures and changes of the feed polyolefin density distributions. Both hyperspectral imaging and Dual Energy X-ray sensors combine information on composition, particle shape and spatial distribution of feed and product materials.

From the environmental point of view, the urgency of saving resources and reducing humanity's impact on the environment is evident. The need of increasing recycling and improving the quality and homogeneity of recycled materials to minimize environmental pollution and usage of resources is a topical subject for the European Community.

The scientific and technological objective of W2Plastics project was defined in the following ways:

1. To identify all valuable recyclable materials as well as all important contaminants relating to the economic value and ecologic impact of complex wastes, to quantify limits and set standards for waste generating facilities and relate the relevant properties of actual wastes to the acceptance strategies, logistics and process technology of these facilities;

2. To create models, by means of theory and experiment, of the fluid dynamics, chemical engineering, material properties and ultrasound imaging that are necessary to develop the MDS-Ultrasound technology for the bulk recovery of 98%+ pure polyolefin products by European recycling SME's;

3. To develop sensing technologies, hyperspectral imaging based, and related data interpretation models to characterize feed and product streams in terms of the relevant composition parameters and performance in applications of the granulates in manufactured products.

The objectives were attained in a progressive strategy: Simulations and experiments, laboratory tests & performance assessment, small scale demonstrations, ultimately resulting in a technology platform at one of the partner SME's.

The objectives of the project were realized by a work plan consisting of three parallel routes (figure 1.6):

1. Relating the economic and ecologic impact and potential of such wastes to the waste properties and acceptance strategies, logistics and process technology of the facilities that generate these wastes;

2. Creating an environmentally friendly and cost-effective bulk process MDS technology that is suitable to recover high-purity polyolefin products from the float fraction of complex wastes at interesting capacities;

3. Developing process control and quality control technology based on powerful emerging sensor technologies;

The work plan routes are covered by 14 work packages dealing with the research and technology (**1-10, 12**), training and dissemination (**11, 13**) and project management (**14**). The research and technology work packages **4-6** deal with route 2 (innovation in process technology), work packages **7-9** focus on route 3 (sensors for process and quality control), while work packages **1-4** and **10, 12** are concerned with route 1 (maximizing economic and ecologic impact).

The work packages were:

• **WP 1:** Characterization of plastics streams from different sources and locations

• **WP 2:** Market Analysis and applications of high purity secondary plastics usage

• **WP 3:** Test of high purity secondary polyolefins and market exposure

• **WP 4:** Chemical improvement of the quality of recycled polyolefins

• **WP 10:** Green solutions for process residues

• **WP 11:** Transfer of technology to industry

• **WP 13:** Workshops, training and dissemination

The science and technology-related work packages

• **WP 5:** Numerical Simulation of the Magfluid Sorting Equipment

• **WP 6:** Development of the Inverse Magfluid Sorting Technology

• **WP 7:** Ultrasound System Design & Testing

• **WP 8:** Ultrasound Data Processing

• **WP 9:** Sensors for Control Equipment and Quality Assessment

• **WP 12:** Implementation of a Life Cycle Analysis of the application of such technologies to specific waste streams

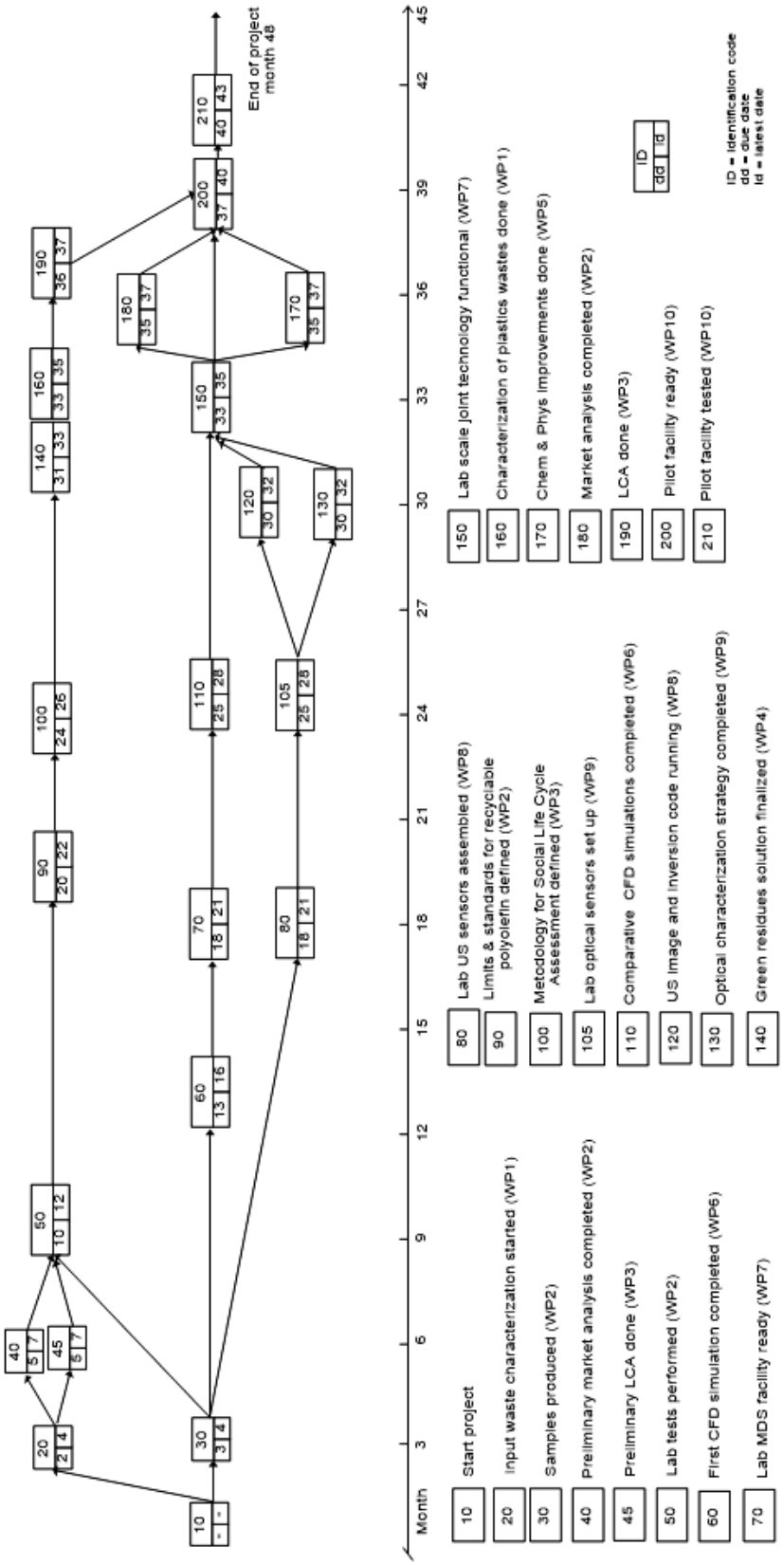

Figure 1.6. W2Plastics work plan consisting of three parallel routes [16]

The connections between work packages are presented in figure 1.7.

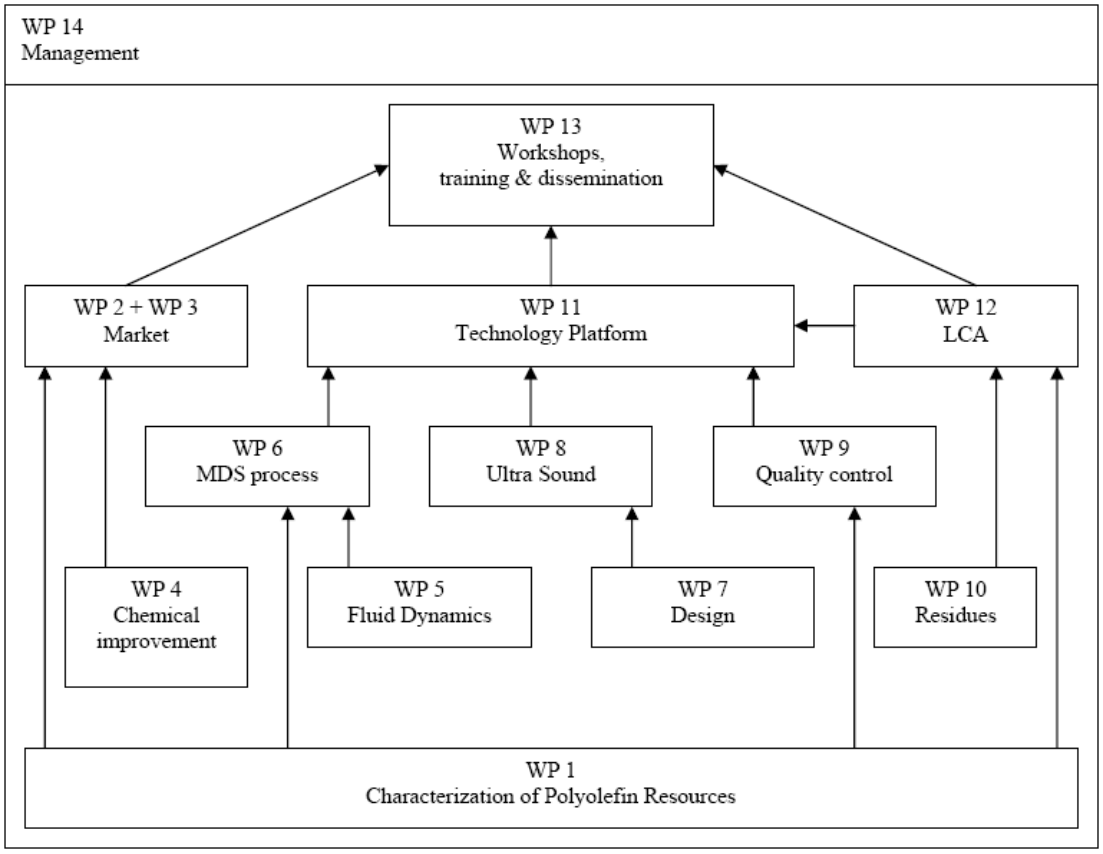

Figure 1.7. Interdependence of WPs (Pert) [16]

The participants were universities, research centres and SME as it shown below (table 1.4.).

Table 1.4. Participants in FP7 Project [16]

Part. No.	**Participant organisation name**	**Country**
1.	Delft University of Technology	The Netherlands
2.	Universita' di Roma La Sapienza	Italy
3.	Technical University of Denmark	Denmark
4.	Transylvania University of Brasov	Romania
5.	Barcelona Supercomputing Centre Centro Nacional de Supercomputación	Spain
6.	Budapest University of Technology and Economics	Hungary
7.	Recycling Avenue	The Netherlands
8.	Alcufer kft	Hungary
9.	Urban S.A.	Romania
10.	Oldelft	The Netherlands
11.	DV – Tecnologie d'Avanguardia s.r.l.	Italy
12.	REDOX Waste Recycling B.V	The Netherlands

Transilvania University of Brasov was involved in the work packages: WP1, WP2, WP3, WP7, WP8, WP10, WP12, WP13 and WP14.

Density separation by flotation means an immersion of the mixed particles in a liquid medium with a density intermediate between those of the heavy and the light particles. The particles with lower density float while the particles with higher density sink.

Using water as liquid phase (1000 kg/m^3), it is possible to separate for example PE (950 kg/m^3) by PET (1070 kg/m^3). Using aqueous salt solutions (in 2 steps): PS (1030 kg/m^3), PMMA (1016 raw materials kg/m^3), PET, or alcohol aqueous solutions (2 steps): PP (900 kg/m^3), LDPE (930 kg/m^3), HDPE (950 kg/m^3). The use of water as liquid phase separation does not allow a high efficient raw materials separation of polymers with close densities. Addition of additives to water (salts or alcohol) leads to an excessive increase of the price.

Magnetic Density Separation (MDS) is a sink-float separation in which the separation medium is a magnetic liquid. This is a colloidal liquid made of nanometre-size ferromagnetic particles suspended in water. Placing this liquid in a magnetic field, the weight of the liquid becomes the sum of gravity and the vertical component of the magnetic force. In this way, the separation medium can be artificially lighter or heavier according to direction and magnitude of the magnetic force. The gradient of the magnetic induction decreases with the distance to the magnet (figure 1.8.a). Placing the magnet below the magnetic fluid, the density of the fluid increases (figure 1.8.a, blue curve). If the magnet is above the magnetic fluid the density of the fluid decreases (figure 1.8.a, red curve) and the process is named inverse magnetic density separation (IMDS).

Because the density of the polyolefins (0.88…0.97 g/cm^3) in below the water density for polyolefins separation the magnet must be placed above the MDS channel. If different polymer balls are introduced inside magnetic fluid, there were suspended according the density, the low-density polymer being on top (figure 1.8.b).

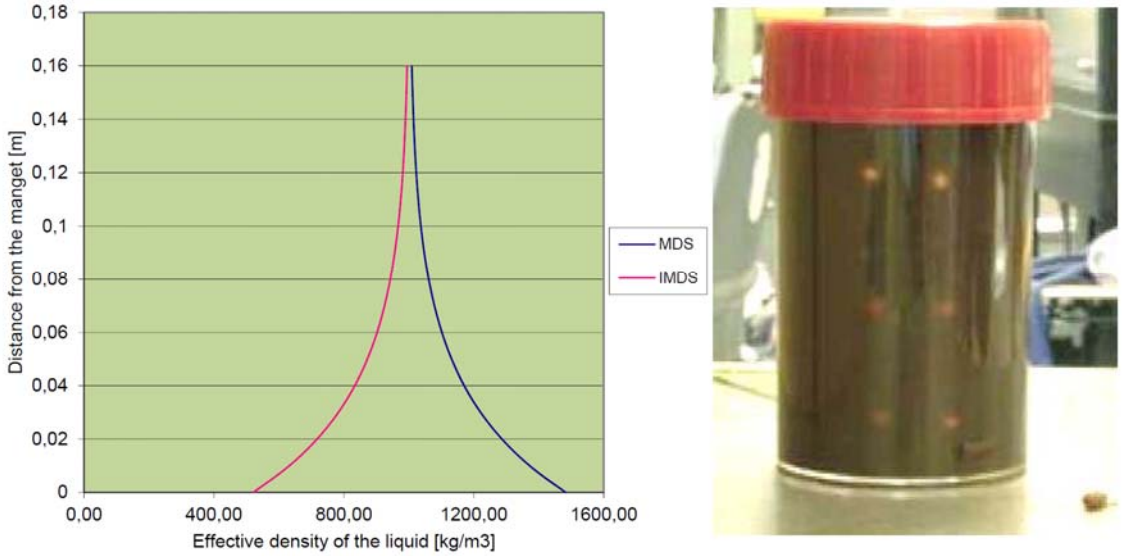

a) b)

Figure 1.8. Magnetic Density Separation principle: a) variation of the effective density of the magnetic fluid for MDS and IMDS, b) polymer balls suspended in magnetic fluid [16]

The mixture of wetted particles is mixed with the process fluid in a turbulent flow, which disperses the various materials over the cross-section of the channel. This way, the particles enter the magnetic separation zone with maximum mobility, i.e. with minimal particle-particle interaction. Then, entering the magnetic separation zone, the fluid must become as laminar as

possible in order to let the magnetic forces create the separation without turbulent mixing. The magnetic field acts with a body force on the process fluid, so as to oppose the gravity force on any volume of the fluid. Since the magnetic field increases exponentially towards the ceiling of the channel, the upward force on the fluid also increases exponentially, and the weight of a volume of fluid (gravity minus magnetic attraction) decreases towards the top of the channel. Since the particles that are to be separated, plastics, glass, non-ferrous metals, are not magnetic; the magnetic field does not oppose the gravity force on these particles. This means that particles will tend to collect at a vertical position in the channel where their gravity is just balanced by the combination of gravity and magnetic force on an equivalent volume of fluid. In other words, materials of different densities collect at different strata in the flow, provided that the mixing effect of turbulence is small enough. After being separated into strata, the flow must be split into several product streams without back-mixing or blocking (figure 1.9.).

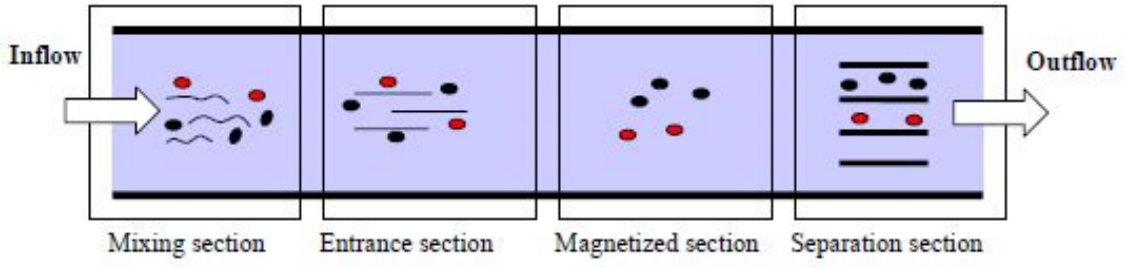

Figure 1.9. The separation channel and the flow of the polymers at different heights [16]

Advantages of the MDS separation:

- Magfluids have no densities limits
- Magfluids have different densities at different positions: multiple products
- Magfluids for plastics separation can be used as ordinary water

The principle of the installation is presented in the figure 1.10. [16]

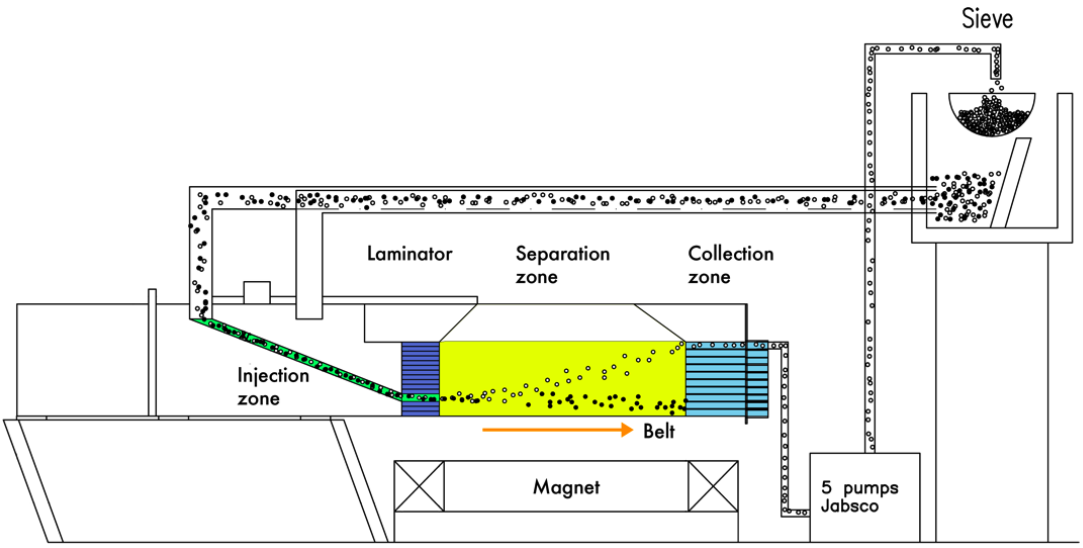

Figure 1.10. MDS equipment principle [16]

To simulate the flow 512 computers from the total of 16384 computers from Barcelona Supercomputing Centre were used.

The 3D model of the flow and the flow simulation are presented in figure 1.11. [16]

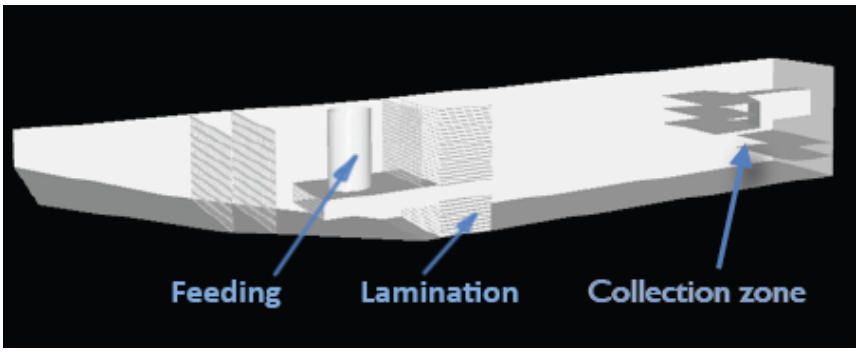

a)

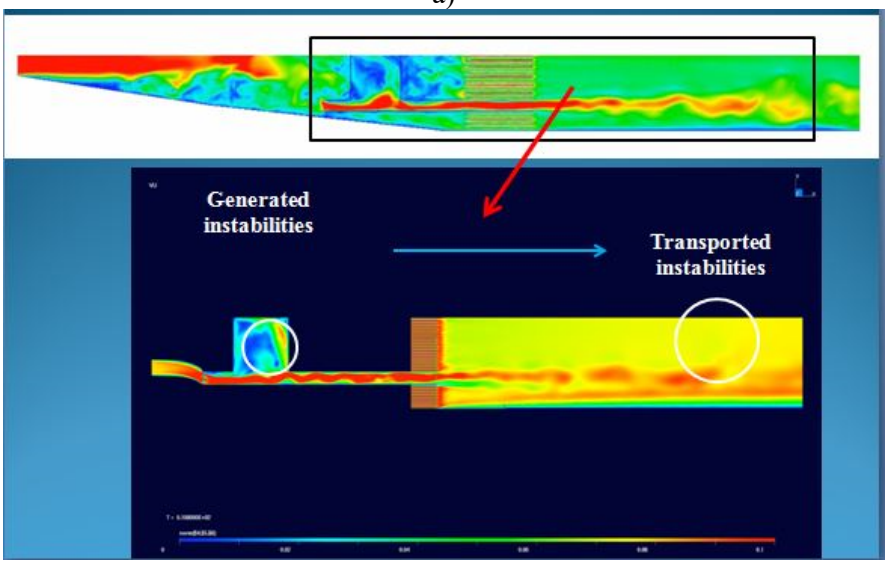

b)

Figure 1.11. The 3D model of the flow (a) and the flow simulation (b) [16]

Ultrasound test for the polyolefins is presented in figure 1.12. The PP particle is brighter than the LDPE particle (figure 1.12.a). The ratio of the pixel intensity of PP to LDPE is 1.5 which confirms the strong reflection of PP particles. Ultrasound test principle and the images of PP and PE particles are presented in figure 1.13.

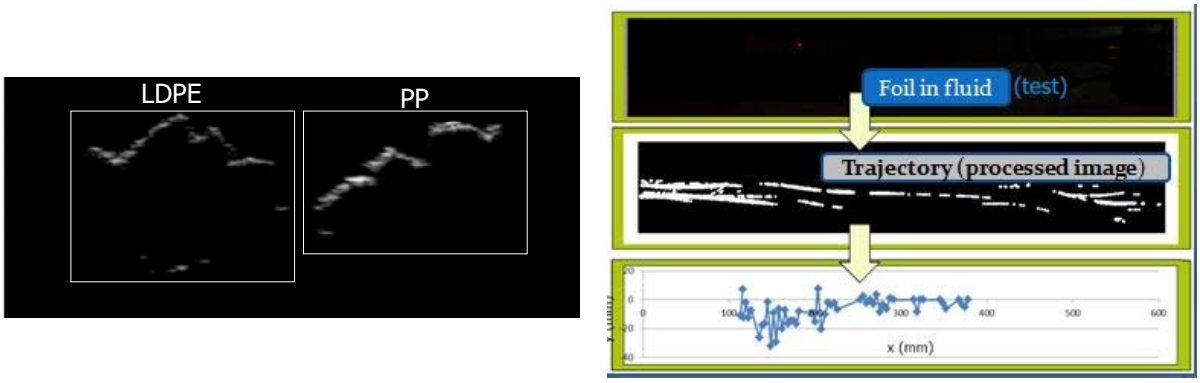

a) b)

Figure 1.12 Ultrasound test for the polyolefins: a) ultrasound image of polyolefins, b) foil trajectory [16]

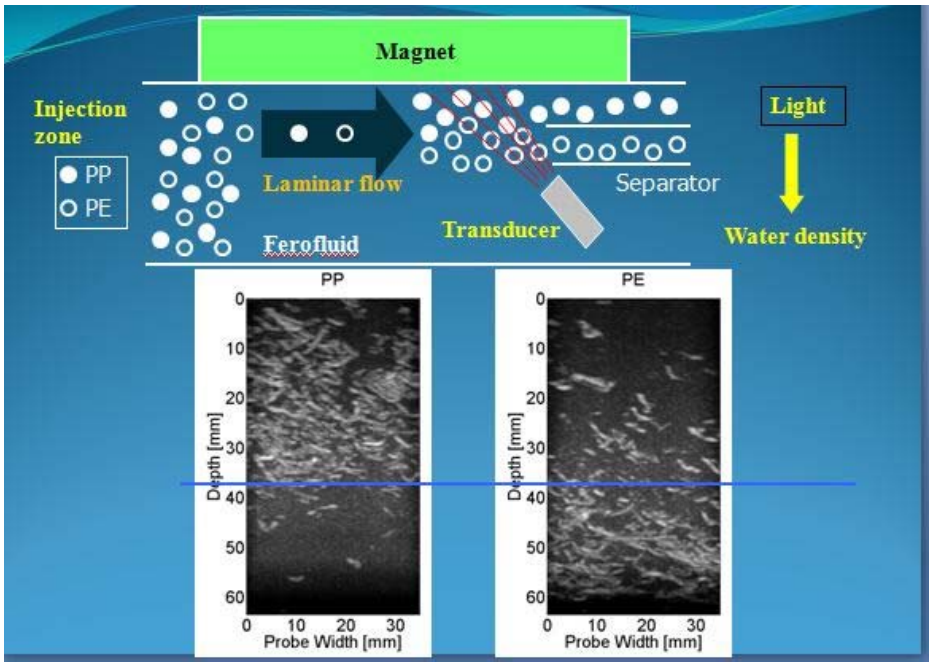

Figure 1.13. Ultrasound test principle [16]

The MDS equipment is presented in figure 1.14. [16]

Figure 1.14. Industrial MDS equipment [16]

1.3 . Trends in selective collection of the household waste [17]

Under the FP7 project, considering that most of the materials used in the research work were polymers as secondary raw materials from municipal solid waste, it was opportune to analyse some aspects related to the trends in selective collection of the household waste at the 2009 level.

The EU regulations stipulate the basic principles relating to waste collection, elimination, reuse and treatment and which can be schematically summarised as two principles:

- the Polluter-Pays principle.
- subsidy, the principle of prioritising the treatment procedures.

The "landfill" directive (1999/31/EC) defines three types of landfills corresponding to three types of waste:

- ❖ class I landfills, for hazardous waste;
- ❖ class II landfills, for non-hazardous waste;
- ❖ class III landfills, for inert waste.

The objective for the EU Members is to reduce the proportion of landfilling and provides that only waste that has undergone prior treatments, shall be admitted. The waste will be monitored for thirty years after its disposal. The European directive on waste incineration (2000/76/EC) sets out new environmental thresholds, in particular those governing dioxin emissions; the threshold for dioxin emissions should not exceed 0.1ng/m.

There is a strong movement in many countries to reduce the volume of wastes to be dumped. Composting allow to the organic fraction of waste to be converted into a useful and commercial product with a higher value. For inert materials, wastes as raw materials are needed to obtained new products.

Development of new materials from recycled materials will also encourage sorting of solid waste.

Conventional waste management systems will provide small gains only. Other alternatives and efforts indicate that:

• onsite treatment and utilisation will reduce need for transport;
• waste minimization is a socially desirable goal;
• subsidy on products generated from recycled materials will encourage socio-economic changes;
• waste that has severe risks and excessive problems in disposal should be identified and that which cannot be neutralized may need to be restricted at the point of creation or entry;

• a database on waste that is available will provide information to possible users of waste.

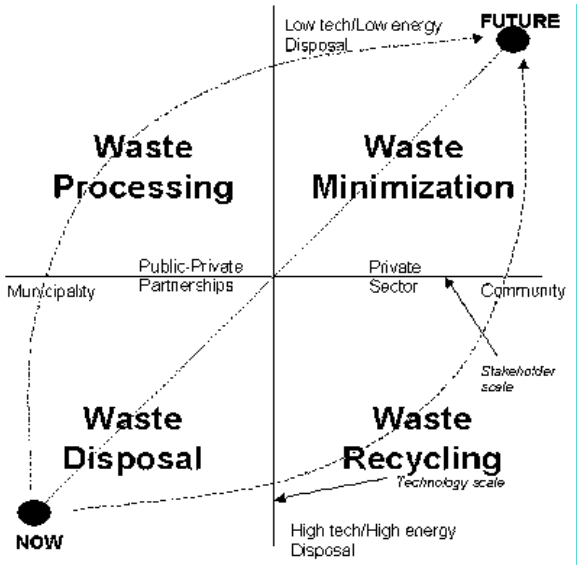

Figure 1.15. Evolution of waste treatment [17]

Four key aspects of waste management are very important: disposal, recycling, processing, and minimization (figure 1.15.). These four issues have been put into a dual axis. One is the horizontal stakeholder scale, ranging from municipalities and local governments to the community. The other is the vertical technology scale ranging from high tech/high energy disposal systems to low tech/low energy systems [18], [19].

Local governments are looking at waste as a business opportunity.

Table 1.5. presents some appreciations concerning separate collection versus mixed collection [20].

It is known that one way to decrease the waste collection is to produce less.

For example, in Romania, from the 1st of January 2009, it is forbidden to give free plastic bags. The same rule was applied in Ireland since 2002. Romania adopted the Waste Management Evidence and the Waste European Catalogue since 1999. At the end of 2005, the 1281 Rule (1281/16.12.2005) of the Environment and Water Management Ministry concerning the waste containers colours was adopted (figure 1.16.): black/grey for unrecoverable/unrecyclable waste; brown for compost/biodegradable waste; white/green for white/coloured glass waste; blue for paper/cardboard waste; yellow for metal/plastic waste; red for hazardous waste.

Table 1.5. Separate collection vs. mixed collection [17]

Separate collection	Mixed collection
Extends landfill life. Removes potential recyclables from the waste stream. Lowers net disposal costs.	It is not time or space consuming for the residents.
Done by the household. No extra cost for the community.	The facility does not need additional space to handle recyclables.
Highly applicable to residential waste.	Basic technology is needed
Industrial waste may be recycled through industrial waste exchanges.	The effectiveness of the collection system does not depend on how people prepare recyclables.
An effective and reliable tool for recycling.	There is no need for established secondary markets.
Can be implemented on small-scale, then expanded.	
Recyclables are usually uncontaminated by garbage and other debris.	

A Romanian citizen generates around 5 kilos of household waste per week, half of it is biodegradable, a half of a kilo is glass and another half of a kilo is paper and cardboard [21]. The rest is shared between other types of waste, 250 grams textiles and 200 grams polymers and PET.

Figure 1.16. Containers for selective collection in Brașov county [17]

In Romania (2008) the selective collection of household waste against waste recovery of main materials: paper and cardboard, glass, metals, plastics it's not a usual practice; it is applied at local level in pilot projects initiated by Waste Recycling Companies and City Halls in co-operation with companies which produce packaging and packaging products. These programs are in progress with inhabitants' associations, schools, institutions, and companies and according to the obtained results and available funds, the projects are extended [23]:

The selective collection is anticipated to be approached in three stages as is presented in figure 1.17. [22], [23]:

• 2004 – 2006: experimental phase (pilot project), population aware;
• 2007 – 2017: enlargement of selective collection at national level;
• 2017 – 2022: implementation of selective collection in difficult to access areas (countryside area, mountain area).

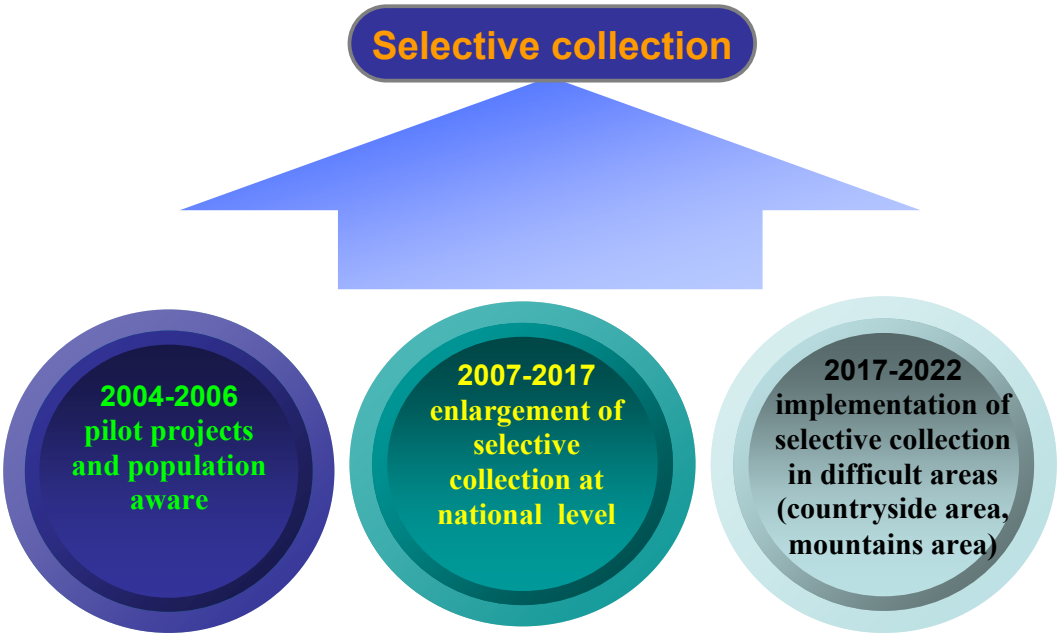

Figure 1.17. Stages of selective collection in Romania [17]

Figure 1.18. presents the collection of polymers waste in Brasov. A significant difference between 2007 and 2008 and the important contribution of the industry waste in the total amount can be observed. Increasing of polymers waste quantity can be observed. The collection is lower in the spring months than in winter, caused probably by the increasing of liquids consumption.

An important step for municipal councils is to stop considering environmental problems as a matter to be solved by a single company or group or companies involved in waste collection.

The selective collection is a problem of municipality, citizens and waste collection companies.

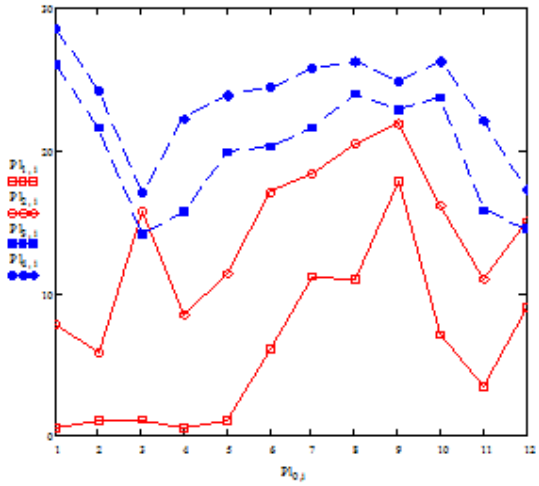

Figure 1.18. Selective collection of polymers waste in Brasov city by Urban Co. [17]

The factors that reduce the selectivity of the waste are: individual effort required by the method; distance between residence of the citizens and containers; low availability of space at citizen's home; low availability of time; comfort and dimensions of the containers; recurrence of old habits of the users.

Some factors are influenced by the age of the waste producers, the occupation, the degree of education, place of residence, the level of income; the rest of them are affected by the environment, the community, politics and civic rules.

The environmental education must be integrated into municipal action plans, thereby offering simple and updated information in an attractive and easily understandable way, and distributing this information so that it reaches the largest part of the population.

This education can be done by: 1. local administrations, through visits and meetings with representatives of the various municipal institutions; 2. large image promoters, through visits to the large waste production centres and the business associations that represent them; 3. citizens, through printed materials distributed to the entire population (brochures, signs, etc.) and through informative talks and itinerant exhibits; 4. visitors, through the placement of signs and the distribution of brochures in areas with a large flow of tourists; 5. schools, through the preparation of specific materials on waste prevention and management and distribution of the materials at educational centres.

The waste collection companies can contribute to the increasing of selective collection by changing the design of the recipients and the availability of them according the users. They can also organize periodically contests on selective collection and give prizes to the top neighbourhoods.

Chapter 2

CHARACTERIZATION OF THE POLYOLEFINS AS SECONDARY RAW MATERIALS

Extensive use of plastics in all areas of human activity leads to the accumulation of huge amounts of waste, mostly non-biodegradable. This creates major environmental problems by polluting soil, water and atmosphere due to their uncontrolled degradation and emission of toxic compounds. Plastics recycling have become a necessity.

A number of variables in plastic waste such as colour, type of additives used, form of the polymer (film, foam, compact) will influence both the separation process and the properties of the material derived from these secondary raw materials.

There are a lot of plastics sources such as Municipal Solid Wastes (MSW), automotive shredder residues (ASR), building and construction waste (B&CW), etc. which generate a lot of types of plastics materials, the quantitative ratio of these plastics is close related to the economic development of the country, the country's population, the people life-level, national customs, seasons, etc.

Plastic waste will be collected and separated as secondary raw materials that can replace partially or totally virgin polymers in obtaining products made of plastics [11], [24], [25], [26], [27], [28]. But their use is still at a low level because of both objective and subjective reasons. Objective reasons are related to continuous collection and separation possibilities of waste and insufficient amounts to provide the rhythmic need of raw materials for industrial production. Also the effectiveness of separation methods must ensure reproducible quality of plastics separated. Contaminants can decisively influence the quality of final products. Also very important are the prejudices and psychological thresholds related to acceptance in everyday use of waste as secondary raw materials. Finally, yet importantly, given that the concept of waste (especially the household) is mentally linked to the notion of dirt, infection, decay, bacteria, microbes, their use is drastically limited.

Exponential growth of the population and decreasing oil supply (the raw material of synthetic polymers) are two key reasons for the development and acceptance of goods from recycled plastics for use in common areas of activity. The need for common use of spaces and objects require antimicrobial nature of materials that lead to the production of floors, panels, furniture, toys etc. so they do not become vectors to transmit pathogens, causing epidemics [29].

The possibility of using the plastic waste as fuel determined the evaluation of the calorific power of those materials.

So characterization of polymeric wastes is compulsory. The paper ***Composition Determination of the Romanian Municipal Plastics Wastes*** [30] (in the frame of the European Project FP7 W2-Platics), presents just the characterization of polymeric wastes selected by Urban Enterprise, from MSW of Brasov County, Romania, in September 2010. The selected plastics have been washed, frozen and ground (fig.2.1.) in a ZM 2000 centrifugal mill and separated based on their density by sink floatation.

Figure 2.1. Cut polymeric wastes selected by Urban Company, from MSW of Brasov, Romania prepared for separation process (W2Plastics/D4.1) [16]

Five samples of polymeric wastes have been separated in 13 fractions (table 2.1.), having different densities using water (ρ = 0.997 g/cm^3) and solutions with different densities: ethylic alcohol + water (ρ = 0.788 g/cm^3, 0.880 g/cm^3 0.908 g/cm^3, 0.923 g/cm^3, 0.935 g/cm^3, 0.964 g/cm^3) and aqueous salts solutions of NaCl and Na_2CO_3 (ρ = 1.0053 g/cm^3, 1.1029 g/cm^3, 1.1469 g/cm^3; 1.197 g/cm^3, 1.27 g/cm^3).

The aim of this action was to separate polyolefins from the MSWP, that means fractions with the density range of: 0.8848 and 0.964 g/cm^3. The lighter and heavier fractions are considered polyolefins contaminants. The separated density fractions have been analyzed by gravimetric method, image analysis and FTIR spectrometry.

2.1. Gravimetric analysis of the contaminants from MSW, Brasov Romania

To have a general view of the polymeric fraction coming from MSWP of Brasov, Romania, an average has been calculated for the percental repartition of the fractions (table 2.2.). The blue zones correspond to the lighter and respectively heavier contaminants fractions of the polyolefins. The PO-s are coded as orange colour.

Approximately 21% from the total waste weight are contaminants for polyolefins. Only 0.82% are lighter polymers, the heavier fraction of contaminants being dominant.

To be closer to the reality, photos of each density fraction were done (figure 2.2.) and the image analysis of all the obtained photos were applied. In this way, it was possible to calculate the percent of each colour from each fraction. Then, infrared spectroscopy analysis was performed, for samples of each colour present in each fraction. By identifying of each coloured polymer, from each density fraction was possible to calculate the percent of each polymer type from a fraction.

2.2. Image analysis of MSW from Brasov, Romania

Figure 2.2. presents the photos of density fractions for the samples separated from the polymeric wastes coming from MSWP from Brasov, Romania. It could be noted that each fraction is formed by pieces of polymers having different colours. Taking into account that each fraction corresponds to a quite narrow interval of density, it could be assumed that same raw materials colour corresponds to the same polymer in the frame of one density fraction. The image analysis has been made by using Photoshop CS5 software.

Table 2.1. Density fractions obtained by separation of the polymeric wastes coming from MSW of Brasov, Romania, selected by Urban [30].

MSW Brasov

S1		S2		S3		S4		S5	
density fraction	percent	density fraction	percent	density fraction	percent	density fraction	percent	density fraction	percent
<0.788	0.026	<0.788	0.026	<0.788	0.018	<0.788	0.027	<0.788	0.014
0.788-0.884	2.045	0.788-0.884	0.459	0.788-0.884	0.397	0.788-0.884	0.492	0.788-0.884	0.579
0.8848-0.908	9.293	0.8848-0.908	5.379	0.8848-0.908	4.289	0.8848-0.908	4.435	0.8848-0.908	5.786
0.908-0.923	6.759	0.908-0.923	7.825	0.908-0.923	6.303	0.908-0.923	10.330	0.908-0.923	9.567
0.923-0.935	6.106	0.923-0.935	4.766	0.923-0.935	6.242	0.923-0.935	5.974	0.923-0.935	5.112
0.935-0.964	56.914	0.935-0.964	56.222	0.935-0.964	63.598	0.935-0.964	59.117	0.935-0.964	59.972
0.964-0.997	1.741	0.964-0.997	3.652	0.964-0.997	2.171	0.964-0.997	3.082	0.964-0.997	1.950
0.997-1.005	0.276	0.997-1.005	0.806	0.997-1.005	1.944	0.997-1.005	0.535	0.997-1.005	0.751
1.005-1.102	5.977	1.005-1.102	7.027	1.005-1.102	3.831	1.005-1.102	3.479	1.005-1.102	4.769
1.102-1.146	1.164	1.102-1.146	1.449	1.102-1.146	1.644	1.102-1.146	1.346	1.102-1.146	0.876
1.146-1.197	2.525	1.146-1.197	3.124	1.146-1.197	2.211	1.146-1.197	2.681	1.146-1.197	2.651
1.197-1.27	0.333	1.197-1.27	0.181	1.197-1.27	0.244	1.197-1.27	0.561	1.197-1.27	0.064
> 1.27	6.841	> 1.27	9.085	> 1.27	7.108	> 1.27	7.941	> 1.27	7.908

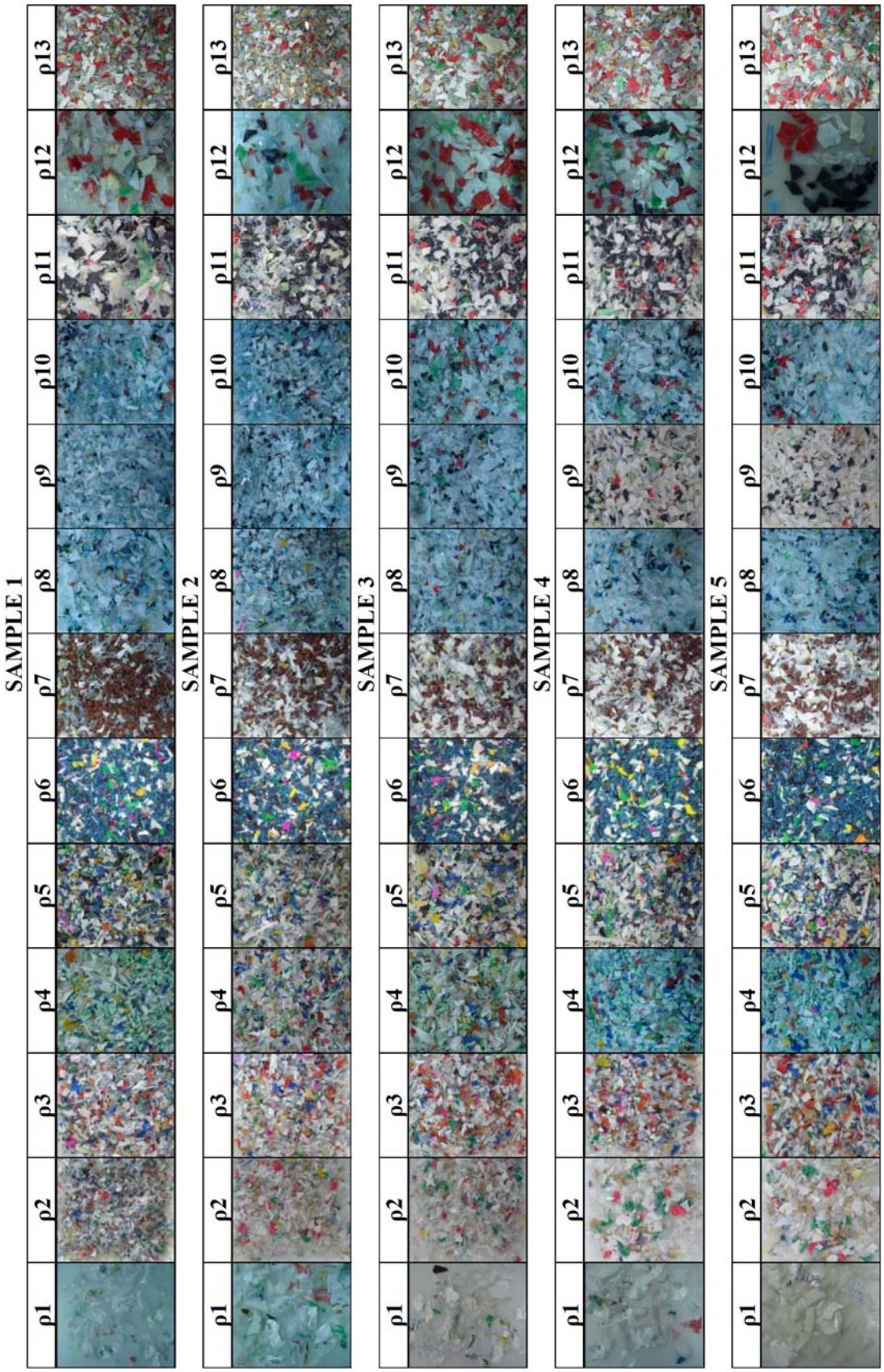

Figure 2.2. Photos of the density fractions from the polymeric wastes separated from MSW from Brasov, Romania, by Urban [16]

Table 2.2. The composition of the polymeric fractions coming from MSW of Brasov, Romania [30]

Fraction Nr.	1	2	3	4	5	6	
Density fraction (g/cm^3)	<0.788	0.788-0.884	0.884-0.908	0.908-0.923	0.923-0.935	0.935-0.964	
%	0.022	0.795	5.836	8.157	5.640	59.165	
%	0.817		78.795				
Fraction Nr.	7	8	9	10	11	12	13
Density fraction (g/cm^3)	0.964-0.997	0.997-1.005	1.005-1.102	1.102-1.146	1.146-1.197	1.197-1.27	> 1.27
%	2.519	0.862	5.017	1.296	2.638	0.276	7.777
%	20.385						

The steps that have been followed for image analysis are: image loading in Photoshop software, determination of the total number of the pixels from the image, selection of the colour that will be analysed, selection of the similar colour on the whole image. After the selection of all zones with the same colour (ex. red), the software will calculate the number of pixels corresponding to the chosen colour the right part of the screen, as it could be seen, red- marked in Figure 2.3. With all the obtained data, it could be calculated the percent of each type of colour from the analysed fraction [16].

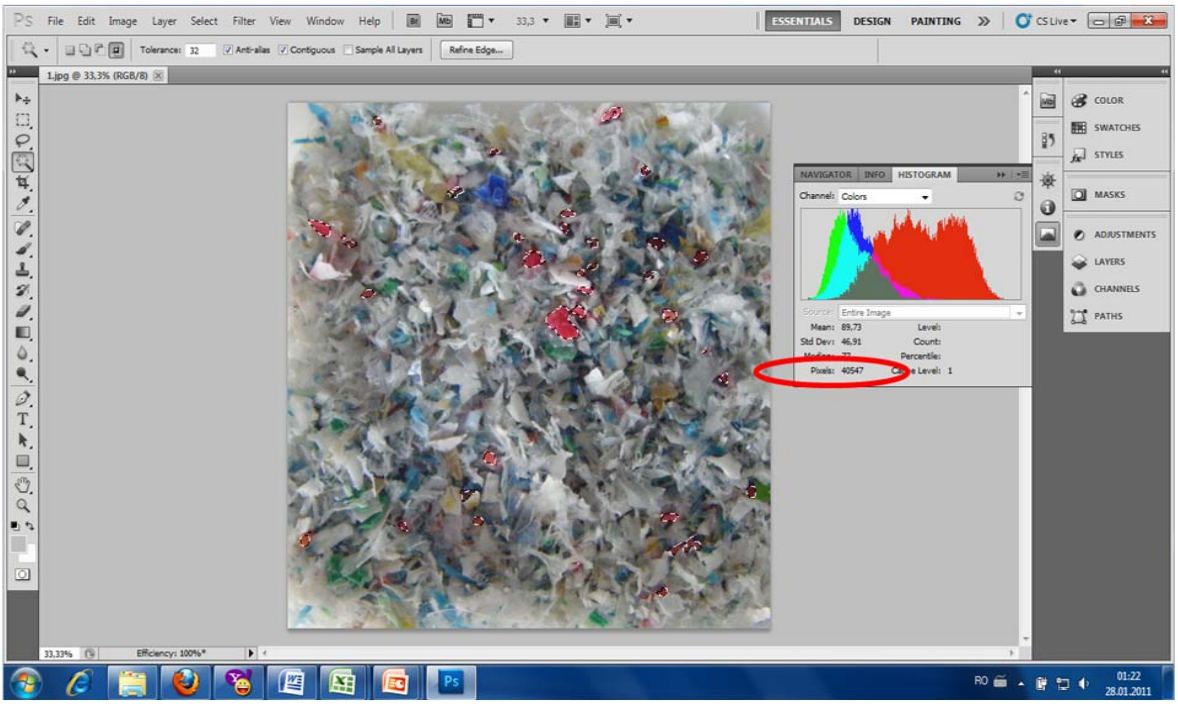

Figure 2.3. Calculation of the pixels corresponding to the chosen colour in Photoshop [16]

As example, table 2.3. present the data obtained for the fraction with density interval: 0.788-0.88 g/cm3 from the Sample 1.

Table 2.3. Percents of coloured polymers from the fraction having the density interval 0.788-0.884 g/cm^3, obtained by separation from the Sample 1 [30]

FTIR index	Colour	Total pixels	Component pixels	%
1	green	323712	5027	1.553
2	light-green		658	0.203
3	blue-indigo		7815	2.414
4	light-blue		13803	4.264
5	blue-transparent		653	0.202
6	transparent/light blue polymeric film		10690	3.302
7	white/grey		34180	10.559
8	red		10840	3.349
9	red/orange light		963	0.297
10	transparent with yellow lines		16542	5.110
11	golden		11300	3.491
12	transparent		190645	58.893
13	white transparent- (soft bag)		4263	1.317
14	yellow pellicle		2556	0.790
15	yellow		2058	0.636
16	light green pellicle/white		3253	1.005
17	white pellicle with bright blue-green lines		4947	1.528
18	white pellicle with red letters		3137	0.969

2.3. Infrared analysis of MSWP fractions from Brasov, Romania

Each coloured type material has been analysed by FTIR spectroscopy by using a Perkin-Elmer BXII Fourier transform infrared spectrometer, equipped with an attenuated total reflectance (ATR) device with a resolution of 4 cm^{-1} in the 4000-600 cm^{-1} interval. To identify the types of polymers from each fraction, Essential FTIR data base has been used.

The identification has been made based on the highest value of the correlation coefficient. Figure 2.4. presents the obtained spectra for the polymers having different colours from the light density fraction coming from the Sample 1.

The obtained spectra have been processed by Essential FTIR data base and the results are presented in table 2.4.

The coefficients of correlation range between 0.91 and 0.989. It is considered them acceptable due to the additives (dyes, pigments, plasticizers, stabilizers) and possible oxidation degree associated to the polymer aging.

Based on the above presented ways of analysis, the composition of all the separated fractions was obtained and it is shown in table 2.5. The identified polymers from each density fraction have been quantified and the percents of these polymers were also included in table 2.5.

It could be noted that the lightest fractions (0.788-0.884g/cm^3, and below) are quantitatively, very low (approx. 0.8% from the wastes) and they are composed by PP and PE. At such low density, only the presence of foam polymers and very thin pellicles, that were stick to the foams particles, could explain the presence of PP and PE in the lightest density fractions. At a more attentive and detailed visual examination of these fractions, foams and thin pellicles have been identified indeed. The heavier density fraction contains seven polymer types (PP, PE, PS, PET, PVC, PA and PC) and some metals traces. Table 2.5. emphasizes the repartition of these polymers in the frame of each density fraction.

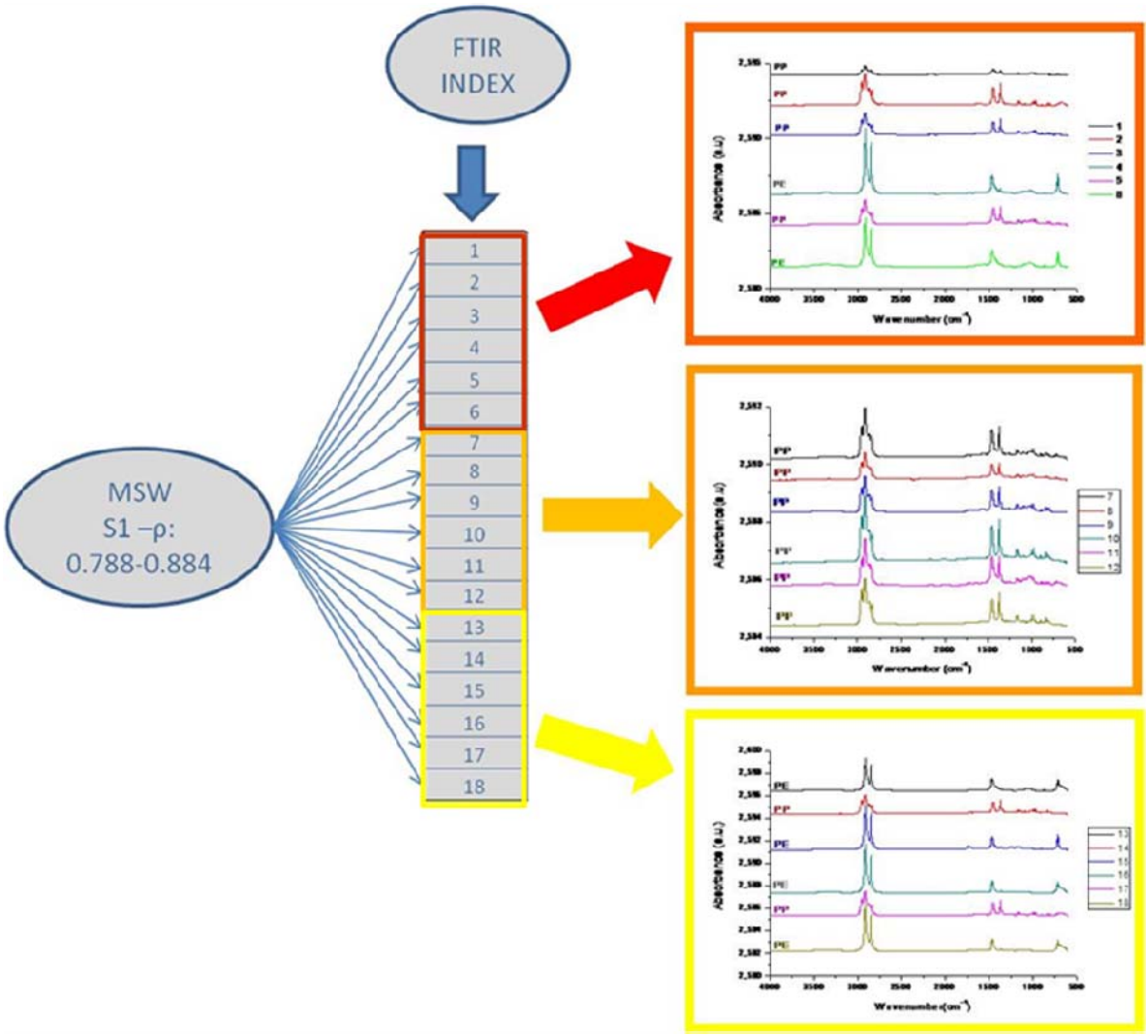

Figure 2.4. FTIR analysis of the identified by colour polymers from the light density fraction of the Sample 1 [30]

Table 2.4. Type of polymers identified by Essential FTIR soft-ware based on the obtained FTIR spectra of each type of coloured polymer from each density fraction [30]

FTIR index	Colour	Total pixels	Component pixels	%	Identified as	Correlation coefficient
1	green		5027	1.553	PP i (Tg=-26)	0.9291
2	light-green		658	0.203	PP i (Tg=-26)	0.9645
3	blue-indigo		7815	2.414	PP i (Tg=-26)	0.91
4	light-blue		13803	4.264	PE (LDPE Mw=50000)	0.9484
5	blue-transparent		653	0.202	PP i (Tg=-26)	0.923
6	transparent/light blue polymeric film		10690	3.302	PE bag	0.9567
7	white/grey		34180	10.559	PP i (Tg=-26)	0.9159
8	red		10840	3.349	PP i (Tg=-26)	0.9651
9	red/orange light		963	0.297	PP i (Tg=-26)	0.9052
10	transparent with		16542	5.110	PP i (Tg=-26)	0.9422

	yellow lines	323712				
11	golden			0.000	PP i (Tg=-26)	0.9194
12	transparent		190645	58.893	PP i (Tg=-26)	0.989
13	white transparent-(soft bag)			0.000	PE bag	0.9227
14	yellow pellicle		2556	0.790	PP i (Tg=-26)	0.9039
15	yellow		2058	0.636	PE (LDPE Mw=50000)	0.941
16	light green pellicle/white		3253	1.005	PE (LDPE Mw=50000)	0.9296
17	white pellicle with bright blue-green lines		4947	1.528	PP i (Tg=-26)	0.9483
18	white pellicle with red letters		3137	0.969	PE (LDPE Mw=50000)	0.9175

Table. 2.5. Repartition of the density fractions in the polymeric wastes selected from MSW Brasov, Romania and repartition of the identified polymers in each fraction. Highlighted fractions are polyolefins [30], [31]

	Δρ g/cm³	**Fraction weight g**	**Fraction percent %**	**Polymer type**	**Polymer percent %**	**Polymer weight g**
ρ1 (MW1)	< 0.788	1.0051	0.022	PE	42.235	0.4245
				PP	56.543	0.5683
ρ2(MW2)	0.788-0.884	36.4899	0.798	PE	10.788	3.9365
				PP	83.891	30.6119
ρ3(MW3)	0.884-0.908	267.1800	5.843	PP	86.997	232.4383
				PE	13.003	34.7414
ρ4(MW4)	0.908-0.923	372.7600	8.152	PP	99.817	372.0786
				PE	0.183	0.6810
ρ5(MW5)	0.923-0.935	258.2300	5.648	PP	76.604	197.8140
				PE	23.396	60.4157
ρ6(MW6)	0.935-0.964	2706.9000	59.201	PP	1.917	51.8832
				PE	95.986	2598.2396
				PS	1.815	49.1356
				Nylon (PA)	0.282	7.6362
ρ7(MW7)	0.964-0.997	114.5300	2.505	PP	38.065	43.5954
				PE	11.995	13.7381
				PS	11.147	12.7669
				PET	2.098	2.4033
				PVC	35.970	41.1960
ρ8(MW8)	0.9974-1.005	39.5568	0.865	PP	15.049	5.9530
				PE	19.411	7.6782
				PS	51.735	20.4648
				PET	3.852	1.5236
				PVC	2.962	1.1717
ρ9(MW9)	1.005-	228.6250	5.000	PE	1.658	3.7904

	1.102			PP	0.090	0.2048
				PS	65.182	149.0212
				PC	5.185	11.8540
				PVC	19.654	44.9335
				PET	3.886	8.8844
				PA	0.269	0.6157
ρ10(MW10)	1.102-1.146	59.1743	1.294	PE	0.102	0.0604
				PP	0.000	0.0000
				PA	1.317	0.7791
				PET	70.133	41.5007
				PS	6.694	3.9609
				PVC	18.755	11.0980
				PC	2.999	1.7745
ρ11(MW11)	1.146-1.197	120.3830	2.633	PC	28.747	34.6061
				PA	0.000	0.0000
				PVC	9.017	10.8554
				PET	59.843	72.0404
				PE	0.016	0.0194
ρ12(MW12)	1.197-1.27	12.6257	0.276	PET	89.404	11.2879
				PA	4.755	0.6003
				PVC	5.703	0.7200
ρ13(MW13)	> 1.27	354.9460	7.763	PET	59.049	209.5921
				PVC	40.889	145.1339
				PA	0.017	0.0603
				metals	0.954	3.3875

By composition analysis of the contaminants fractions from MSWP from Romanian wastes, it could be noted that in fact, the lightest density fraction contains only polyolefins in the foam form or as very thin pellicles. So, the lightest fraction of the MSWP selected from Brasov, could be recycled together with the polyolefinic fractions without the contamination danger (Figure 2.5).

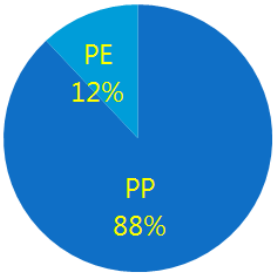

Figure 2.5. Repartition of the polymers from MSWP, from Brasov County, Romania, in the light fraction (MW1-2) [30]

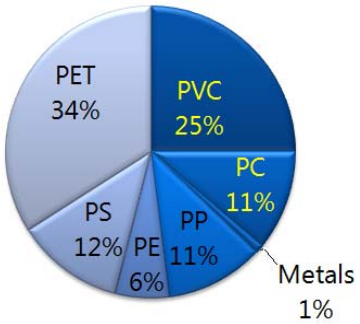

Figure 2.6. The perceptual repartition of the components of the heavier density fraction (MW7-13) [30]

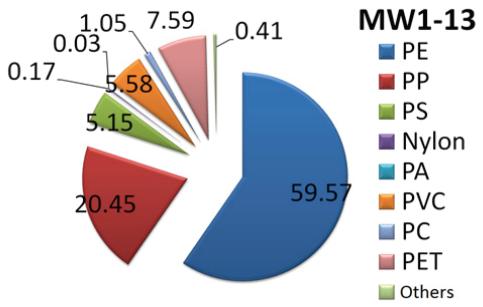

Figure 2.7. Composition of MW1-13 [31]

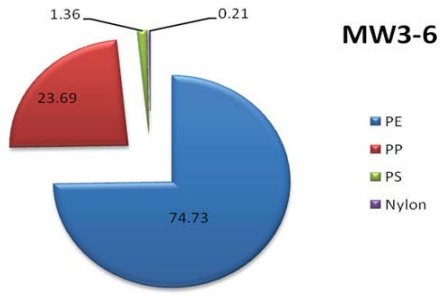

Figure 2.8. Composition of MW3-6 [31]

From Figure 2.6. it could be noted that a higher non-homogeneity characterizes the heavier fraction of Romanian wastes. **It is difficult to recycle this complex polymeric mix, due to the incompatibility of the components.** It also could be noted that PP and PE are present both in lighter and heavier fraction of all the separated wastes: 100% in lighter fraction and 16.5% in the heavier fraction of Romanian MSWP. This means that both PP and PE are used in complex materials such as composites having polyolefins only at the surface. FTIR analysis used in reflection mode gives information only concerning the surface structure. The presence of the other interior layers contributes to the increase of the density of these materials, and as consequence, they have been found in the heavier fraction. Composites with polymeric foams, having PP or PE at the surface, or being their self PP or PE foam, could determine their identification by ATR FTIR only as PE or PP, while their density is lower than those of the pure and compact PP or PE.

This aspect is confirmed by the calorimetric analysis too, results that will be presented a little later.

Generally, the polymers having higher density are characterized by lower calorific power [32], [33]. As PE and PP were found, both in the lighter and heavier fractions of wastes, the calorific power of these fractions will become higher, due to the higher polyolefinic caloric power. So, the incineration of the heavier fraction of MSWP with energy recovery could be taken into account as an alternative to polymeric wastes recycle.

The paper **Microbial safety of plastic materials obtained from wastes** [31]**,** present an antimicrobial comparative study between virgin polyolefins and those considered as secondary raw materials.

Three types of virgin polyolefins (POs) have been used: polypropylene (PP homopolymer trade name Moplen HP400R provided by Basel Polyolefins; MFR 25 g/10 min – at 230°C and 2.16 kg, ρ = 900 kg/m^3), high density polyethylene (HDPE trade name HDPE B5823 provided by Sabic; MFR 0.16 g/10 min – at 190°C and 2.16 kg, ρ = 958 kg/m^3), and low density polyethylene (LDPE trade name Lupolen 3010 D purchased from Lyondell Basel Industries; MFR 0.25 g/10 min – at 190°C and 2.16 kg; ρ = 927 kg/m^3).

Plastic wastes used in this study were collected and selected from Municipal Solid Wastes (MSW) by specialized Urban Enterprise from Brasov, Romania, in September 2010, in the frame of the European Project FP7 W2-Platics and characterized in the preceding paper presented.

Pure polymers and three samples obtained from waste were subsequently frozen and ground in a ZM 2000 centrifugal mill to obtain a homogeneous mixture (0.5-1 mm particles). Then pure polymers were melting mixed in a Brabender extruder at temperatures of 130, 140 or 175°C depending on the nature of the polymers used, at a mixing speed of 60 rpm for 10 minutes. Time of mixing has been chosen at 10 minutes and it was kept constant in all the experiments, aiming to ensure a good homogenization of the melt material, proved in case of

wastes, which particles have different colours, by the uniformity of the sheet colour. For samples obtained from wastes, higher temperatures have been used for melt mixing, because of the complex composition of fractions: 180°C for fractions having higher content of polyolefins and 220°C for fraction with higher content of contaminants. The resulting mixture was then pre-melted for 10 minutes, and pressed in a Carver press at 140, 150 or 180°C for 6 minutes, obtaining sheets of 150x150x1mm (LxWxH).

In all samples only Irganox 1076 (0.5%) has been used as antioxidant.

2.4. Mechanical analysis of materials obtained from virgin and waste polymers [31]

Bone-shaped specimens according to EN ISO 527-1 STAS were mechanically tested using a Zwick Z020 mechanical testing machine, 10 mm/min, according to SR EN ISO 527-12/1996 determining the tensile strength, Young's modulus and relative elongation.

Since practical applications of products made from polymers require a good mechanical strength, tensile tests for both virgin polyolefins and samples made from waste were performed. The results are presented in table 2.6. Note that MW3-6 fraction, predominantly consisting of POs, shows the best strength. The sample is stiffer than virgin polymers; it shows a higher elasticity modulus and a substantially lower relative elongation than polyethylene, but close to that of PP.

This is possible due to the crosslinking between oxidized groups of the components as well as between unsaturated groups (vinyl) formed during life cycle. Tensile strength is close to that of PE, as dominant component of the fraction. Currently products on the market made from composite materials are used on panelling, panels, flooring with similar properties [34]. MW7-13, heavy fraction, considered a contaminant for POs, because of its very complex composition, because of incompatibility of polymers and because of very different degradation and melting temperatures, which does not allow the melting temperatures to ensure homogenization, shows the weakest mechanical properties. MW1-13 un-separated mixture, due to the POs content, shows mechanical properties similar to PE but the relative elongation is much smaller. Mechanical properties obtained for both materials prepared out of MW1-13, but especially those prepared out of MW3-6 encourages their proposal for various practical applications. Good mechanical properties of materials made from wastes are not the only ones that can ensure the development of their practical applications.

Table 2.6. Mechanical properties of virgin POs and wastes fractions [31]

Sample	Young Modulus (MPa)	Tensile strength (MPa)	Elongation (%)
LDPE	261.77	13.23	269.54
HDPE	738.16	25.87	393.41
PP	1153.65	31.63	5.09
MW1-13	587.29	13.60	0.70
MW7-13	1007.73	6.72	0.29
MW3-6	1466.77	18.15	1.10

2.5. Determination of material crystallinity of materials obtained from virgin and waste polymers [31]

All measurements were performed using equipment from Perkin Elmer Diamond DSC in an inert atmosphere (N_2) from 0ºC to 300ºC with a heating rate of 10°C/min, 10-15 mg of the sample were closed in an aluminium capsule. In all cases, there were two heating cycles, the first cycle aimed at removing the influence of heat treatments on materials and consequently on their properties. X-ray diffraction (Bruker-AXSD8 Advance Cukα1, λ=154016Å, 2θ = 10 ÷ 600) by

which both absolute crystallinity of the material analyzed and the presence of other crystalline substances (additives) was determined.

All the significant 2θ crystalline peaks have been taken into account according to Eq. (2.1.):

$$\chi_{XRD} = \frac{\sum A_c}{\sum A_c + \sum A_a} \quad (2.1.)$$

where:
χ_{XRD} - is the total crystallinity of the sample,
Ac – crystalline peak area,
Aa – amorphous peak area.

DSC method by which the crystallinity index was calculated by dividing the melting enthalpy of the mixture to the enthalpy of the 100% crystalline polymer as given by Eq. (2.2.) [35]:

$$\chi_{DSC} = \sum_{i-1}^{n} \frac{\Delta H_{mi}}{\Delta H_{mi}^{0}} a_i \quad (2.2.)$$

where:
ΔH_{mi} is the melting enthalpy of *i* component from the mixture,
ΔH_{mi}^{0} is the melting enthalpy of *i* component 100 % crystalline,
a_i is the percent in which the polymeric *i* component is present in the mixture.

By DSC measurements it was obtained a higher crystallinity index in the case of virgin polymers: HDPE (69.72%), PP (42.02%) and LDPE (36.77%) than in the case of waste based materials. The fraction containing the most POs, MW3-6, has the highest crystallinity index (29.11%) while the waste undivided into fractions reveals a lower crystallinity index of 15.39%. For the contaminant fraction, by DSC, it was impossible to determine this feature, as the thermogram highlighted predominantly amorphous character.

The same issues can also be highlighted by X-ray diffraction which determines the total crystallinity of samples (including inorganic additives). Thus, according to XRD analysis, in the case of wastes, the highest crystallinity was obtained for fraction MW3-6 (76.91%) and the lowest for the sample obtained from contaminant fraction MW7-13 (50.88%).

2.6. Determination of contact angle of materials obtained from virgin and waste polymers [31]

Measurements were made with type SCA20 goniometer (Data Physics Instruments) and its software. The software enables the calculation of the contact angle formed between the tangent to the circle that describes the outline of the droplet and the surface of the material to be analysed, thereby determining the wetting ability of the liquid used in the analysis. Test liquids used were water, glycerine and 1-Br-naphthalene. Values of surface tension and polar and dispersive components are found in the literature [36].

Measurements were performed in at least five different points, for each fluid, and the average value was reported. During the tests, the volume of the droplet was kept constant at 10 μl, and the contact angle was recorded immediately after the droplet felt on the analysed surface. Also the surface free energy of materials obtained was determined, based on the relationship

developed by Owens, Wendt, Rabel and Kaelble [37], [38], [39], (Eq. 2.3.), which took into account dispersive (d) and polar (p) components (Eq. 2.4.) of the surface tension γ [40].

$$\gamma_{SL} = \gamma_{SV} + \gamma_{LV} - 2\left(\sqrt{\gamma_{SV}^{d}\gamma_{LV}^{d}} + \sqrt{\gamma_{SV}^{p}\gamma_{LV}^{p}}\right)$$

$$\gamma_i = \gamma_i^d + \gamma_i^p$$

(2.3.), (2.4.)

In Eqs. (3, 4) the symbols and notations have the following meanings:

γ_i - is the surface tension at the interface liquid-solid (solid/vapours or liquid/ vapours).

It has two components:

γ_i^d - representing dispersive component of the surface tension

γ_i^p - that represents the polar component of the surface tension.

Due to the influence of the surface electric charge on the bacteria adhesion and colonizing, the surface energy of the samples has been calculated also by using the Lifshitz-van der Waals and Lewis Acid-Base (LW/AB) approach, with the help of the instrument's software. According to this approach, the surface energy (γ) is decomposed into a Lifshitzvan der Waals (γ^{LW}) dispersive component as well as into a polar component - γ^p - with Lewis acid (γ^{p+}) and Lewis base (γ^{p-}) contributions respectively (Eq.2.5.) [41].

$$\gamma = \gamma^{LW} + \gamma^{p} = \gamma^{LW} + 2\sqrt{\gamma^{p+} \cdot \gamma^{p-}}$$

(2.5.)

The initial contact angle θ_0, which is the contact angle at the beginning of wetting process (for $t = 0$) for the test liquids was used in the calculation of surface energy.

Using experimental values of the contact angle one may calculate the surface energy of the samples. Thus, it was determined that LDPE and HDPE have similar values of surface energy (38.13 and 38.28 mN/m, respectively) while PP shows a lower value (36.29 mN/m), which demonstrates a more pronounced hydrophobic PP. In all cases, the dispersive component is dominating (85-90%).

In the case of waste, there is a noticeable decrease in surface energy: MW3-6=17.8 mN/m, MW1-13 = 23.5 mN/m and MW7-13 = 26.5 mN/m. These values show a more pronounced hydrophobic behaviour than virgin POs, probably due to crosslinking or to elimination of polar groups obtained either by photo-oxidation occurring during the life cycle or due to thermal reprocessing. Dispersive component remains dominating (75-85%) but decreases compared to materials obtained from virgin polymer in favour of the polar component. The resulted values show a more pronounced decrease of surface energy as the content of the POs increases. This happens due to prevailing thermal degradation of POs through mechanisms similar to Norish I which consists of the elimination of CO or their crosslinking. In general, hydrophobic bacteria better adhere to hydrophobic surfaces. However, tests show that the hydrophobicity of material's surface plays the most important role in bacterial adhesion by comparing to the bacterial surface hydrophobicity [42].

Considering the obtained results, materials prepared from wastes (more hydrophobic) should favor bacterial growth compared to those obtained from virgin polymers (more hydrophilic). In the same time, it was determined that Gram negative bacteria (such as *E. coli*) are more hydrophilic then Gram positive bacteria [43].

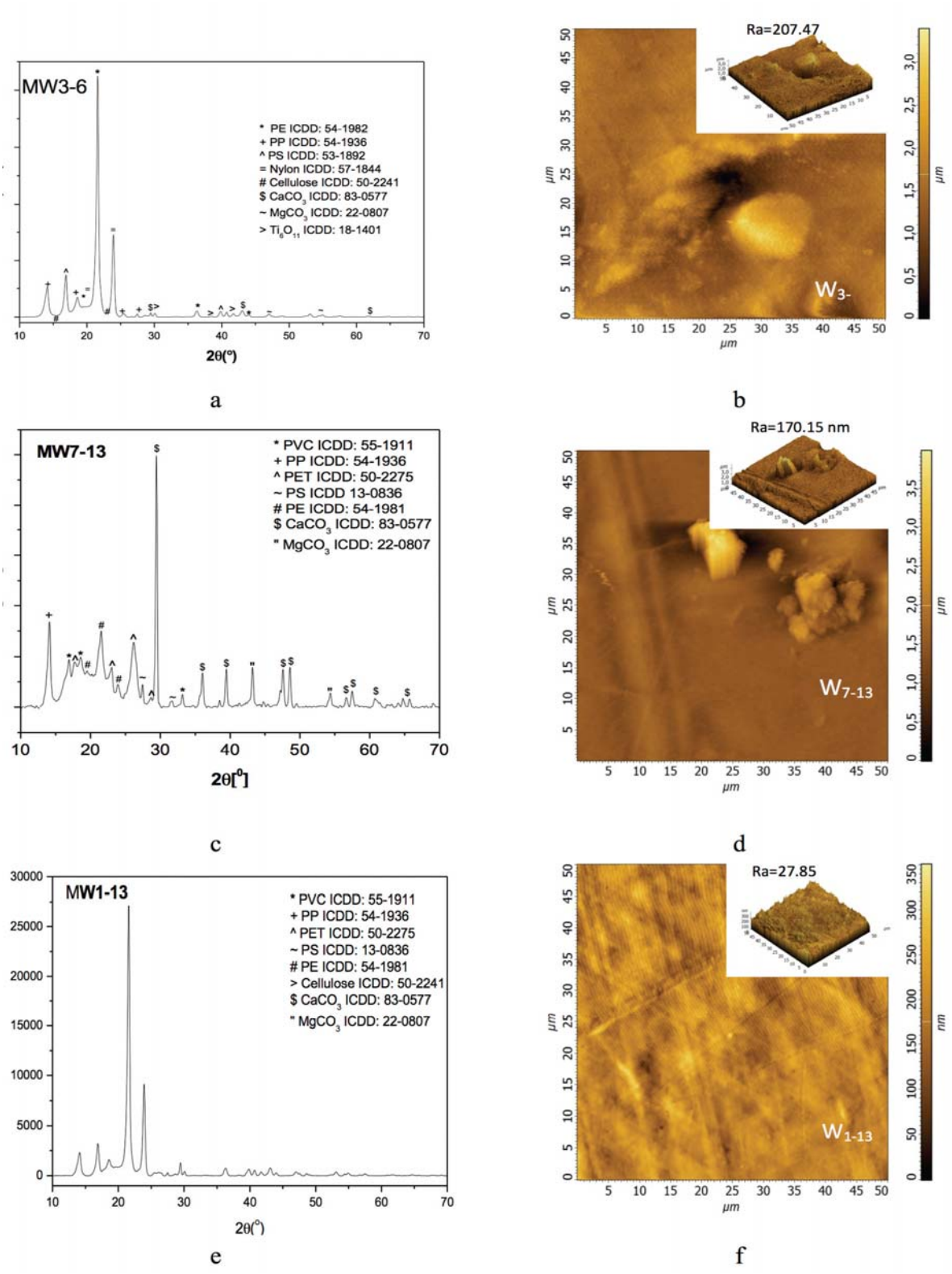

Figure 2.9. XRD and AFM characteristics of the waste based materials (a) and b) for MW3-6 fractions, c) and D) for MW7-13, e) and F) for MW1-13) [31]

So, they better adhere on more hydrophilic surfaces, in our case, on HDPE samples. By using the Lifshitz-van der Waals and Lewis Acid-Base (LW / AB) approach one may determine the surface electric charge of the material.

The obtained values for Lewis base components (γ^-) are dominating compared to Lewis acid components (γ^+) and vary depending on the composition of materials obtained from wastes as follows: MW1-13 = 3.42 mN/m; MW7-13 = 7.43 mN/m and MW3-6 = 16.49 mN/m. Note that the surface of materials is predominantly negatively charged. This reduces the ability of negatively charged bacteria to adhere to the surface of materials even if their hydrophobic behaviour is emphasized. Taking into account that bacteria preferentially adhere and colonize porous surfaces [42] it was determined the roughness of samples obtained from polymeric waste included in the study.

2.7. Determination of roughness by Atomic Force Microscopy of materials obtained from virgin and waste polymers

Surface morphology was studied in semi contact mode using atomic force microscope Scanning Probe Microscope Solver PRO-M, NTMDT, with scan sensor cantilever type NSG 10-Au (features: 3.4 X1, 6x0, 3 mm cuboidal body sensor tip (L) 95 x (W) 30 x (T) 2 mm, with 240 kHz resonance frequency and force constant 11.8 N/m). The analysis was conducted under laboratory conditions 25°C air temperature, and the images obtained were processed using the software on the device, aiming to determine the roughness of studied surface.

AFM measurements of roughness reveal average values for virgin POs (ie 87.2063 nm for PP), higher values for MW3-6 fractions (207.47 nm) and MW7-13 fractions (170.15 nm) and lower values for fractions MW1-13 (27.85 nm). According to previous studies reported in the literature [42], more pronounced roughness increases the contact surface with the medium favouring bacterial growth. However, if the conformation of roughness does not dimensionally fit the characteristics of bacteria then it reduces the contact surface of bacteria with the material and their adhesion is hindered (figure 2.9.).

2.8. Qualitative determination of water vapours adsorption from the atmosphere of materials obtained from virgin and waste polymers

Qualitative assessment of adsorption of water vapours from the atmosphere on analyzed samples was performed by determining the difference between the absorption bands areas of OH groups (3400 cm^{-1}) from FTIR spectra corresponding to samples conditioned in laboratory atmosphere and those conditioned in a $CaCl_2$ desiccator.

POs are by definition hydrophobic materials, however FTIR spectroscopy has shown that virgin POs undergoes minor thermal oxidation during processing, that leads to the formation of polar groups OH (υ = 3400 cm^{-1}) and C = O (υ = 1510- 1800 cm^{-1}) (figure 2.10.) [44].

These favour adsorption of water vapours from the atmosphere on the samples surface. After performing ATR FTIR analysis on samples maintained in laboratory atmosphere (humidity 45 ± 5%, temperature 25 ± 2°C) and on samples conditioned at 25°C in desiccator with CaCl2, one may observe a change in the intensity (area) of absorption band from 3400 cm^{-1} (Table 2.7.).

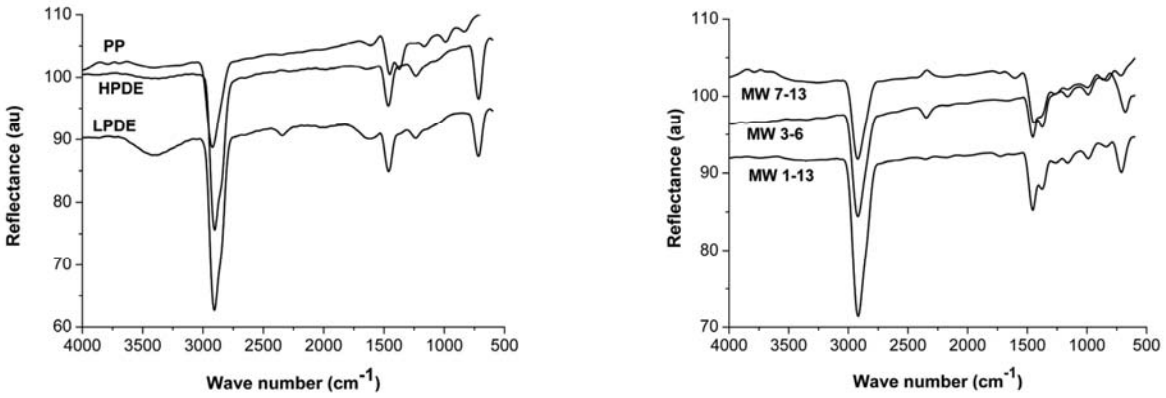

Figure 2.10. FTIR ATR spectra for virgin PO and for tested waste fractions [31]

Adsorption of water vapors at the surface may promote further growth of bacteria. From Table 2 it could be also noted that HI for wastes based materials is in the same range of magnitude with POs' HI. CI is much smaller than that of virgin POs suggesting a thermal degradation of wastes based materials during the thermal processing that follows a mechanism similar to Norish I.

Table 2.7. Area of the absorption bands characteristic for OH and C=O groups, hydroxyl index and carbonyl index of materials based on virgin POs and wastes [31]

Sample	A_{OH} (au)		HI	ΔA_{OH} (au)	$A_{C=O}$ (au)	CI
	A_{lab}*	A_{dry}**				
LDPE	210	150	0.17	60	1265	2.14
HDPE	300	290	0.3	10	410	2.26
PP	160	150	0.04	10	233	0.55
MW1-13	170	-	0.11	-	160	0.10
MW7-13	302	-	0.22	-	252	0.18
MW3-6	136	-	0.23	-	84	0.14

This statement is sustained also by comparing the determined average carbonyl index of MW1-13 before (0.72) and after thermal processing (0.1). The decrease of carbonyl groups number after thermal processing is due to the CO release (similar to Norish I photo-degradation mechanism).

These results are in good agreement with those recently reported by Gardette et al. [45] that show that both photo and thermal oxidation of polyolefins lead to the same products, only the relative concentrations of these products are dramatically different in the two processes.

2.9. Determination of adsorption of water at samples immersion

Of each type of composite, cylindrical samples (dxh: 10x1 mm) were cut using a perforating
punch. These samples were conditioned in an oven at 80°C for 24 hours and then were weighed (m), considering the sample at time t0 (all calculations of adsorption of water will relate to this value). Each sample was immersed in 20 ml of distilled water and weighed using analytical balance at determined period after the excess water was removed from the sample's surface. Using recorded data, the percentage of water retained (*S*) by each sample was calculated, according to Eq. (2.6.):

$$S = \frac{m_s - m}{m} * 100 \quad (2.6.)$$

where:
m_s - is the sample's mass at a defined immersion time (g),
m- is the initial mass of the sample (g).

Changes in polarity and crystallinity of materials also influence sorption of water during material's immersion. The small amounts of water adsorption (0.1-2.38%) are characteristic to hydrophobic and highly crystalline materials. This aspect highlights the reduced possibility of polymer structure swelling by adsorption of water and thus the reduced release of antibacterial agents from the polymer matrix during the life cycle, respectively during washing and separation by flotation method.

This argument is in favor of maintaining antibacterial agents in the material for a long time, even after it became waste. The high crystallinity obtained for waste materials is consistent with the low values of their water adsorption (0.89-2.38%) and suggests the minimum possibility of releasing the antimicrobial agents from their structure.

2.10. Microbiological tests

To determine the surface contamination of analysed samples, three types of tests were conducted [31]:

- Swab Check test allows qualitative determination of total bacterial contamination.

Microbiological tested surface is wiped with a cellulose buffer. Thus, any bacterium is transferred through the buffer in a special medium that contains a dye indicator. The tube is subjected to incubation at 37°C for 24h. A single bacterium is sufficient to cause a colour change. This means that SwabCheck is about 1000 times more sensitive than conventional adenosine triphosphate ATP method. The benefits of the SwabCheck test are that it is sterile, packaged and ready for use. It is also easy to handle, provides fast results and has a long life. SwabCheck is used as an indicator of hygiene for different surfaces. Colour change from red to yellow indicates a microbiological contamination. The change in colour is based on the reaction of the acid from the medium composition with the pointer. A quick change in color indicates high levels of bacteria in the tested sample. SwabCheck is useful in determining levels of sanitation of surfaces in areas of food processing, beverage, dairy factories, restaurants, hospitals, microbiology laboratories etc.

- Contact plates tests allow determination of the total number of germs (NTG) and the number of *Enterococci* from the surface of the analysed material. Contact plates are provided on each side with a slide containing culture medium. Slides are placed in plastic tubes, fitted with a lid.

The medium on one side is Plate Count Agar, orange, to determine the total number of germs, and on the other side is VRBG Agar (Violet Red Bile Glucose) Agar, red, for determining *Enterococci* (figure 2.11.). Bacteria and fungi on tested surfaces are put on slides surface. The tubes where the blades are inserted are subject to incubation for 24-48 hours, and the results are compared with images of the diagrams in figure 2.12. Results are expressed in CFU/cm^2. The slides are compared to charts after 24 hours, reintroduced in the incubator and compared again after other 24 hours.

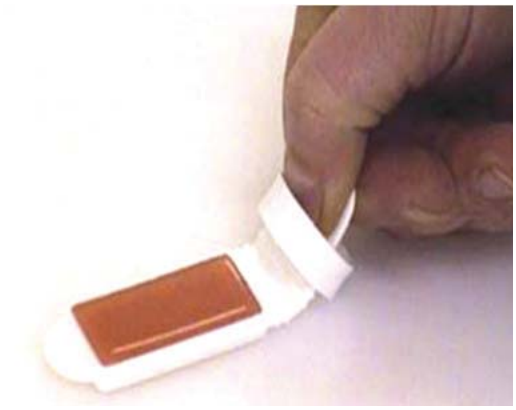

Figure 2.11. Contact plates tests [31]

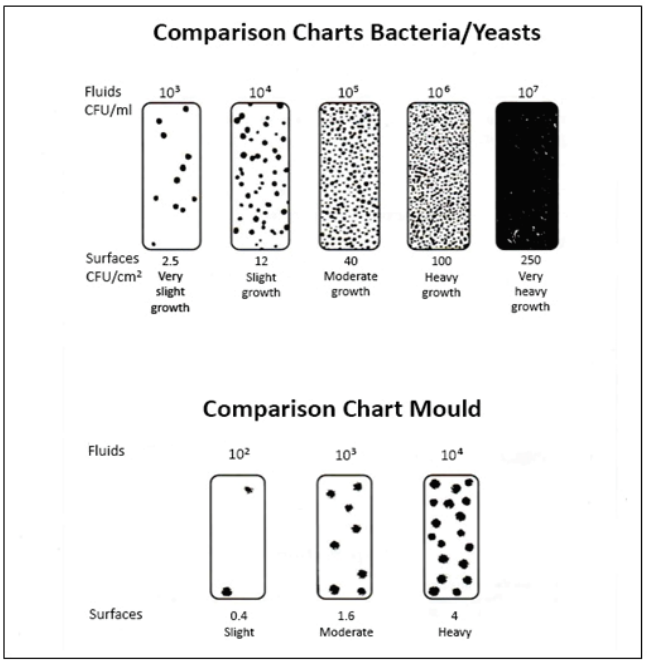

Figure 2.12. Comparison charts bacteria (Dipslides for industrial and Environmental Monitoring of Bacteria and Fungi, Prospect, VWR International GmbH, Wien, Austria) [31]

Each polymer sample was brought in contact with both sides of the plate. The plates were placed in plastic tubes and then were subjected to incubation at 37°C for 24 and 48 hours respectively, after which they were compared as in figure 2.12.

- *E. coli* test determines quantitatively the number of colonies of *E. coli* developed over the surface. This test uses a reference stock culture to obtain pure populations of individual microorganisms with known and predictable growing demands, with selective and differential properties, with biochemical or phenotypic activity, serological, response tests, known antimicrobial susceptibility features that are reproducible to authentic reference cultures.

a) Achieving primary culture

Kwik-STIK *E. coli* ATCC 25922 units was left open at room temperature for thermal equilibration. Kwik-STIK unit is removed and stuck to the primary agar plate for identification. The gelatine tablet is positioned at the bottom of the device and the hydrating fluid reservoir is positioned on top of the device. The hydration fluid is released and then immediately the inoculation material is transferred on the agar medium with nonselective growth (primary culture). The inoculated area is stroke off 10-20 times with a sterile loop and then the rest of the agar surface is stroke off to obtain isolated colonies. The medium is immediately incubated, which determines the selection of representative well insulated colonies, to be used for transfers in Petri plates where the polymer samples will be applied.

b) Achieving the secondary culture

On the seventh day since processing references strain for obtaining primary culture, a test culture in nonselective agar medium is prepared: representative, well isolated colonies from primary culture are harvested with a sterile loop and are dispersed on the medium, inoculating a circular area with a diameter of 25 mm and then stroke off 10-20 times the inoculated area to get isolated colonies. The subculture is then incubated for 24 hours at 37°C.

c) Inoculation

The previously obtained subculture is used for seeding the Petri plates in which SOY AGAR Tryptone medium was previously introduced. Seeding was done as follows: lactose-positive bacteria colonies, which were previously heated at 37°C for 2 hours, are inoculated on plates with a flamed loop. A sample of polymer was placed in each Petri box. They were incubated for 24 h at 37°C. After incubation results were evaluated by determining the number of colonies developed.

Tests applied to bacterial growth on the surface of studied materials led to the results shown in table 2.8.

Table 2.8. Results of microbiologic test [31]

Sample	Swabcheck	NTG (CFU/cm^2)*	Enterococci (CFU/cm^2)	E. coli (CFU/cm^2)
LDPE	-	0	0	0
HDPE	+	4	0	1(around the sample)
PP	-	1	0	0
MW1-13	-	0	0	0
MW7-13	-	0	0	0
MW3-6	-	0	0	0

Significant images of the microbiological tests are presented in figure 2.13. Higher resistance of materials obtained from waste to bacterial growth can be explained by the fact that while sheet samples made from virgin POs were obtained in the laboratory without supplementary additives than antioxidant, materials obtained from waste may also contain antibacterial (nisin, naftamicyn) or bacteriostatic substances, used in the initial processing, especially for food packaging, which still retain their activity after one product life cycle. Antibacterial substances are generally added in a small amount and that makes them undetectable by FTIR spectroscopy. Also, a number of dyes (methylene blue, Blue Toluidines A) and pigments (ZnO and TiO_2) used to develop packaging, may have antimicrobial behaviour and impart this behaviour to polymeric waste that contains them. Both in the heavy fraction MW7-13 and in the un-separated waste, PVC has been identified. Its presence and possible degradation during the life cycle can generate HCl or chlorine based compounds showing antibacterial nature. The "others" category highlighted of plastic waste composition (figures 2.5. and 2.6.) may also include acrylic esters commonly used as adhesives for labels.
They are also known as antibacterial substances. Thus, small amounts of antimicrobial agents coming from different antimicrobial packaging may exercise their character, even synergistically in materials obtained from waste. Also, increased stiffness of materials coming from waste (a high Young's modulus) determines the impossibility of multiplying bacteria initially attracted by the rough surface, because of hindering their elongation as essential step in cell division [46].

The high crystallinity obtained for waste materials is consistent with the low values of their water adsorption (0.89-2.38%) and suggests the minimum possibility of releasing the antimicrobial agents from their structure.

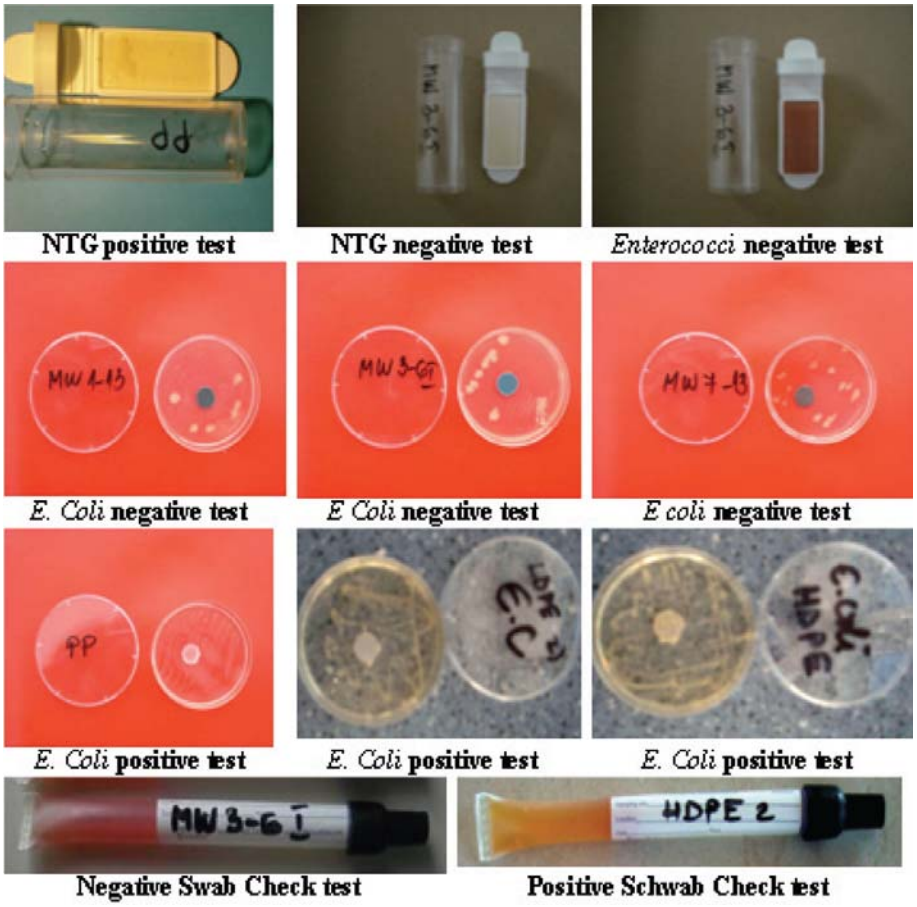

Figure 2.13. Significant images of microbiology tests [31]

2.11. Measuring of heat of combustion (calorific value) of polymers

The equipments used in the paper **Investigation on Energy Density of Plastic Waste Materials** for the energy density tests were: XRY-1C Oxygen bomb calorimeter, XRY-1C software and Kern & Sohn ABJ 220-4M analytical balance. Because the tested material is a fuel, the energy density measurement means the determination of the heat of combustion. The gross calorific value at constant volume (higher heating value or gross energy or upper heating value or higher calorific value) is the absolute value of the specific energy of combustion, in Joules, for unit mass of a solid recovered fuel burned in oxygen in a calorimetric bomb under the conditions specified. The products of combustion are assumed to consist of gaseous oxygen, nitrogen, carbon dioxide and sulphur dioxide, of liquid water (in equilibrium with its vapour) saturated with carbon dioxide under the conditions of the bomb reaction, and of solid ash, all at the reference temperature. (W2Plastics/D41) [16].

The net calorific value at constant volume (lower calorific value) is the absolute value of the specific energy of combustion, in Joules, for unit mass of a solid recovered fuel burned in oxygen under conditions of constant volume and such that all the water of the reaction products remains as water vapour (in a hypothetical state at 0.1 MPa), the other products being, as for the gross calorific value, all at the reference temperature.

The calorific value as determined in an oxygen bomb calorimeter is measured by a substitution procedure in which the heat obtained from the sample is compared with the heat obtained from combustion of a similar amount of benzoic acid whose calorific value is known.

These measurements are obtained by burning a representative sample in a high-pressure oxygen atmosphere within a metal pressure vessel - called a bomb. The energy released by this combustion is absorbed within the calorimeter and the resulting temperature change within the absorbing medium is noted. The calorific value of the sample is then calculated by multiplying the temperature rise in the calorimeter by a previously determined energy equivalent determined from previous tests with a standardizing material. With the bomb calorimeter is measured the gross calorific value [47], [48], [49].

The tested polymeric wastes come from three sources: Urban Enterprise, Brasov County, Romania, automotive shredder facility from Austria and building and construction sector from France.

MSW was washed, cut and separated in two kinds of samples. First sample has been frozen in liquid nitrogen and then cut in the frozen state with Retsch ZM200, centrifugal mill. This sample contains a mix of polymers wastes. The second sample was separated in 4 density categories: $\rho<0.88$ g/cm3; $0.88<\rho<0.965$ g/cm3; $0.965<\rho<0.998$ g/cm3 and $\rho>0.998$ g/cm3. After separation and exclusion of the polyolefins fraction ($0.88<\rho<0.965$ g/cm3) the samples were frozen and cut.

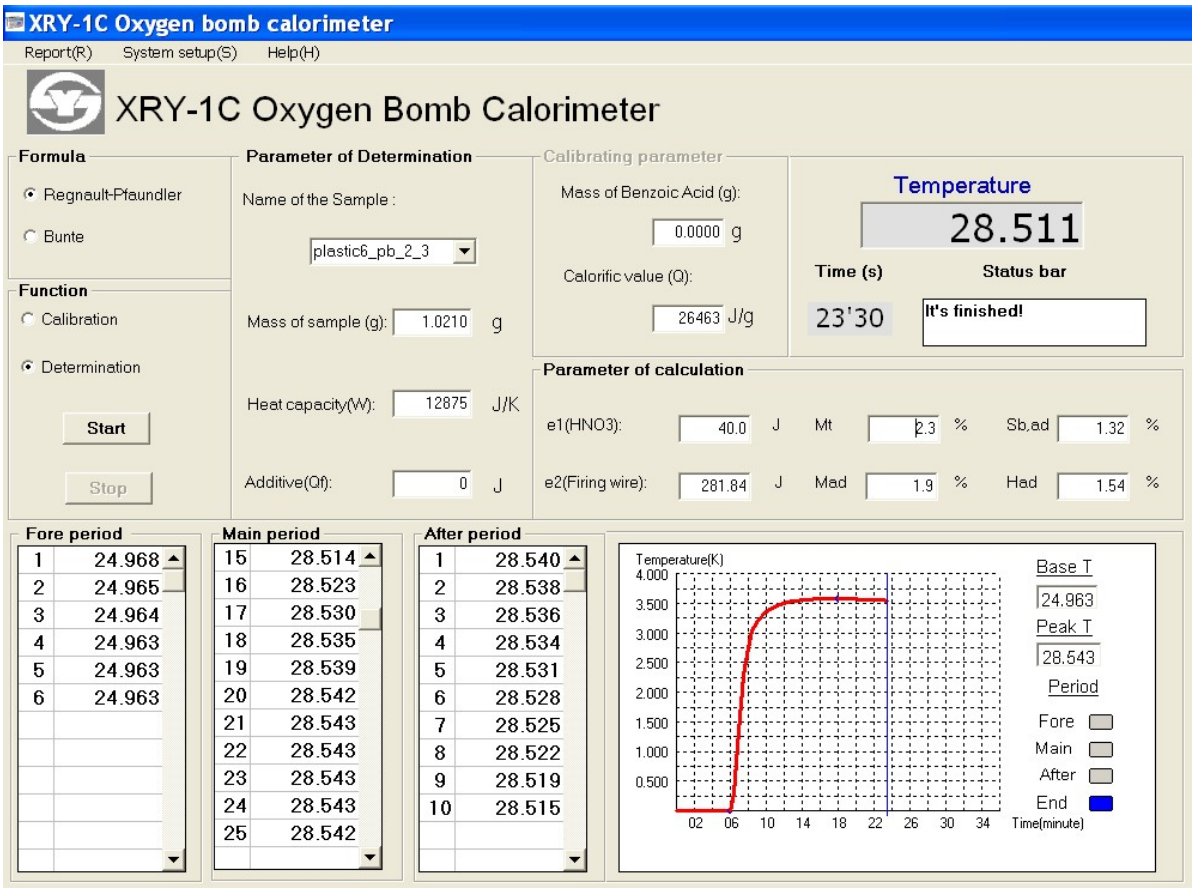

Figure 2.14. The XRY-1C software result of the Romanian MSW after extraction of polyolefins, density $\rho < 0.88$ g/cm^3 [50]

Because were received only the light fraction (after flotation in water) of the ASR and B&CW, the tests were performed only on the fraction with $\rho<0.998$ g/cm3, including polyolefins, and on density categories having $\rho<0.88$ g/cm3; $0.965<\rho<0.998$ g/cm3, without polyolefins fraction.

Before determinations of the calorific value of samples, it is necessary to do the calibration of oxygen bomb calorimeter. This consists in a reverse procedure. Having the heat of combustion of benzoic acid as 26435 J/g, it is determined by the same kind of test the thermal capacitance of the calorimeter, W, burning in crucible the benzoic acid and knowing its mass. For each sample, in the XRY-1C software there were introduced the input data: the mass of ignition wire in grams; the mass of cotton fuse in grams; the calorific value of wire [J/g]; the calorific value of cotton [J/g] and the mass of test sample in grams. After burning the software plotted the graph temperature-time (figure 2.14.) and calculates the gross calorific value.

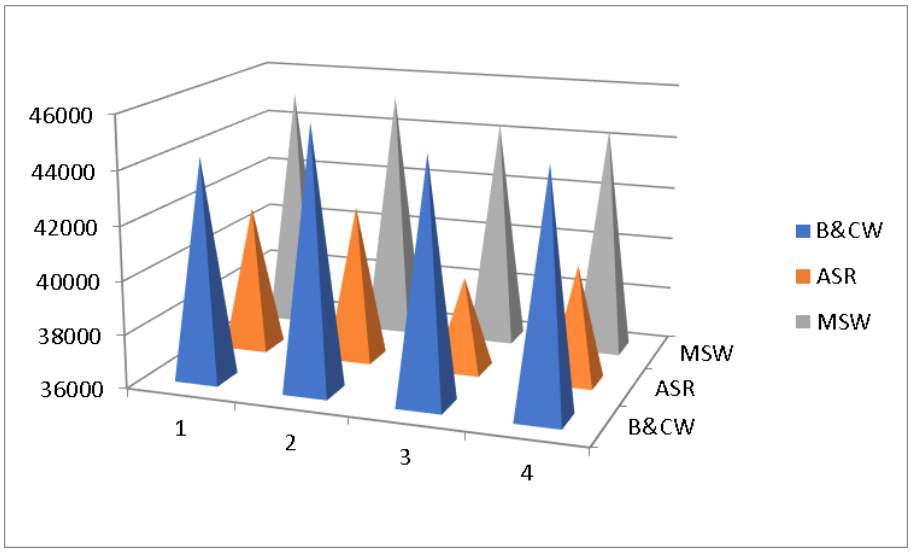

Figure 2.15. Gross calorific value [J/g] of the B&CW France, ASR Austria and MSW Romania before extraction of polyolefins [50]

The results obtained for mixed plastic waste were recorded for Qb,ad – burning calorific value, adiabatic, qs = Qgr,ad - gross calorific value, adiabatic and Qnet,ad - net calorific value, adiabatic. Also the results of calorimetric analysis of residues (after extraction of polyolefins) were noted.

Diagrams have been drawn according to the Qgr,ad - gross calorific value, adiabatic.

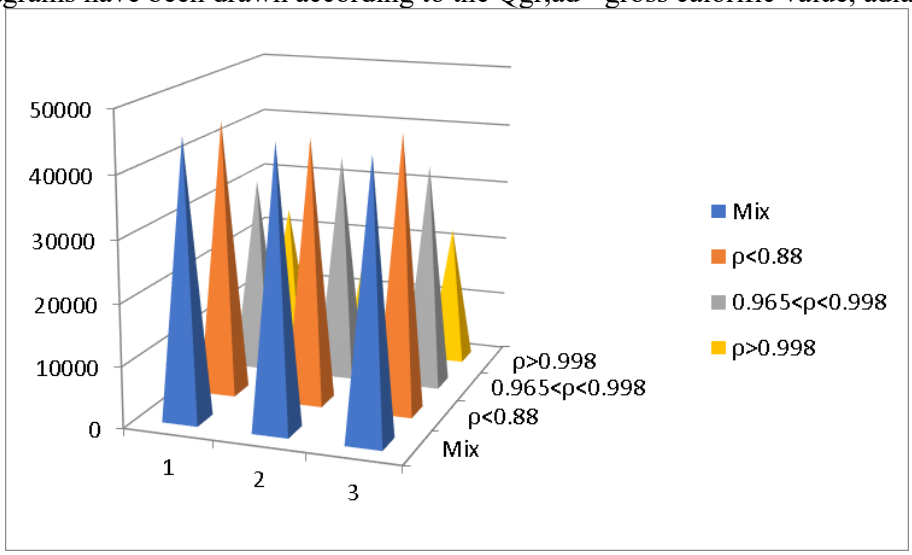

Figure 2.16. Gross calorific value [J/g] of the Romanian MSW before and after extraction of polyolefins (ρ is density measured in g/cm^3) [50]

Figure 2.15. presents the gross calorific value [J/g] of the B&CW France, ASR Austria and MSW Romania before extraction of polyolefins.

It can be observed a small variation of gross calorific value, even the B&CW France and ASR Austria samples don't contain the heavy fraction, $\rho>0.998$ g/cm^3.

From figure 2.16. it could be seen that the calorific power of the MSW from Romania decreases with the increase of the fraction density. This result is in agreement with the data from the literature, as it could be seen in table 2.9., according to the composition change of the fractions.

Because the calorific power of polyolefins is higher than those of other polymers, the extraction of polyolefins decreases the calorific power of the residues.

Table 2.9. Calorific power of some polymers and fuels

Polymer type	Calorific power (MJ/kg)	Ref.
Polyethylene (PP)	46.40	[51]
	45.80	[33]
Polypropylene (PE)	46.30	[51]
	47.74	[33]
Polystyrene (PS)	41.40	[51]
Polyvinyl Chloride (PVC)	18.00	[51]
Poly Ethylene Terephtalate (PET)	24.13	[51]
Poly carbonate bisphenol A (PC)	31.53	[51]
Wood, Dry. Average	20.00	[51]
Unsaturated Polyester	26.00	[51]
Epoxy Novolac, catalytic cure (phenoxy-N) [028064-14-4]	31.70	[33]
ABS	39.84	[33]

From figure 2.17. it could be noted that low density fraction has a lower calorific power, but the differences are quite small, around 12%. The calorific power of the mix is higher than calorific power of light fraction with 25% and higher than calorific power of heavy fraction with 15%.

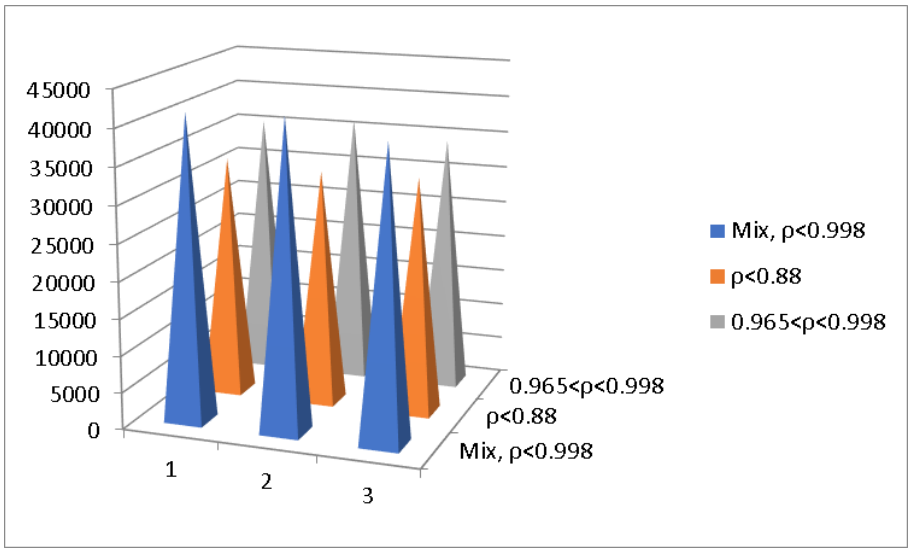

Figure 2.17. Gross calorific value [J/g] of the Austrian ASR before and after extraction of polyolefins (ρ is density measured in g/cm^3) [50]

Figure 2.18. shows the decrease of the calorific power with the increase of the fraction density, according to the literature data. The calorific power of the mix is higher than calorific power of light fraction with 10% and higher than calorific power of heavy fraction with 15%.

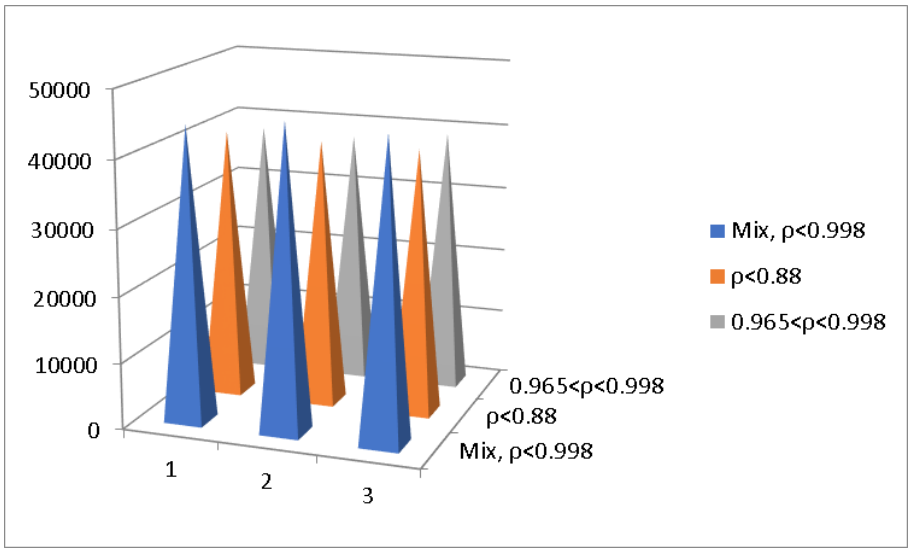

Figure 2.18. Gross calorific value [J/g] of the French B&CW before and after extraction of polyolefins (ρ is density measured in g/cm^3) [50]

From figure 2.19 it could be noted that for the lighter fraction, the calorific power for wastes coming from household is the highest, then follows that of the B&CW and the ASR exhibits the lowest value. The decrease of the calorific power of MSW is with 9% by comparing with that of B&CW and with 27% by comparing to ASR.

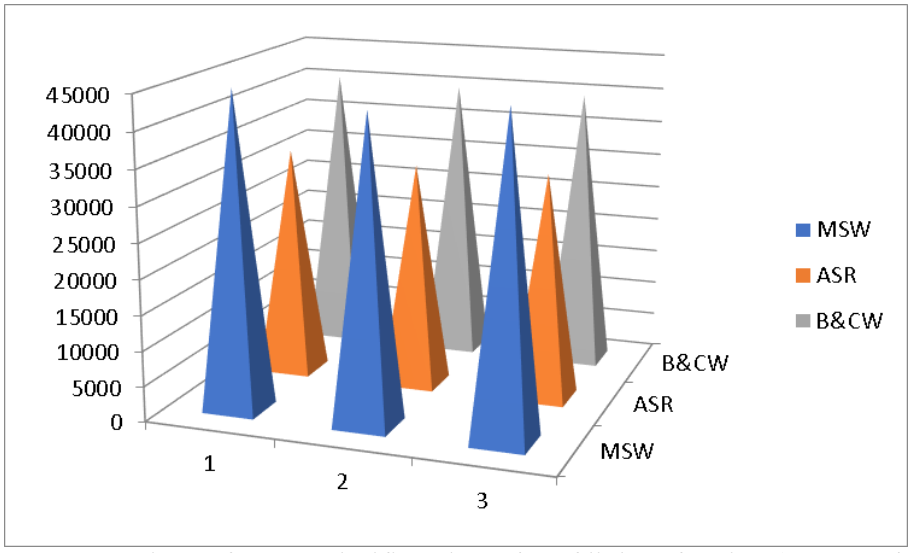

Figure 2.19. Comparison of gross calorific value [J/g] of lighter fraction (ρ<0.88 g/cm^3) [50]

Figure 2.20. shows that in case of heavier fractions the decrease of the calorific power of ASR and MSW is approximately with 8.5% by comparing to that of B&CW. It could be noted, by comparing figures 2.18 and 2.19, that the variation of the calorific power of different fractions of wastes is higher in case of the lighter fraction and lower in case of heavier fractions.

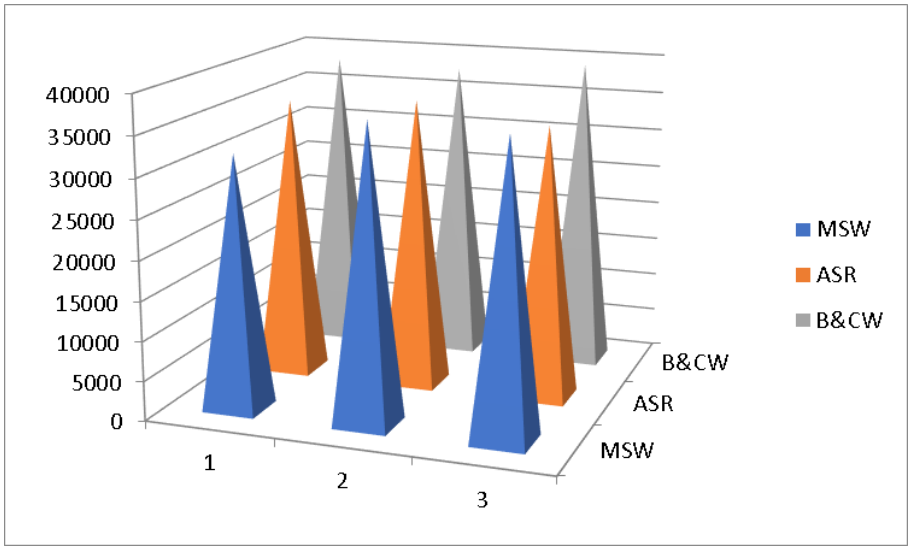

Figure 2.20. Comparison of gross calorific value [J/g] of heavier fraction ($0.965<\rho<0.998$ g/cm^3) [50]

After polyolefins characterization as secondary raw materials some conclusions have been highlighted.

2.12. Conclusions

Limits of the separation possibilities of polymers, based on their density differences, have been evidenced. Both lighter and heavier fractions, out of the interval of 0.8848 and 0.964 g/cm^3, contain polyolefins. They could be thin films or foams in lighter fraction or composite materials in heavier fractions. Also limits in the polymers identification possibilities were found: composite materials could be analysed only at the surface while the internal composition and structure could be different. Polyolefins separated in the range of 0.8848 and 0.964 g/cm^3 could be recycled together with lighter fraction without contamination danger. The heavier fraction has a complex composition, still containing PE and PP and could be used for energy recovery from polymeric wastes by incineration.

These results evidenced multiple and complex problems that have to be taken into account in both wastes separation, analysis and results interpretation, highlighting the difficulties of the recycling of polymeric wastes.

The surface of materials obtained from polymeric wastes by melt mixing and pressing does not allow bacteria (*E. Coli* and *Enterococci)* and germs (NTG) to adhere and colonize.

Materials obtained from waste seem to be sanitary safe and could be used for obtaining products that are commonly used by many people, without any contamination risk with the tested bacteria and germs. This property is due to: (1) the reduced capacity of materials based on wastes to swell in water or atmosphere moisture, minimizing the release of the small amounts of antimicrobial agents initially introduced into packaging materials; (2) high material hydrophobicity; (3) low negatively charged surface that repels the negative charged bacteria; (4) surface conformation that even rough seems to be not fitted with the tested bacteria shape and dimensions; (5) material rigidity that hinders the eventually adhered bacteria into grooves and scratches to elongate in order to divide and colonize the surface.

The calorimetric analysis reveals a high capacity of the mixed plastic wastes to be used as fuel. The calorific power of those materials has a high level, compared to those of petroleum derivatives. The ASR and B&CW have a reduced calorific power compared with MSW, because

the polymers in these kinds of products are present especially as resins for composite materials, rather than single material as there are find in MSW.

Extracting the polyolefins from the mixed plastic waste, the calorific power decreases for all kinds of waste. Generally, the polymers having higher density are characterized by lower calorific power. As the PE and PP were found, both in the lighter and heavier fractions of wastes as composites, the calorific powers of these fractions will be higher, due to the higher polyolefinic calorific power.

Even after extraction of polyolefins, the calorific power of residues is still greater than those of different sorts of coals and these materials could be burned to obtain a reasonable amount of energy.

Chapter 3

IMPROVING THE QUALITY OF THE SECONDARY POLYOLEFINS USING MAGNETIC DENSITY SEPARATION

The commercial applications used in polymers separation are usually restricted to particles of 6.4 to 10 mm in size and throughput tonnage is limited due to the rates of separation for the other techniques [52]. Because both PP and PE float in water, it is difficult to separate one from the other. Using floating-in-water technique, the polyolefins can be separated from the heavy plastics present in the plastics streams, but another technology is necessary to separate PP from PE. Because it is compulsory to have different densities of the fluid, floating in alcohol could be used, but the process must be repeated in many steps, using different concentrations [53]. This technology is very expensive, dangerous and has limited separation flexibility.

Bezati et al. (2010) [54] define one of the possibilities of plastic separation technologies based on X-ray fluorescence spectroscopy. The sorting process is very expensive and the efficiency is limited. In general, it is difficult to obtain high purity for separation of materials very close in density [24].

Another separation technology is based on fluidization. Carvalho et al. (2009) [55] developed this technology in tap water. The same technology was tested by Yoshida et al. (2010) [56] in a gas-solid fluidized bed separator with silica sand. The float-sink of the plastics was affected, as the authors noted, by the air velocity for fluidization, the float-sink time and the feed amount of plastics. The possible causes of the effects were discussed by the authors, focusing on the apparent density of fluidized bed, the fluidization intensity, the size segregation of fluidized particle, the shape of the plastics and the interaction between the plastics during the float-sink process.

Gent et al. (2009) [52] present the plastic separation using cyclone separation. As the lowest cost recycling process, density separation methods are presently used in virtually all the automated industrial plastics recycling processes as a cleaning and/or pre-concentration and/or preparation phase for subsequent processing methods, or in some instances, to produce a marketable product.

3.1. Magnetic density separation technology and equipment for sorting of secondary polyolefins from waste

In the frame of FP7 project „Magnetic Sorting and Ultrasound Sensor Technologies for Production of High Purity Secondary Polyolefins from Waste", it was developed a magnetic fluid equipment for sorting PP and PE from polymers mixed waste streams. The project uses the emerging technology called Magnetic Density Separation (MDS) [57], [58], [59] to separate a complex mixture into many different materials in a single step, using one and the same liquid. The goal of the project was to develop cost-effective and clean technology based on MDS and ultrasound process control to recover high-purity polyolefins from complex plastic wastes [60], [61]. The paper **Magnetic fluid equipment for sorting of secondary polyolefins from waste** [62] presents the research made on lab scale equipment showing the fruitful results.

The tests were performed using three types of polyolefin streams: Romanian and Dutch household waste, French demolition waste and Austrian automobile shredder residues. The properties of Romanian household waste were presented by Baltes et al. (2009) [17] and Patachia et al. (2011) [30]. The properties of the demolition waste were presented by Serranti and

Bonifazi (2010) [63]. The properties of car shredder light fraction were presented by Vajna et al. (2010) [64].

In ordinary floating, at equilibrium, the particle density is equal to the liquid density (Archimedes principle). In MDS the ferrofluid is attracted both by the Earth and by magnets and its weight varies with distance to magnet (figure 3. 1.). The Archimedes principle applied for ferrofluid: the particle is at equilibrium if it has the same weight as the volume of replaced ferrofluid [65], [66].

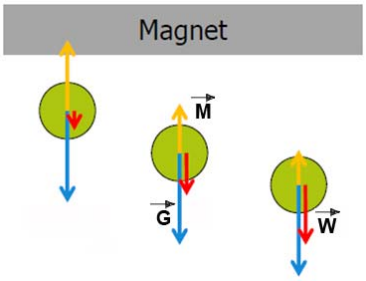

Figure 3.1. Particle of magnetic fluid loaded by: M = magnetic force (variable), G = gravity (constant), and W = G-M, weight

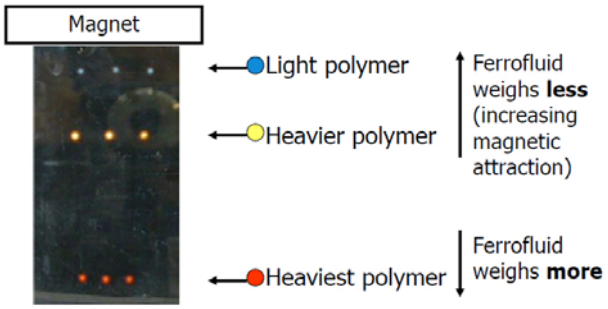

Figure 3.2. Floating of different plastic particles in ferrofluid [67]

Based on these properties of the ferrofluid, the floating in ferrofluid is a feasible method for plastic particles separation (figure 3.2.). Considering the density separation between PP and PE as 915 kg/m^3 [68], it is possible to apply the MDS to polyolefins separation (figure 3.3.).

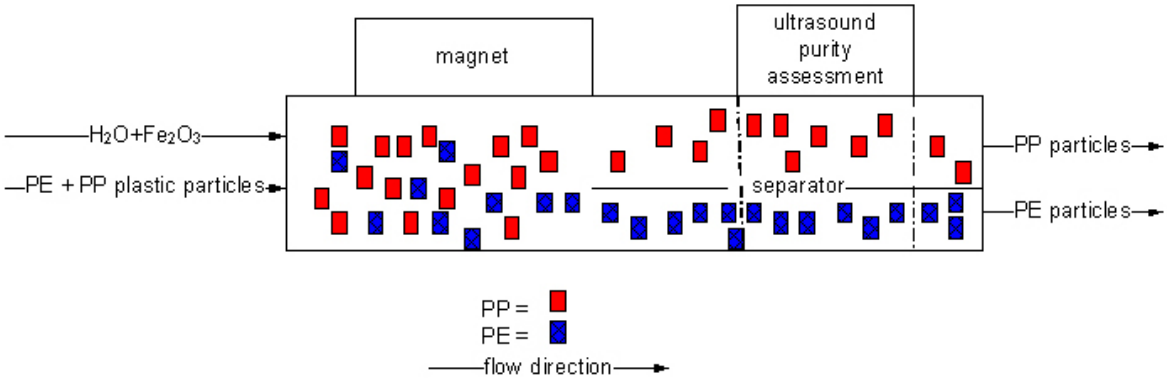

Figure 3.3. MDS and ultrasound assessment applied to polyolefins separation [16]

The separation process flowchart is presented in figure 3.4. As input in the process is used the fraction that float in water of the polymers waste, collected from household solid waste, building & construction waste and automobile shredder residues.

After granulation and flake thickness classification follows the cooking of the polymers, this means boiling in water with $CaCO_3$ and dewatering to remove all air bubbles from the surface, which can alter the floating process.

The output of MDS separation is three types of polyolefins: PP (density = 840…915 kg/m^3), PE I (density = 915…960 kg/m^3), PE II (density = 960…990 kg/m^3) and residues, collected in big bags after ferrofluid extraction.

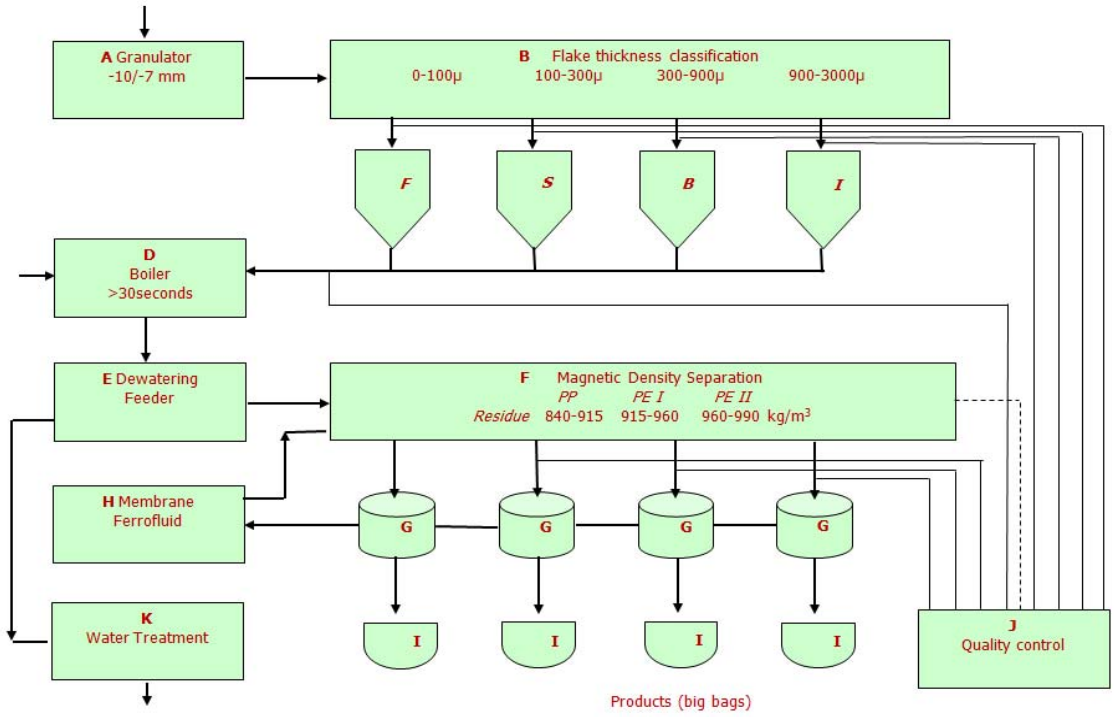

Figure 3.4. Flowchart of the separation process based on MDS [62]

The residues were light particles ($\rho<840kg/m^3$) and heavy ($\rho>1000kg/m^3$). These residues can be treated by incineration or pyrolysis, to extract energy and oils, or to be used as filling material in construction. After treatment, the water can be reused in the MDS process, as well as the ferrofluid.

All the process is controlled using ultrasonic inspection with sensor array and hyperspectral imaging to ensure the purity of the PP and PE [69], [70], [71], [72], [63], [73], [74].

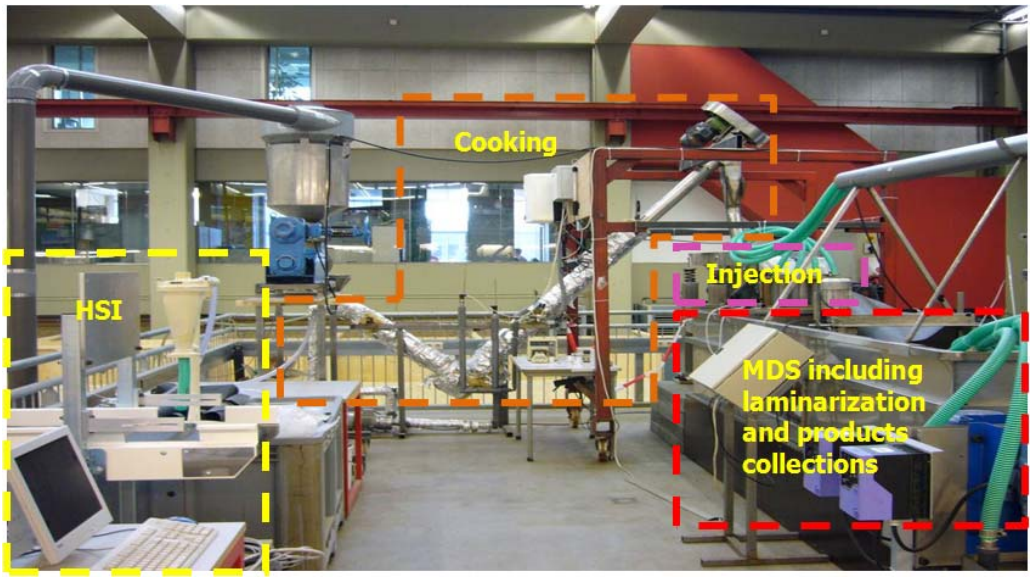

Figure 3.5. Lab scale equipment for polyolefins separation based on MDS [62]

Lab scale equipment was realized at the Technical University of Delft (figure 3.5.) based on the previous experience of the project team [75], [57], [58], [59].

This equipment was designed for cooking, feeding, flow in MDS and process control experiments. In the back, the cooking unit, using electric heating, prepares the plastic flakes for feeding, reducing the air bubbles on the surface and decreasing the contact angle. On the back right side, the injection assembly feeds the MDS with plastic flakes having an expansion box to drop the speed. On the right side the MDS realizes the separation of the polyolefins in ferrofluid bath. Because this is the critical point of the whole equipment, the experiments were focused on particle flow and MDS accuracy, in different working conditions. On the top of the MDS bath, the ultrasonic sensor array inspects the process. At the end of ferrofluid bath there are the separation channels, where the PP, PE flakes and residues are collected and removed by pumps. On the left side, the hyperspectral imaging equipment controls the accuracy of the process. The tests were performed on the MDS lab scale equipment.

Presence of the air bubbles on the surfaces decreases the density of the flakes (figure. 3.6.). The presence of 2 mm^3 air on the flakes surface reduces the density of 200 mm^3 flake with 10 kg/m^3. For 0.5 mm thick flakes the effect is 4 times worse. The result is a strong inaccuracy of the separation, because PE (910-920 kg/m^3) are likely to mix with PP. For this reason, the removing of air bubbles is necessary. There were two ways for wetting: in boiling water and in vacuum. To study the boiling influence on wettability, the contact angle (polymer-water-air) was measured. The boiling of polymer flakes decreases the contact angle to below 90° (figure. 3.7.).

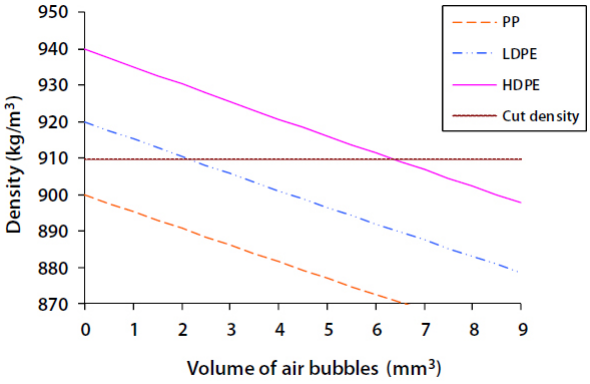

Figure 3.6. Density of the polyolefins flakes vs. volume of air bubbles [65], [66]

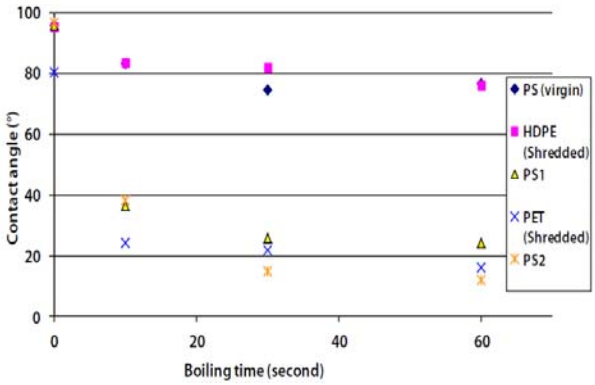

Figure 3.7. Contact angle of polyolefins flakes depending on boiling time [62]

To study the boiling time, mixtures of PE flakes and PP flakes were sink-floated in calibrated alcohol water liquids to get six samples of PP with densities within 5 kg/m^3 and another six samples of PE with densities within 5 kg/m^3. Test samples 1 of PP and PE were not boiled. The other five test samples were boiled for 10 s, 30 s, 60 s, 120 s, and for a long time, respectively. One by one, the test samples of PP and PE are immersed in ferrofluid in the magnetic field and the floating position of the samples was recorded, and compared to the expected floating position for the density range of the polymer flakes. Figure 3.8. presents the equilibrium position if polyolefin flakes in MDS function of boiling time. The polymer densities were in the interval indicated by dotted lines. The resulted safe boiling time was 60 seconds.

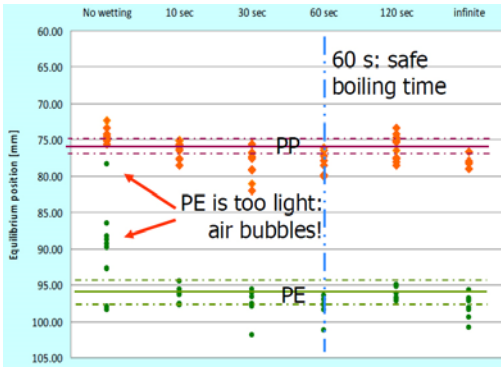

Figure 3.8. Equilibrium position (mm) if polyolefin flakes in MDS depending on boiling time [62]

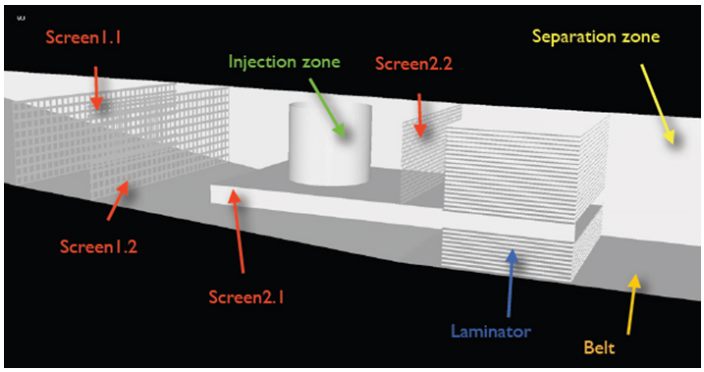

Figure 3.9. 3D model of the feeding and MDS channel [62]

Both boiling and wetting in vacuum remove all air bubbles from the surface of the flakes, and they work for all tested polymers. Wetting in vacuum is more expensive, needs to be done in batch, but can also remove air from polymer particles with an air pocket, e.g. tubes. It does not result in permanent wetting (not after air-contact). Boiling is cheap and results in "permanent" wetting (even after the flakes are brought again into the air atmosphere) because of the formation of a microscopic layer of $CaCO_3$. However, it cannot remove air pockets efficiently. Boiled flakes need to be cooled before MDS. Shredded plastics wet better than virgin plastics; sometimes shredding is sufficient to achieve wetting.

To study the feeding transport in the MDS channel and separation, the simulation of plastic particles flow in the ferrofluid was performed. This simulation was done at Barcelona Supercomputing Centre, using 512 CPUs from the 16384 CPUs of the supercomputer and Alya code [76]. The 3D model of the feeding and MDS channel (figure 3.9.) was simplified to a 2D model (figure 3.10.) to reduce the computational costs.

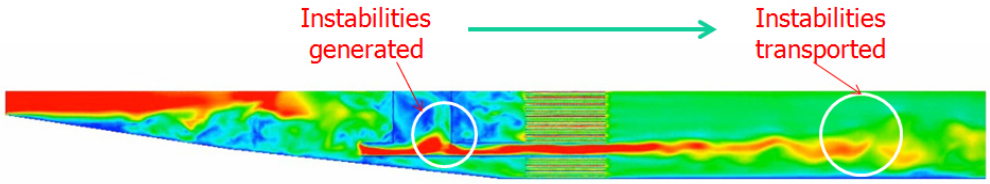

Figure 3.10. Instabilities in the first version of 2D model [62]

The tests made on lab scale equipment reveal the dispersion of the polymers at collector, which decrease the efficiency of the separation process. The same problem was observed on the simulation (figure 3.10.). The injection cylinder is responsible for this turbulence.

Simulations with different dimensions and shapes of the feeding channel were performed. The intermediary results and final design are presented in figure 3.11. In the first version, the instabilities are still present, due to large perpendicular feeding channel (figure 3.11.a). Reducing the size of the feeding channel decreases the vertical oscillations of the particles, but the turbulence is still too high (figure 3.11.b). Having an inclined narrow feeding channel, there are no macro instabilities (figure 3.11.c). The final design of the entrance in the MDS channel includes also a laminator which tried to make the flow laminar in the shortest distance as possible.

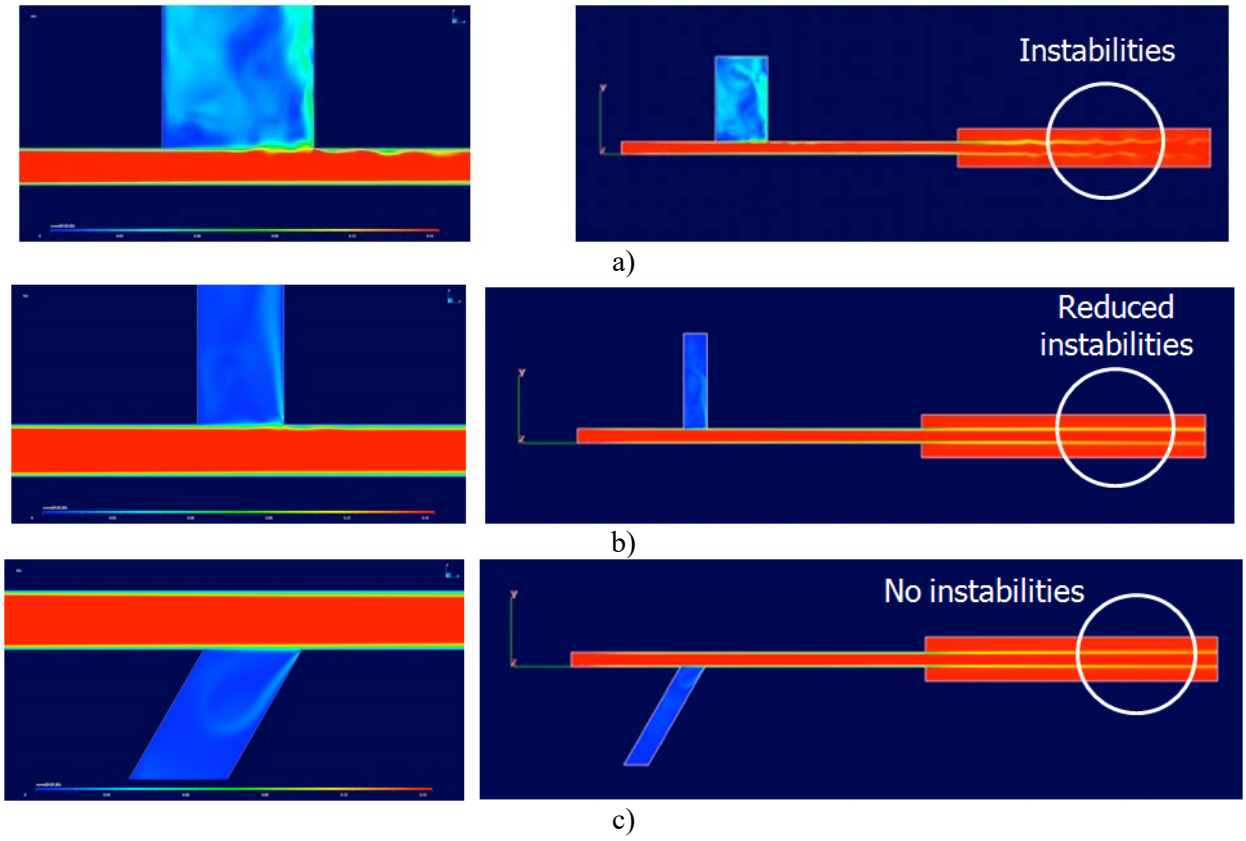

Figure 3.11. Flow simulation steps and improvements of the 2D model: Optimisation of the feeding area: a) wide, b) narrow, c) inclined + laminator [62]

Micro turbulences are necessary at the beginning of the MDS channel because help to release the particles if they are happened to stick on each other and reduce big scale turbulences in the channel. These micro turbulences should decay fast and reduce to an acceptable scale before reaching the splitters at the end of the separation channel.

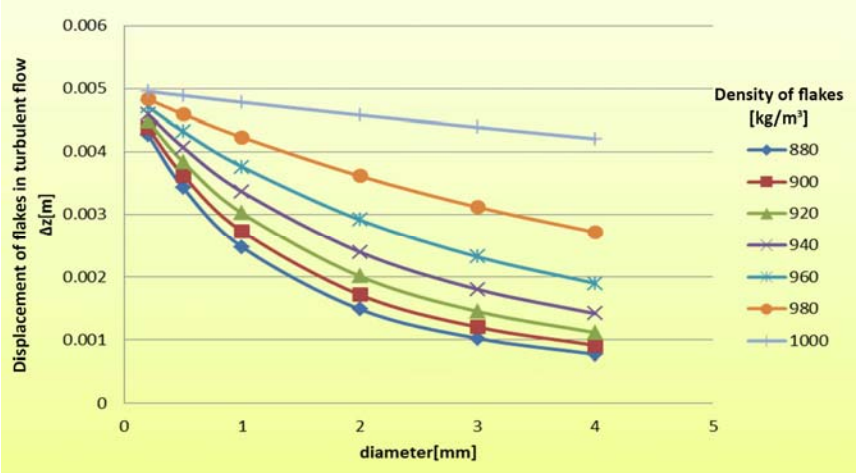

Figure 3.12. Displacement of flakes in the MDS channel turbulence [62]

Figure 3.12. presents the displacement of flakes in the channel turbulence flow (vertical velocity, Vy = 0.01 m/s, period = 2 s) function of particle diameter and density. The displacement decreases with increasing of diameter and decreasing of density.

3.2. Feasibility study of the MDS technology, for production of secondary polyolefins from polymer waste [77]

In the previous subchapter was presented the MDS equipment as an industrial prototype for an input of 400 kg/h. For industrial implementation, is required a feasibility study, to allow the owners to decide the opportunity this equipment with increased capacity.

The feasibility study is an analysis and evaluation of a proposed project to determine if it is technically feasible, if it is feasible within the estimated cost and if it will be profitable [78], [79], [80], [81]. The feasibility study is a process based on a cost benefit analysis of the project viability and is used to support the decision-making.

The paper **Feasibility study of the production of secondary polyolefins from the plastic wastes using magnetic density separation** the description of business, the project overview, the operational plan, the flowchart of the process, the energy consumption, the investment costs, the variable operating costs, the fixed operational costs and funding. The output of the study is the cost per unit. The feasibility study provides all data necessary for the investment decision.

For the purpose of this study, it is assumed that the input has been pre-treated so as to guarantee:

- a very low ferrous metal (including stainless) and glass/stone content (less than 0.01 mass %),
- a low sink fraction content (less than 10 mass %),
- a low rubber/wood/non-ferrous metal content (less than 2 mass % in total),
- a low moisture content (< 1 mass %),
- a low content of organic contaminants (only relevant for polyolefin fraction of household waste).

It is expected that commercial versions of this process will be designed in multiples of 3000 kg/h, which is equivalent to 25000 tons/year. This assumption is based on the fact that existing plastics recycling companies often process volumes in the range of 25000 to 50000 tons/year.

The process flow consists of:

1. **Receiving the order and contract preparation** - this stage is to analyse the performance capability of the order and after this the contract shall be drawn up and signed.
2. **Ordering the execution** - the launching graph is drawn, execution and control, which is transmitted to the production department, and the necessary of materials will be submitted to the Supply department.
3. **Supply** - supplied materials fall into the following categories: polymers, ferrofluid, pH control liquid. Their transportation is provided by the suppliers.
4. The **technical process** consists of the following steps (figure 3.4.):

A. *Fine granulation.* The input is milled to a size below 10 mm (or alternatively to below 7 mm, depending on the requirements of the outlet). This step requires the input to be free of ferrous metals (including stainless steel) and glass/stone because of the otherwise fast degradation of the cutting knives. Fine copper wires may be present at low concentrations.

B. *Classification.* The flakes are classified by wind sifting or ballistic separation into four ranges of flake thickness: 0-100μ (*F*: mainly foils, fibres and dust); 100-300μ (*S*: mainly EOL products moulded from sheet); 300-900μ (*B*: mainly blow-moulded EOL products); 900-3000μ (*I*: mainly injection moulded EOL products). The exact thickness ranges may

vary somewhat for specific inputs. This process step requires a dry input. Slip streams of the four streams of 0.1-1 kg/h each (10000 flakes per hour, the actual mass flow depends on the flake thickness range) are deflected towards the Hyperspectral quality control unit (process step J), in order to analyse the grades and make a commercial evaluation of the input.

C. *Intermediate storage.* The four thickness ranges of flakes are stored in silos. The remainder of the process acts only on the three thick-walled flake mixtures (*S*, *B* and *I*). The foil fraction *F* is sold as it is.
D. *Boiling.* One of the flake mixtures *S*, *B* or *I* is fed from its silo and submerged in boiling water for at least 30 seconds. This step coats the flakes with a thin layer of water to avoid the possibility of air bubbles attaching to the surface of the flakes during density separation. At the same time, residual amounts of organic and oil contaminants are dissolved from the flake surface and bacterial activity is reduced, to protect the magnetic process liquid from degradation (step E in the process). The minimum of 30 seconds frees the polymers from air. The actual residence time may be longer depending on the contamination of the input. At the beginning of this stage, a dry slip stream of the material is deflected towards the Hyperspectral quality control unit (step J in the process), in order to analyse the input MDS grade.
E. *Dewatering.* The boiled flakes are dewatered to below 7 mass% moisture and cooled to below 35ºC on a dewatering screen/feeder, to reduce the influx of water into the magnetic process liquid and protect it from degradation by heat. The dewatering screen feeds the material into the MDS (step F in the process). The reclaimed water is purified in a water treatment facility (step K in the process).
F. *Magnetic Density Separation (MDS).* The wet flakes are mixed into a flow of magnetic process liquid (total flow rate 200 – 300 m^3/h, density =1006 kg/m^3) and separated according to flake density into five categories: <840 kg/m^3 (light residue); >990 kg/m^3 (heavy residue); 840-915 kg/m^3 (polypropylene); 915-960 kg/m^3 (polyethylene I); 960-990 kg/m^3 (polyethylene II). The flow of flakes is monitored at the splitter by ultrasound sensing, in order to detect problematic flow conditions whenever they occur. The ultrasound sensor creates continuous statistics of the reflection brightness distribution (material type, presence of air bubbles), horizontal speed and the volumetric flow of each of the four types of product and compares this to the expected product flows based on the input quality analysis.
G. *Process liquid recovery.* The products of MDS are taken from the MDS unit and centrifuged to moisture content below 0.5-2 mass % (depending on flake thickness, thick flakes below 0.5% mass moisture).
H. *Process liquid control.* The reclaimed process liquid is passed through a membrane to extract water, add concentrated ferrofluid, and add pH control liquid, in response to a pH sensor, a magnetization sensor and a level control. The resulting concentrate is fed back to the MDS unit main input before a static mixer.
I. *Storage.* The products are stored in silos. Before storage, slip streams of the three main products, Polypropene, Polyethene I, Polyethene II, are deflected to the hyperspectral quality control in order to check for purity, and compute actual recovery of the valuable components from input.
J. *Quality Control*. Samples taken continuously from the pneumatic transport lines are evaluated on-line for grade by hyperspectral analysis.
K. *Water treatment.* Water from the dewatering-feeder is cleaned of mainly organic pollutants in order to be re-used.

5. **Delivery** - will be made in polyethylene big bags, the transportation being done by the customers, after the preparation of the delivery documents.

A significant amount of energy is involved in the hot-wash. For the material recycling of household waste, an industrial facility needs an extensive hot-wash while this step is not needed for demolition waste and automobile shredder residues. Since hot-wash is not specific for the W2Plastics technology, this step is not included in this analysis, but an estimate is given for the energy consumption for completeness. Note that due to their small wall thickness, plastic foils and films require considerably more energy for cleaning per ton throughput than thick plastic flakes. A foil/film washing line of basic technology and with a design throughput of 500 kg/h require 400 kWh/ton including hot washing, thermal drying and foil-compacting, whereas a plastic bottle washing line of the same capacity only consumes 200 kWh/ton (also including hot washing and thermal drying). It appears that this data mark the upper limit in plastic washing due to the small throughput and basic technology applied. Proceeding from a mix of 65 wt-% foils and 35 wt-% rigids in plastic packaging waste recovered from household waste and an actual throughput of 3 tons/h per processing line, it was estimated the average power consumption in the cleaning and fragmentation step using state-of-the-art technology at 200 kWh/ton.

As it was already mentioned it is provided that production of PP and PE will be 25000 ton/year at the end of three years following the implementation period. The costs' structure is:

Investment costs. The estimated cost of components of the W2Plastics equipment for the full commercial scale (3000 kg/h) is 1340000 €.

Variable operating cost. Below, the variable operating costs involved in running the process are estimated.

Electricity cost. The estimated installed power breakdown of the full-scale facility is 573 kW. Assuming an overall electricity consumption of 32% of installed power, it is estimated that the electricity costs for the W2Plastics process are 61 kWh/ton of input.

It is estimated that *maintenance* of the knives of the granulator occurs once every week of operation. Estimated cost of maintenance is 2500 €, or 5€/ton of input.

The loss of *magnetic process liquid* is estimated at 1.5 vol% of the input, or 15 l/ton of input. Since the process liquid is made by diluting concentrated ferrofluid 50 times with water, the loss of concentrated ferrofluid is about 0.3 l/ton of input. Ferrofluid is sold at prices ranging from 12 – 30 €/l, depending on the amount purchased. It is therefore estimated that the cost of ferrofluid will be about 6 €/ton of input. The cost of pH control liquid is negligible.

Fixed operational cost. The crew needed to run the process consists of an operator (5 shifts), a shovel driver (5 shifts), a lab technician (1 shift), and a mechanic (1 shift). Depending on the embedding of the activity (green field or inside an existing company) there may be a need for an engineer, a commercial director, a financial director and a general director.

General maintenance (excluding maintenance of the knives of the granulator) is estimated at 1% per year of the investment cost of the process line.

Funding. Investment fund will be made through a bank loan within 10 years with an interest rate of 7.65%.

Cost per unit. Taking into account the costs from the Romanian economy [82], the production cost of secondary polyolefins (PP, PE) will be 182.79 EUR/ton.

It is assumed that return on investment will be in 10 years from the starting of the production. In the cost computing it was considered the composition of raw material:

- 50% polymer waste from household waste,
- 25% polymer waste from automotive shredder residue,
- 25% polymer from building and construction waste.

Assuming the yearly production of 25000 tons, the production cost will be 182.79 EUR/ton. This cost is very competitive comparing with the minimum international prices of secondary polyolefins (LDPE=435 EUR/ton, HDPE=800 EUR/ton, PP=660 EUR/ton) [83], [84].

3.3. Monitoring the separation process of the polymeric materials immersed in a magnetic fluid

Separation of plastics waste using MDS technology with magnetic fluid allows different immersion depth for different type of polymers; it is of great importance the determination of the acoustical properties of polymeric materials (longitudinal ultrasounds velocity).

The paper **Labview in ultrasound plastic materials measurement** [85], proved the flexibility of LabVIEW (Laboratory Virtual Instrumentation Engineering Workbench) - graphical programming software – when it is used in connection with applications of ultrasound measurements in the field of polymeric materials characterization.

Table 3.1. Type of samples [85]

Simple layered sample		Double layered sample	
Type	**Thickness [mm]**	**Type**	**Thickness [mm]**
PP	2.53	PMMA	10 + 4
HDPE	1.3	-	-
PS	1.53	-	-
PMMA	10 + 4	-	-

Table 3.2. Magnetic fluid properties [85]

Magnetisation Ms [Gs]	**Particle density d [g/cm^3]**	**Temperature of measurements [°C]**
97	1.088	29
130	1.132	29

In the research, emission and reception of the acoustical waves were made with EPOCH XT instrument, and the first step was to adapt this device at LabVIEW requirements for determination of acoustical properties of the plastics. The developed LabVIEW applications offer a better support in ultrasound materials measurements and characterization: data interpretation (characterization of the shape and height of the peaks, determination of the wave attenuation); control of the instrument for signal measurement (input/output data management; device setup and control); saving the Data Base on PC (for future data computations) [86].

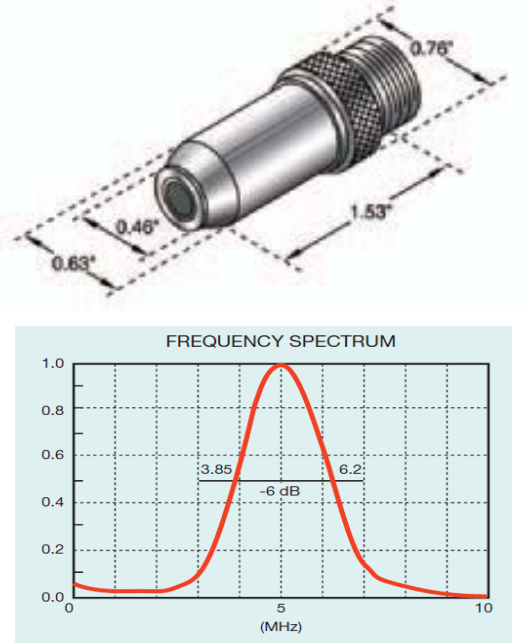

Figure 3.13. Immersion sensor and his frequency spectrum [85]

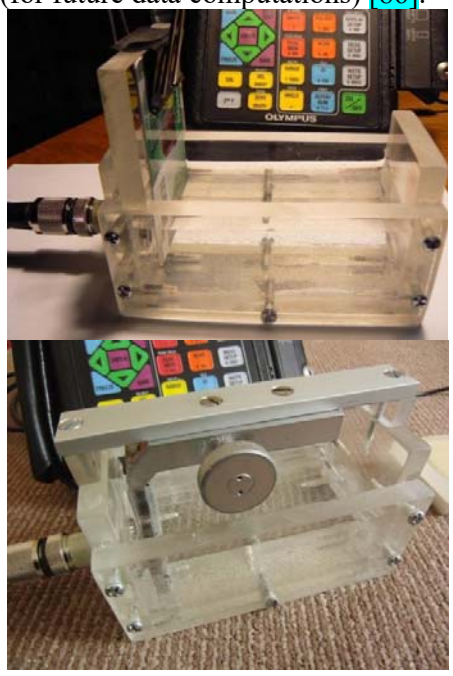

Figure 3.14. Measurement tank and the sample holder and positioning system [85]

The classes of polymers investigated in the research were presented in table 3.1.
As was mentioned above, the measurements were made in water and in a magnetic fluid with Ms=130 Gs and 1/29 ratio dilution. This nano-magnetic fluid was produced by Laboratory of the Magnetic Fluids, in Timisoara-Romania (table 3.2) [87], [88].

As generator and receiver of the ultrasounds was used EPOCH XT (from OLYMPUS): with tunable square wave pulsing, selectable digital filters, gain range 0-110 dB, peak memory and peak hold, adjustable PRF, 0.01 mm measurement resolution, two gates with programmable alarms, etc. In the liquid medium (water or magnetic fluid) was placed one immersion sensor A310S-SU with the role of transmission/reception transducer (figure 3.13.).

The measurement setup was made from PMMA and is shown in the figure 3.14, with the special positioning of the sensor and with the adjustable sample holder (on the right), at micrometric precision.

The polymers studied are presented in the table 3.3. [89].

The input data, for all of the experiments were: Frequency = 5.00 MHz (for some measurements: 1 MHz to 7.14 MHz); Energy = 75 V; Damping = 50 Ohms; Filter = 1.5-8.5 MHz.

For all the polymer samples was measured the thickness using a digital micro meter with a better precision like the thickness measured with the Olympus EPOCH XT device. These results were used as input data for the ultrasound measurements [90], [91].

The gates length was setup in a position so that to have the first expected peak inside of the first gate and the second expected peak inside the second gate. The ultrasound velocity was adjusted so that to obtain the sample thickness with 0.01 mm precision in upper-right corner (figure 3.15).

Table 3.3. Sample properties [85]

VICAT soldering temp. [°C]	Dens. [g/cm^3]	Melt flow rate [g/10min.]	Prop.
150	0.905 – 0.917	14-18	SS-12: Midilena lll -J800 Polyproylene (PP)
72	0.960	8	Hostalen GC 7260 Polyetylene (HDPE)
96	1.050	12	Styron 485 Polystyrene Resins

Figure 3.15. EPOCH XT screen and signification of the values [85]

To extracting the measured data was designed a preliminary LabVIEW application, with the role of conversion for the EPOCH XT saved data file (one EXCEL file) and representation of data in on WaveFormGraph (WFG).

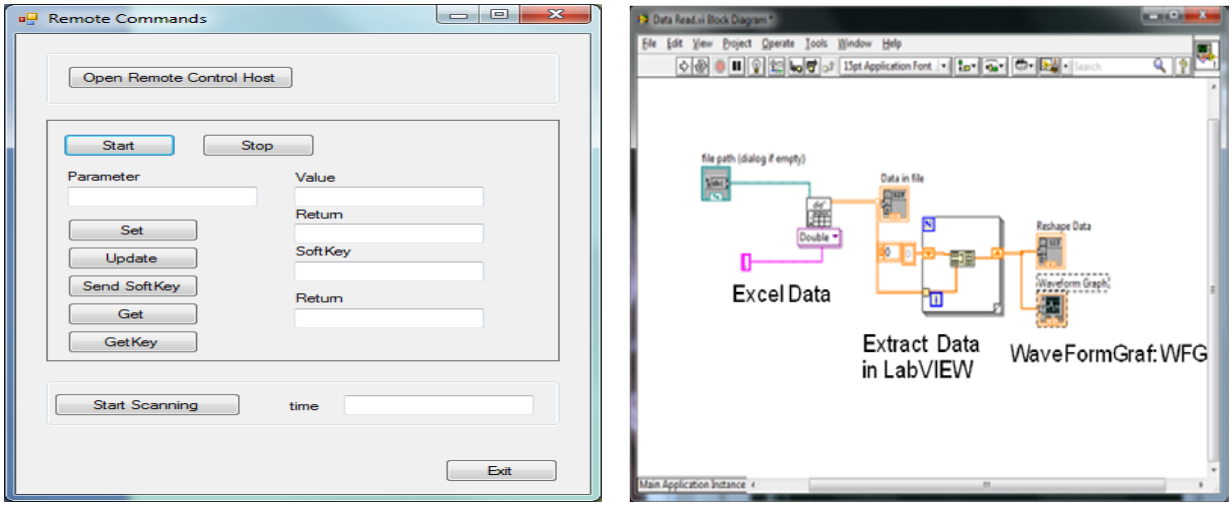

Figure 3.16. Remote control panel and program for conversion, extract and WFG [85]

In the figures 3.16 are shown Remote Commands application and the developed LabVIEW program. After this preliminary application, it was developed a second LabVIEW application. This application integrates the necessary Remote Commands and offer a full LabVIEW control of the Olympus EPOCH XT device.

Table 3.4. Ultrasounds longitudinal sound velocity in water [85]

Plexiglas (PMMA)	Styron 485 Polystyrene Resins	SS-12: Midilena lll -J800 Polyproylene (PP)	Hostalen GC 7260 Polyetylene (HDPE)	Type of polymer
10 transparent 10 white 4 yellow	1.53 yellow	2.53	1.30 translucent	Thickness [mm]
2614 2471 2578	2204	2478	2324	Longitudinal sound velocity [m/s] Experimental
2750 2650	2320 2290 2340	2740	2430 2241-2271 2460	Longitudinal sound velocity [m/s] Literature

For the experiments conducted in water, the synthesis of the measurements is concentrated in the table 3.4., the results of measurements in the magnetic fluid (1/29 ration dilution) in the table 3.5.

Table 3.5. Ultrasounds longitudinal sound velocity in magnetic fluid [85]

Plexiglas (PMMA)	Styron 485 Polystyrene Resins	SS-12: Midilena lll -J800 Polyproylene (PP)	Hostalen GC 7260 Polyetylene (HDPE)	Type of polymer
10 transparent 10 white 4 yellow	1.53 yellow	2.53	1.30 translucent	Thickness [mm]
2614 2471 2578	2204	2478	2324	Longitudinal sound velocity [m/s] Experimental
2677 2521 2631	2243	2654	2053	Longitudinal sound velocity [m/s] Literature

The experimental device with magnetic fluid inside is presented in figure 3.17.

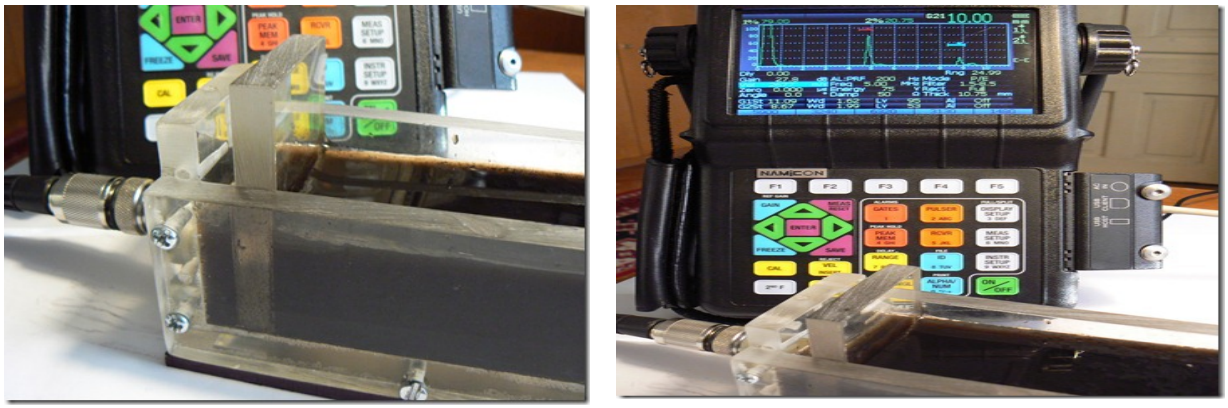

Figure 3.17. Measurements in magnetic fluid [85]

3.4. Conclusions

MDS method is adequate for the separation of high quality secondary polyolefins from different plastic waste streams. Before the MDS process, the polymer waste particles must be prepared by boiling 60 seconds in water with $CaCO_3$ and dewatering, to remove air bubbles from the surface and to decrease the contact angle below 90°.

Using the CFD was determined the shape and dimension of the feeding channel. With an inclined narrow feeding channel, there are no macro instabilities. Only micro turbulences were obtained, which helped the separation process.

The researches made on lab scale equipment show fruitful results that encourage us for the next step, the pilot plant MDS equipment, now under development. All the results of this research were applied in the scaling of lab equipment to the pilot plant. After the tests on the pilot plant, the solutions will be ready to be implemented in the commercial version of the MDS equipment.

The feasibility study should provide all data necessary for the investment decision. Applying the presented feasibility study to the company specific data will result in cost of

production of secondary polymers. Comparing the cost with market price, it will be very useful for the price strategy.

The final product of a successful feasibility study is a project proposal for management or financing institutions concerning the opportunity of introduction of magnetic sorting technology of secondary polyolefins from waste.

The marketing strategy is focused on gaining and maintaining competitive superiority through quality service and attentive relationship with customers.

Concerning the monitoring process of the MDS process, OLYMPUS EPOCH XT instrument has been adapted for measurement of acoustic properties of plastic materials using LabVIEW environment;

Some LabVIEW application has been developed to: enlarge the interpretation possibilities of the detected signals coming from ultrasound investigations; make easier the input/output device control; reduce the measurement time.

Longitudinal ultrasounds velocity in different plastic materials has been determined both in water and in magnetic fluid with enough accuracy and well correlated with the literature.

Chapter 4

APPLICATION OF THE SECONDARY POLYOLEFINS IN COMPOSITES MATERIALS

Polymers have specific properties, advantageous for many applications: low density, high chemical resistance, high resistance to environmental conditions (humidity, solar radiation, pH), high mechanical strength, easy processing. In addition, their properties can be modified and adapted to the application needs by modifying the structure (modification of the molecular mass and its dispersion in the system, branching or crosslinking, obtaining of co-polymers with different distributions of the monomers in the chain), morphology (modification of the degree of crystallinity, shape and size of the crystals, the production of compact or porous polymers), or by mixing with other polymers or blending with organic or inorganic fillers (in the form of powders, woven or non-woven fibres, particles of different sizes) . The ways of controlling the properties of polymers are virtually infinite. Applications of virgin and secondary polymers in composite materials are in the attention of researchers around the world. Therefore, today, there is no field of human activity that does not profit from the benefits of using polymers.

To improve the polyolefin waste using it is necessary to obtain composites materials with different types of composition. Polyolefins composite materials domain is very large due to the multiple combination possibilities that have developed over the years. The possibility of replacing in specific applications the virgin polyolefins from composites materials by second raw materials coming from polymeric wastes is of real interest.

Glass fibre reinforced polyester composites (GFPCs) are currently used in a plethora of applications such as construction structures, automotive covers, boat hulls, blades for wind turbines and so forth. Thus, studies regarding the influence of UV radiation on the GFPCs structure and properties under prolonged exposure are of outmost importance. Usually, these studies could be assessed by complex structural analysis, such as scanning probe microscopy, FTIR spectroscopy, correlated with colorimetric or mechanical analysis, which are expensive and time consuming [92], [93], [94], [95], [95], [154].

Calcium carbonate is the fourth most frequently employed category of filler used for the production of thermoplastic matrix composites, especially polyolefin-based (polyethylene and polypropylene), after talc, silica and montmorillonite. The addition of calcite in the polyolefin (PO) matrix leads, in principle, to a diminishing of the final cost of the material and to the improvement of its mechanical properties (rigidity, hardness, impact resistance and flexural resistance), and could constitute an effective method to an efficient valorisation of both polyolefin and calcite wastes [96], [97], [98], [99], [155].

In the following, it will be presented parts of the research work of the author and the team in this field.

4.1. Investigation on the friction coefficient of the composite materials obtained from plastics wastes and cellulosic fibres [100]

Because these composite materials can be used in applications requiring mechanical friction, this paper presents determination of static coefficient of friction on flat surfaces. The selection of polymeric composites from waste as materials for sliding components of machines and devices is a very important aim for tribologists as well as tribological behaviour of non-polymer-on-polymer tribosystems. The best tribological combination practically confirmed is

steel on polymer; therefore the tests were done with this system. Based on research of [101], [102] and [103], Z. Rymuza presents for non-polymer-on-polymer contacts in [104] that mechanical and adhesive interactions are located in the very thin surface layer of polymer being in frictional contact. The ratio between mechanical and adhesive component depends in particular on roughness of the counter-body. The coefficient of friction is usually very high at small roughness because of high adhesion, and it decreases to minimum value at increase of roughness and then increases at further increase of roughness when mechanical component of friction force becomes very high. The similar tendency was confirmed also experimentally in the case of wear rate. But the minimum value of friction coefficient, wear rate, and also the shape of the characteristic curves are fairly similar. In conclusion, the polymeric tribosystems can operate without lubrication. Very wide possibilities to modify polymeric materials by fillers, lubricants and many other additives give very good perspectives to find polymeric composites that show excellent tribological properties both as matched with non-polymer or with another polymeric component.

As Georgescu comments, generally the additions of reinforcement and/or lubricating materials improve the tribological behaviour [105]. The additives with lubricant role cause the decrease of surface energy and also the decrease of material resistance due to the weak joining. The reinforcement materials increase the polymeric tensile strength but can drastically modify the surface roughness. So, the friction coefficient could increase, also the surface roughness, but the protective and uniform transfer film will no longer form. Not all additives in the polymers composition enhance the matrix characteristics. For example, in certain conditions, the presence of fibers causes the wear deterioration. Evans and Lancaster note that the fibers additions in polymers generally have benefic effects on the wear but seldom produce the decrease of this property [106]. An increase of other characteristics was observed: decrease the deformation under the load without affecting the conformability, sometimes the friction coefficient is smaller and constant; some additives facilitate the quick heat removal [107]. The huge interest and the polymeric composites consumption in recent years highlight the limits in properties optimization [105], [108], [109]. N. K. Myshkin and A. V. Kovalev evidenced that in the range of moderate loads of 0.02 to 1 N the friction coefficient decreases with load increase [110]. Such behaviour may be explained by the elastic deformation of surface asperities. Also, theoretically, the friction force should not depend on the sliding velocity. For polymers, however, this statement is true only if the temperature within the contact area has negligible increase. Usually there is a complex dependence of the friction coefficient on the velocity explained by variations in the relaxation properties and physicochemical activity of macromolecules. A.S. Pouzada et al. consider that in injection moulds an important factor arising from the model is that the static coefficient of friction between the plastic and metal surfaces in contact is greatly influenced by the surface roughness, contact temperature and some processing variables, such as cooling time, melt temperature and holding pressure [111]. The comparison between experimental data and simulation suggested that substantial errors could derive from not using a coefficient of friction adjusted to the actual processing conditions. As V. Quaglini and P. Dubini remark in [112], it is generally accepted that at low and medium pressure levels plugging of a polymer on smooth metal surfaces can be neglected [113], [114], and friction is explained in terms of the adhesion mechanism only. H. Jiang, R. Browning et al. studied the effect of Ra and contact load on μ_s of a set of model TPO systems. Their conclusions were that the findings show that μ_s increases when contact load increases or Ra decreases. However, the effect of Ra becomes less significant under higher contact loads [115].

Because these composite materials can be used in applications requiring mechanical friction, this paper presents the obtained values of static coefficient of friction on flat surfaces, between polyolefins matrix based composites and steel.

Pure polyolefins and POs resulting from waste recycling, additives and filler materials (figure 4.1.) have been used in order to obtain them. The characteristics of virgin polyolefins are presented in table 4.1. Mixed polyolefins waste with different polyolefin content, resulted from municipal solid waste polymers (MSWP) collected by Urban Company in September 2010 from Brasov County, Romania, were used. Five charges, each of one kilo weight have been collected. Taking into account that the municipal solid waste represents a mixed plastics type, it is necessary to perform selective separation to increase its value, as it was already presented in chapter 2. For the research, it was considered the polyolefins materials with the density between 0.8848 and 0.964 g/cm^3 from the MSWP. The smaller or greater density fraction out of considered interval (mentioned before) was classified as contaminants of polyolefinic waste.

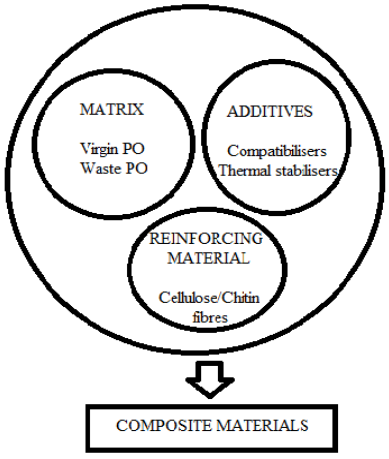

Figure 4.1. Samples composite materials composition [100]

Table 1. Virgin polyolefin characteristics [116-118]

Mat. type	Commercial denomination	Producer company	Material characteristics
PP - homopolymer	Lupolen 3010 D	Lyondell Basel Ind.	Softness index (190˚C; 2.16kg)=0.25g/ 10 min; ρ=927 kg/m^3

After separation 13 density fractions were obtained, our research was focused on to the following: W3: ρ3 = 0.884 – 0.908 g/cm^3, W4: ρ4 = 0.908 – 0.923g/cm^3, W5: ρ5 = 0.923 – 0.935g/cm^3 and W6: ρ6 = 0.935 – 0.964 g/cm^3, taking into account that these fractions include polyolefins (characterization was presented in chapter 2).

As filler material, cellulosic fibres modified with chitin, acquired from Shandong Helon Textile Sci. & Tech. Co., Ltd. China (Mainland), on commercial denomination Chitcel has been used. As additives, thermal stabilizers and coupling agents have been used (table 4.2.). The coupling agents have a double role, on one hand to ensure a proper interface between the components of the polyolefins density fractions and on the other hand to provide the best interface between matrix and fibres (figure 4.2.).

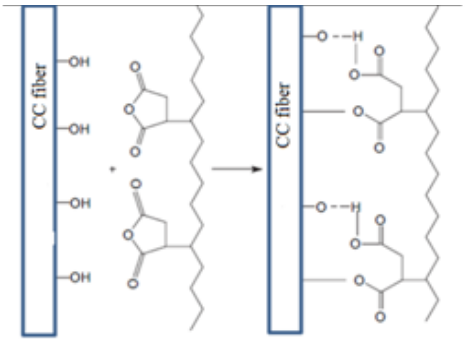

Figure 4. 2. Coupled mode of compatibilizing agents modified with maleic anhydride, on cellulosic fibre [116], [117], [118]

Table 4.2. Thermal stabilizers and coupling agents used for composites materials [116-118]

Additive type	Commercial denom.	Producer company	Function in composite
Octodecil 3 (3,5-ditertbutil- 4-hidroxifenil) propionat	Irganox 1076	Ciba	Thermal stabilizer
Polymer graft with maleic anhydre	PP-MA	Sigma Aldrich	Coupling agent
Vinil trietoxi-silan	VTS	Fluka	Coupling agent

The samples are composite materials with virgin polypropylene (PP) matrix (table 4.3., first four samples), polyolefins from MSWP no separated waste, density fractions 0.884-0.964g/cm3 (table 4.3., last four samples), CC fibres as filler material, according to table 4.3. The composite materials were obtained at "Petru Poni" Institute of Macromolecular Chemistry Iasi, Chemistry Department from Transilvania University of Brasov and Department of Polymer Engineering from Budapest University of Technology and Economics. All details are presented in [30].

Table 4.3. Samples composition [100]

Code	PP %	PE %	PS %	PA %	CC fibres %	Irganox 1076 %
PP	100	-	-	-	-	-
PP2C	97.000	-	-	-	2	0.5
PP10C	89.000	-	-	-	10	0.5
PP30C	69.000	-	-	-	30	0.5
W_{3-6}	23.577	74.356	1.356	0.211	-	0.5
W_{3-6}2C	23.103	72.862	1.329	0.207	2	0.5
W_{3-6}10C	21.207	66.883	1.220	0.190	10	0.5
W_{3-6}30C	16.468	51.937	0.947	0.147	30	0.5

For each sample, the difference up to 100% is the addition of thermal stabilizers and compatible agents.

One stage of the obtaining process is desiccating at 60-80°C, 2 hours drying chamber maintaining, followed by cryogenic frozen and shredder in ZM 200 centrifugal mill, in the polyolefins waste case. For a better intermixing, the particles dimensions are 0.5-1mm. The mixing process and the obtaining of the samples are presented in [30]. After cooling and shredder operations, followed the pressing process in a mould using a Collin hydraulic press. The dimensions of the laminas were L x l x h: 150 x 150 x 1 mm.

Taking into account that obtained composite materials presented above will be able to be used-up in practical applications, it was considered necessary to define de friction coefficient. 1N load was the pressure force on a sample with the dimensions 20x20mm (figure 4.3.).

Figure 4.3. Samples dimensions for friction coefficient [100]

Figure 4. 4. Calibration of the roughness checker [100]

Figure 4.5. The parameters tested with Surtronic 25 [100]

Figure 4.6. Friction coefficient determination in progress [100]

To determinate the friction coefficient it was used a testing machine-a high precision tribometer with prisms, including two planes semi couples, one fix and the other one mobile. The

tribometer worked on the principle of the inclined plane and measure the angle hereupon the sliding phenomena go on. All details concerning the method and the equipment are presented in [119].

This principle consists of correlation between slope angle α and friction coefficient μ (tgα = μ). It is possible to define the static friction coefficients (which appear on the borderland between removal and repose). The friction sheet, part of the ensemble polymer-metal, is steel, because this is the best tribological combination practically confirmed. Each friction coefficient value represents the average of 20 tests on each sample.

The surface roughness was measured using a Surtroni 25 surface roughness tester (Taylor Hobson) [120]. R_a is the arithmetic mean of the absolute departures of the roughness profile from the mean line. The unit contains a drive motor which traverses the pickup across the surface to be measured. The measuring stroke always starts from the extreme outward position. At the end of the measurement, the pickup return to this position ready for the next measurement.

Firstly, the calibration of the instrument checker (figure 4.4.) has been done. The Surtroni 25 stylus can traverse up to 25mm (or as little as 0.25mm) depending on the component. The Gauss filtered measurements were done for an evaluation length of 4 mm (figures 4.5. and 4.6.). Four measurements on each surface have been done and the average values of R_a were recorded.

Steel sheet roughness is 0.34 μm in the sliding direction of the sample. In table 4.4., the obtained values of the friction coefficients of materials are very close.

Table 4.4. Values of μ and Ra for PP and W_{3-6} series [100]

Sample	Average friction coefficient	Standard deviation of friction coefficient	Ra [μm]
PP	0.369	0.022	1.175
PP2C	0.344	0.022	1.155
PP10C	0.340	0.026	0.980
PP30C	0.366	0.035	1.280
W_{3-6}	0.369	0.023	1.350
W_{3-6}2C	0.313	0.053	1.070
W_{3-6}10C	0.352	0.040	0.980
W_{3-6}30C	0.332	0.034	1.195

The addition of the microfibers up to 30% decreases the samples roughness thereafter is identified an increasing of the value. This indicates active participation of polymer matrix fibres in the mixing process. The full effect is exerted in the waste matrix with complex composition. At high concentrations of fibres, their possible agglomeration leads to increase the material roughness.

Although variations in roughness shall attract variation of the friction coefficient, the obtained last values are negligible. This is possible to be explained by a compensatory effect that could be exertion by the variations of other materials characteristics that influence the friction process and consequently the friction coefficient. These include: changing the surface energy of the samples due to compositional differences between samples, material rigidity changes due to crystallinity changes of adding fibres as well as cross linking reactions or fibres transfer that occur both, during the life cycle of materials from waste as well as a result of their thermal processing. Some of these data are presented in papers [121]. Practical applications of materials obtained from waste must involve a careful assessment of all their properties and their correlation, in order to optimize their composition for specific applications.

4.2. Glass fibres reinforced polyester composites degradation monitoring by surface analysis

The aim of this study is to present a simple and time efficient method for assessing the chemical modifications that occur on the surface of different types of GFPCs exposed to artificial ageing under 254 nm UV radiations, namely photographic image analysis of the surface of the composite material. The image analysis method has been successfully applied in some studies in order to assess the roughness profile of wood materials, UV or electron beam degradation of wood veneers [122], [123] as well as the adsorption kinetic and equilibrium of different types of dyes on poly(vinyl alcohol) cryogels [124], [125]. Also, degradation of synthetic polymers or composites has been studied by CIELab method, based on chromophoric group formation during the degrading process that leads to materials yellowing or browning [121].

Even though the CIELab method has been already used for GFR-PCs materials to study their degradation [126], the novelty of this work consists in the following two aspects: (1) characterization of the sample's colour by analysing the photographic image of the sample, using a suitable software and avoiding expansive spectrophotometers use and (2) increase the sensitivity of the coloristic method by enhancing the modifications in the CIELab colour space parameters of the surface by using an ionic or polar dye adsorption on the composite surface.

The novelty of this work consists in enhancing the modifications in the CIELab colour space parameters of the surface of different types of composites when submitted to UV-irradiation, through an ionic or polar dye adsorption on the composite surface. The method relies on the principle that UV irradiation could promote degradation on the surface of the composites, which leads to the formation of polar groups. The polar groups are responsible for a higher methylene blue adsorbed amount, which leads to an intensification of the stain colour, thus providing information about the performance of the material (testing of UV protective coatings, correlation with the water adsorption values). Methylene blue adsorption from aqueous solutions has been widely used in determinations regarding the oxidation degree for cellulosic materials or for surface area determinations of different oxide materials, calcium carbonate [127], graphite, activated carbons, yeast [128], [129] etc. Also, staining with this dye is frequently used in medicine and microbiology in order to enhance the visibility of the cellular components or to highlight possible dysfunctionalities (such as abnormal growth) [130]. Studies regarding the influence of radiation with a wavelength smaller than 300 nm on the structure and properties of polyester composites have not been extensively reported up to date. Most of the studies from the reference literature report the use of prolonged UV-A and UV-B irradiation on several unsaturated and/or aromatic polyester matrices [131], [132]. Our approach, in using a low wavelength UV radiation (254 nm) decreases the necessary time in evaluation of the surface changes and offers permanent information regarding the efficiency of the protective coating.

In this study, two different types of commercial GFPCs with red and white acryl coatings of 0.2 mm thickness have been used. The polymer matrix of the composites is composed of an ortophtalic-based resin (ENDYNE H 68372TA) and the reinforcing agent consists in a glass-fibre mat roving (E-type, Owens-Corning Composites LLC, U.S.A.). The average fibre weight fraction of the composites has been 32%. The red-coated composite consists in a layer of glass-fibre roving embedded between two layers of ortophtalic resin and the white-coated composite contains uniformly distributed glass fibres into the resin. For the image analysis, water adsorption, methylene blue stain-ing and FTIR spectroscopy the composites have been cut into circular specimens of 30 mm diameter (the white coated samples) and 20 mm diameter (the red samples) respectively. The composite material average thickness was 2.50 mm for the white samples and 3.30 mm for the red samples. All of the specimens were washed with ethanol in order to remove the contaminants from the surface, dried at 105°C for 4 h and then conditioned

for a week at 24°C and 54% relative humidity prior to analysis. The average humidity at equilibrium for the two types of conditioned composites was 0.150% for the white samples and 0.206% for the red samples.

1). Accelerated ageing of GFPCs

The conditioned GFPCs have been introduced in an UV-irradiator (Bio-Link 254, Viber-Lourimat) and exposed for a total time of 10 h to a UV radiation of 254 nm, having the irradiance value set at 120 mJ/cm^2. During the irradiation experiments the relative humidity in the chamber was 55 ± 5% and the temperature 24 ± 5°C. Two sets of samples from each types of obtained composite have been exposed to UV on the coated and respectively non-coated side. The notation of the samples in the tests performed is the following: I: initial non-irradiated sample; R: sample with red coating; W: sample with white coating; F: coated side of the sample; B: uncoated side of the sample; UVF: UV-irradiated on the coating; UVB: UV-irradiated on the back (not protected by coating); MB at the end of the codification: samples immersed in methylene blue solution.

2). Water adsorption tests

The conditioned GFPCs were immersed into closed recipients containing 10 mL of distilled water, and their mass has been deter-mined at precise time intervals during a 24 h interval. The relative mass gain at equilibrium (Δm_{eq}) of the samples during water storage was calculated using Eq. (4.1.) [133]:

$$\Delta m_{eq} = \frac{\left(m_{eq} - m_{t=0}\right)}{m_{t=0}} \cdot 100 \qquad (4.1.)$$

where m_{eq} is the mass of the composite (initial and irradiated on various sides) at equilibrium of water sorption and $m_{t=0}$ is the mass of the composite before water immersion (at $t = 0$).

3). Methylene blue adsorption on the composite's surface

In order to determine the possible structural modifications that occur on the surface of the samples during UV irradiation (polar groups formation) the GFPCs samples have been introduced in 10 mL of 200 mg/L aqueous methylene blue solution for 1 h, removed from the liquid and dried for 24 h at room temperature. Then, the pictures of coloured dried samples have been taken and used for the image analysis interpretation, according to next section (Image analysis).

4). Image analysis

Colour changes on GFPCs surfaces due to UV-irradiation were analysed using an alternative technique to those extensively used up to this date. The novelty is the using of photographic image analysis, instead of a photocolorimeter. It was demonstrated that this technique offers good relative results on UV-irradiated wood, in agreement with experimental data obtained by other analysis methods, such as FTIR spectroscopy [122], [123]. Initial photographic images of the irradiated samples and reference, as well as of the samples after MB sorption have been taken with the help of a Sony DSC110 digital camera (3072 × 2034 pixels resolution), under the same lighting conditions. The individual images of the samples have been loaded in Adobe Photoshop and the L*, a*, b* parameters using the CIELAB (8 bit) channel were determined in twenty points for each specimen, and the average value was used in further interpretations.

L* represents the lightness and varies from 100 (white) to 0 (black) while a* and b* represent chromaticity indexes: +a* red, −a* green, +b* yellow, −b* blue.

The colour differences have been calculated using Eqs. (4.2.) to (4.4.) and the total colour difference parameter _E* has been calculated from Eq. (4.5.) for each irradiated sample before and after MB sorption [134]:

$$\Delta L = L_2^* - L_1^* \quad (4.2.)$$

$$\Delta a^* = a_2^* - a_1^* \quad (4.3.)$$

$$\Delta b^* = b_2^* - b_1^* \quad (4.4.)$$

$$\Delta E^* = \sqrt{\Delta L^{*2} + \Delta a^{*2} + \Delta b^{*2}} \quad (4.5.)$$

where subscript 1 denotes the values obtained for the reference and subscript 2 denotes the values after UV irradiation on the coated and uncoated side respectively.

Positive values of Δa* describe a red shift, negative values of Δa* a green shift, while positive values of Δb* represent a yellow shift and negative values of Δb* a blue shift for the colour of the irradiated samples, in comparison to the reference.

5). Optical microscopy imaging

The optical microscopy images have been performed with a Carl-Zeiss Jena metallographic microscope, equipped with a digital USB image acquisition camera, at 500× magnification.

6). Determination of the static friction coefficient

The static friction coefficients (μ_s) of the samples (reference and UV-irradiated samples) on both sides, against metal (stainless steel), have been determined by the inclined plane tribometric method, according to the reference literature [119]. Briefly, the conditioned specimens have been placed onto the surface of the tribometer (at null inclination). The inclination has then been varied until the samples started to slide down the tribometer surface.

7). FTIR spectroscopy

The ATR-FTIR spectra of the composites were obtained with a Bruker-Vertex 70 Fourier transform infrared (FTIR) spectrometer, equipped with an attenuated total reflectance (ATR) device with a resolution of 4 cm^{-1} in the 4000–600 cm^{-1} interval.

8). Surface energy determinations

Contact angle measurements of UV-aged samples and reference using distilled water and glycerol as reference liquids were per-formed at 25°C with an OCA System 20 goniometer, provided by Data Physics Co., Ltd. 5 drops of test liquid, 4μl in volume were deposited onto the coated surface of the same GFPC. The surface energy of the samples was calculated according to the Wu method, with the help of the instrument software. According to this method, the surface free energy is divided into a polar part and a disperse part. According to this approach, the surface energy (γ) is decom-posed into a Lifshitz-van der Waals (γ^d) dispersive component, as well as into a polar component, γ^p, according to Eq. (4.6.) [135]:

$$\gamma = \gamma_s + \gamma_l - \frac{4 \cdot \gamma_l^d \cdot \gamma_s^d}{\gamma_l^d + \gamma_s^d} - \frac{4 \cdot \gamma_l^p \cdot \gamma_s^p}{\gamma_l^p + \gamma_s^p} \quad (4.6.)$$

where γ_l^d and γ_l^p represent the dispersive and the polar components of the test liquid(s), determined from the reference literature and γ_s^d and γ_s^p represent the dispersive and polar components of the tested surface. The initial contact angle θ_o at the beginning of the wetting pro-cess (at t = 0) distilled water and glycerol was used in the calculation of surface energy. The

relative error of the surface energy determinations was 1% for the overall, dispersive and polar components of the surface energy.

Analysing the samples from figure 4.7. it could be observed that in the case of all the irradiated samples, delamination occurs on the uncoated side and this delamination and hence the roughness is more intense in the case of the white sample.

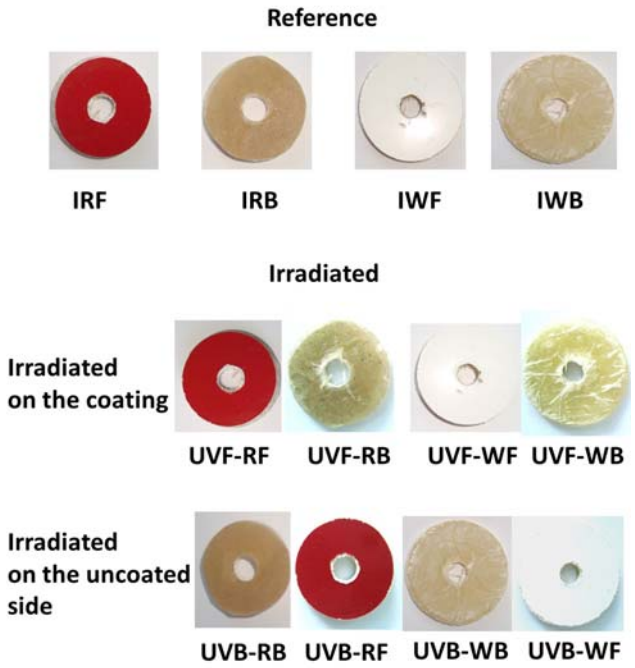

Figure 4.7. Photographic images of the irradiated GFPCs and reference [154]

Also, it could be observed that roughness increase on the uncoated side occurs also in the case of irradiating the sample on the coated side, meaning the UV radiation is able to penetrate into the mass of the material, promoting several structural modifications, also evidenced from FTIR spectroscopy analysis (figures 4.11. and 4.12.).

Table 4.5. illustrates the change in the colour parameters for the irradiated samples, by comparing to the reference. As it can be seen from Table 4.4., the UV irradiation generally determines an overall decrease of the L* parameter, associated with the lightness. This decrease could be correlated with the degradation of the material. Possible cromophore groups formation and π electrons conjugation (O-H, C=O, C=C) on the surface sample, under UV irradiation, determined the darkening of the material colour.

More intense degradation of material means higher number of cromophores that lead to more intense and darker colour. In CIELAB system this situation is described by L* parameter decrease. The most pronounced decrease of the lightness parameter is registered for the uncoated side of the samples exposed to UV, for which also the strongest delamination occurred. UV radiations also determine on the opposite side of the sample a decrease in the lightness parameter, probably due to structural rearrangements of the material.

Table 4.5. Color parameters differences for irradiated samples irradiated on various sides [154]

Irradiation	Photo position	ΔL^*	Δa^*	Δb^*	ΔE^*
UVF	RF	-1	1	-2	2.44
	RB	-5	-13	4	14.49
	WF	0	0	0	0
	WB	2	-9	13	15.93
UVB	RF	2	-2	0	2.82
	RB	-6	1	0	6.08
	WF	-1	-1	-2	2.44
	WB	-8	0	-3	8.54

When irradiating the samples on the coating, a total colour modification (ΔE*) increase of the coating is observed for the red sample, while in the case of the white-coated sample the

colour is maintained. On the opposite face of the samples irradiated on the coating, significant colour modifications occur, towards green (more pronounced for the red sample) and towards yellow for the white sample. Also, the total colour modification of the white sample on the uncoated side, opposed to irradiation, is the highest, which could serve as an additional information that white sample is more prone to degradation than the red sample.

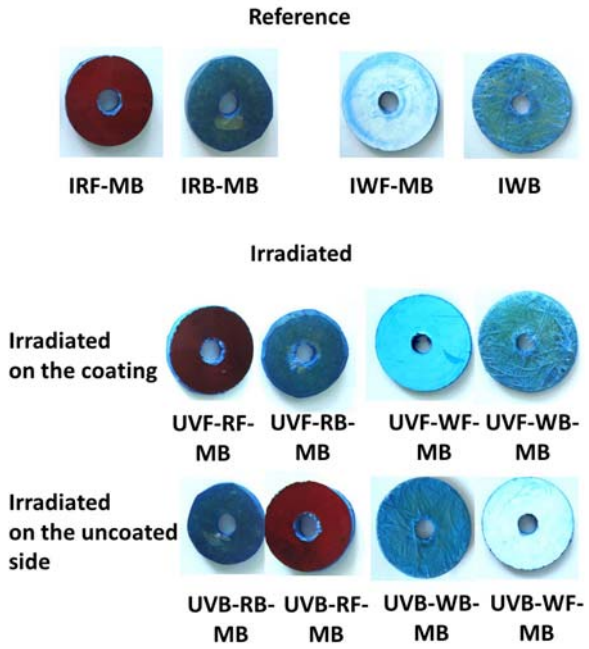

Figure 4.8. Reference and irradiated samples stained with MB [154]

When irradiating the samples on their uncoated sides, a more pronounced modification in ΔL* occurs, while for the opposite side of the irradiation, minimal colour modifications occur, more notably for the white sample, towards blue.

The photographic images of the reference (non-irradiated samples) and UV-aged samples treated with methylene blue presented in figure 4.8. and table 4.6. clearly indicate that surface of the samples is more polar, owing to an increase in the blue colouration of the samples after irradiation, on both sides. The differential increase in polarity of the samples after irradiation proves useful in enhancing several colour differences between the irradiated samples and the reference, thus increasing the sensitivity of the proposed image analysis method. After irradiation, the colour modifications that occur on the irradiated side are almost double by comparing with the non-irradiated sample.

The most important colour modification occurs for the UVB-WB-MB sample.

Table 4.6. Colour parameters difference of the initial and irradiated samples immersed in MB in comparison with the (1) initial non-irradiated samples and (2) initial non-irradiated samples immersed in MB [154]

Sample	Photo position	ΔL^*		Δa^*		Δb^*		ΔE^*	
		1	2	1	2	1	2	1	2
Non-irradiated	RF-MB	-13	-	-24	-	-28	-	39.10	-
	RB-MB	-33		-18		-44		57.87	
	WF-MB	-5		-17		-13		21.97	
	WB-MB	-25		-16		-53		60.74	
UVF	RF-MB	-18	-5	-39	-15	-35	-7	55.40	17.29
	RB-MB	-29	4	-19	-1	-50	-6	60.84	7.28
	WF-MB	-13	-8	-38	-21	-26	-13	47.84	25.96
	WB-MB	-26	-1	-22	-6	-48	5	58.85	7.87
UVB	RF-MB	-15	-2	-30	-6	-30	-2	45	6.63
	RB-MB	-36	-3	-14	4	-54	-10	66.39	11.18
	WF-MB	-1	4	-16	1	-8	5	17.91	6.48
	WB-MB	-34	-9	-14	2	-61	-8	71.22	12.20

In case of the unstained samples, possible light reflection on the coated surface due to the glossiness determines small variations of the colour parameters on both white and red samples.

The adsorbed MB is able to increase the colour differences between the reference and the red sample irradiated on the coating with 600% and respectively 270% in the case of the sample irradiated on the unprotected side.

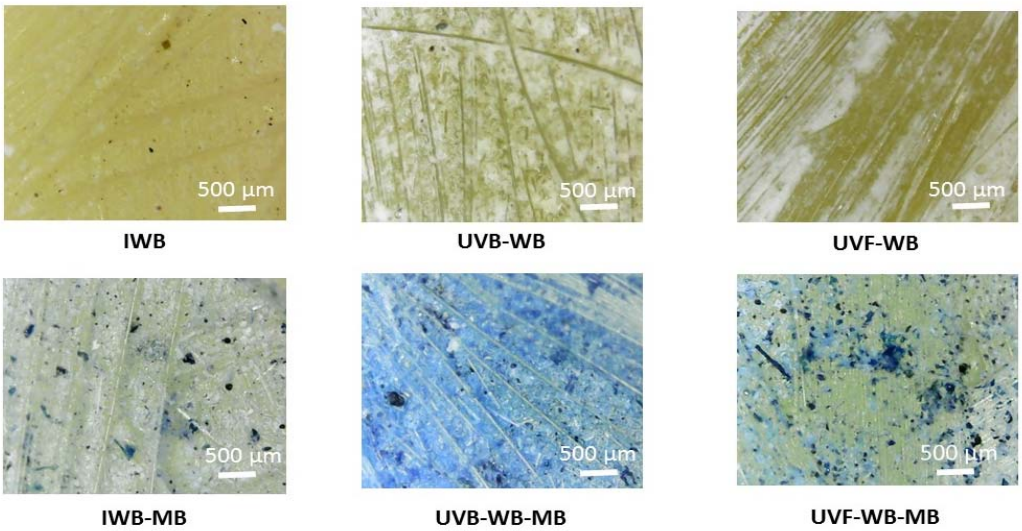

Figure 4.9. Microscopic images of the unstained and MB-stained initial and UV-irradiated white samples on the unprotected side (500 x magnification) [154]

The information regarding the increased susceptibility of the white sample to UV degradation is also maintained in the case of MB staining. Also, by using MB staining technique it is possible to increase the colour differences between the two faces of the samples irradiated on one side, especially for the white sample.

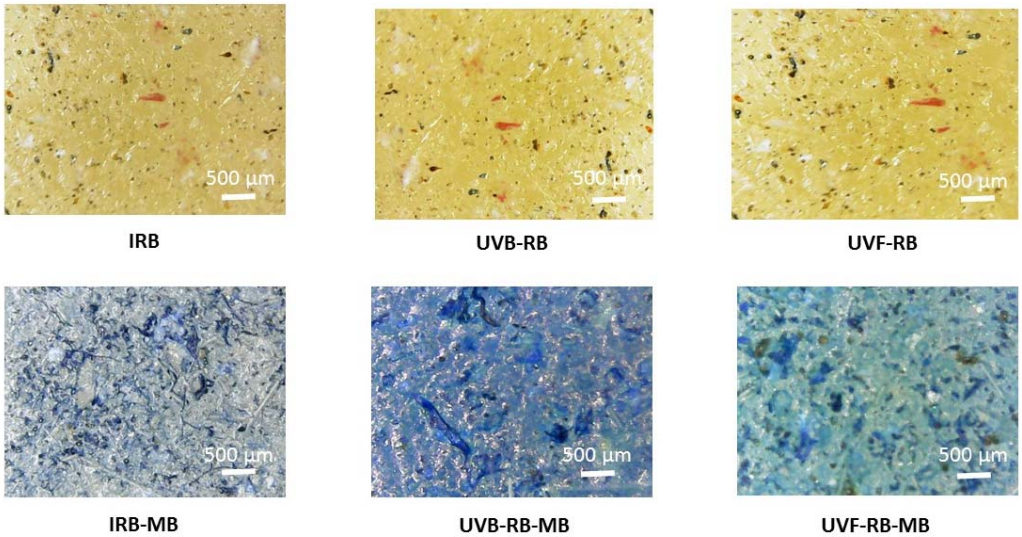

Figure 4.10. Microscopic images of the unstained and MB-stained initial and UV-irradiated red samples on the unprotected side (500 x magnification) [154]

Delamination of the unprotected surface on irradiation for the white sample could be better observed from the optical microscopy images, presented in figures 4.9. and 4.10. In the

case of the initial reference sample, uniform embedding of the glass fibre rowing into the resin could be observed. In the case of the initial red sample, a higher initial surface roughness could be observed, due to the presence of surface microdefects (pores, cracks, etc.).

Table 4.7. Static friction coefficients, average roughness and percental water uptake of the GFPCs [154]

Sample	μ_s	R_a	Sample	Δm_{eq} (%)
IRF	0.1950	2.34	IR	0.534
IRB	0.1411	13.14		
IWF	0.1719	4.52	IW	0.775
IWB	0.1773	27.32		
UVF-RF	0.2024	2.46	UVF-R	0.739
UVF-WF	0.1702	14.38	UVF-W	0.975
UVB-RB	0.2058	16.11	UVB-R	0.807
UVB-WB	0.1720	42.33	UVB-W	1.077

Irradiation of the samples determines delamination of the glass fibres in the case of the white-coated samples and an increase in the porosity of the red-coated samples, as well as an overall increase in the colouration of the oxidized surface when immersed in MB.

Delamination is also sustained by the values of the average roughness of the composite, determined by the image analysis method, as described papers [122], [123], as well as from the values of the friction coefficient, both presented in Table 4.7.

Assuming that static friction coefficient is direct proportional to the roughness of the composite surface, it could be observed from Table 4.7. that irradiated samples with the higher roughness (higher friction coefficient) are the ones irradiated on the unprotected side.

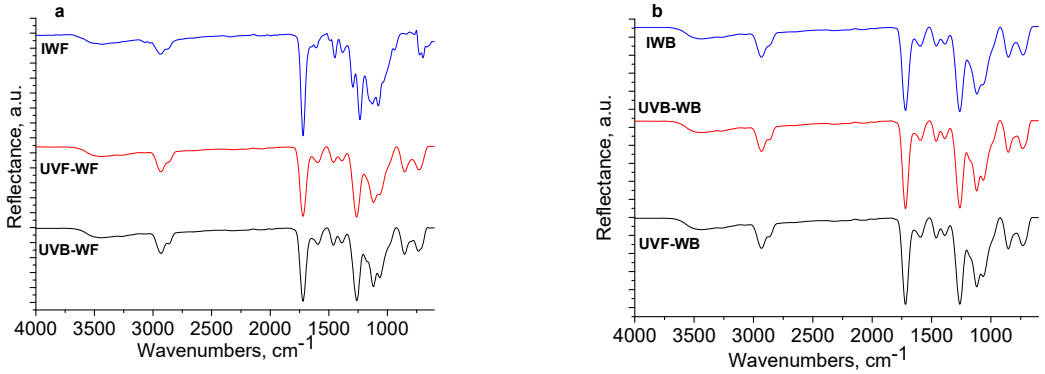

Figure 4. 11.(a): FTIR spectra of the initial and UV-exposed white samples for the coated side; (b): FTIR spectra of the initial and UV-exposed white samples for the uncoated side [154]

From the data presented in Table 4.6., it could be concluded that most affected by UV-irradiation are the white samples, at irradiation on the unprotected side. For all of the samples leaching of ionic compounds into distilled water has been observed, by monitoring the electrical conductivity of the storing water at determined time intervals, using a Consort C835 multiparameter analyzer. The irradiated samples eliminate more ionic compounds into the storing water. The white sample, irradiated on the unprotected side evidenced the higher percentual water uptake. Still the water adsorption values remain at a low value (<1.2%) by comparing to the classic hydrophyllic materials. The FTIR spectra of the initial and UV-

irradiated samples on both the coated and uncoated sides (figures 4.11. and 4.12.) reveal several information regarding the structural modifications that occur on the surface of the samples. The composites analysed on the coated face (figures 4.11.a and 4.12.a) present typical bands ascribed to acrylic resins.

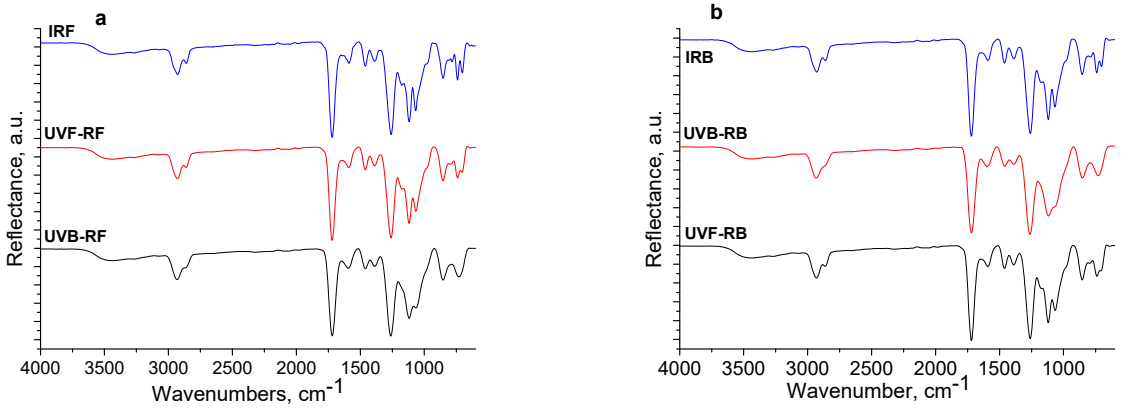

Figure 4.12(a): FTIR spectra of the initial and UV-exposed red samples for the coated side; (b): FTIR spectra of the initial and UV-exposed red samples for the uncoated side [154]

The weak absorption from ~3439 cm^{-1} and 1601–1639 cm^{-1} corresponds to O-H stretching and bending vibration, and respectively to physic-sorbed moisture [136]. The two broad bands in the 2854–2912 cm^{-1} interval, correspond to alkyl stretching modes and the sharp intense stretching vibration at 1721 cm^{-1} is ascribed to C=O groups. The several distinct absorption bands from 1150 cm^{-1} to 1240 cm^{-1} can be attributed to the C–O–C stretching vibration modes from the aliphatic acrylate polyester. The bands from 1388 cm^{-1} to 724 cm^{-1} can be attributed to the α-methyl group vibrations. The band from 987 cm^{-1} is the characteristic overtone absorption vibration of acryl resins (fingerprint band), together with the band at 1082 cm^{-1} [137], [138]. The band at 1441 cm^{-1} can be attributed to the bending vibration of the C-H bonds of -CH_3, whereas the band at 845 cm^{-1} could be ascribed to the inorganic filler from the coating [92].

Regarding the initial composites analysed on the uncoated side (figures 4.11.b and 4.12.b), typical aromatic polyester bands could be observed. The band centred at ~3445 cm^{-1} (IWB) and ~3451 cm^{-1} (IRB) is related to the stretching vibration of O-H groups [139]. As this stretching vibration is shifted to higher wavenumbers for the case of the IRB composite, a stronger interaction of the polyester matrix with the glass fibre could be possible, accounting for the higher UV resistance of the red-coated composite. The weak bands from 3075 cm^{-1} (IWB) and 3078 cm^{-1} (IRB) could be assigned to the aromatic C-H vibrations. The bands in the 2840–2960 cm^{-1} could be ascribed to the C-H stretching vibrations of the aliphatic alkyl groups from the polyester matrix. A sharp intense band attributed to C=O stretching vibration could be observed at 1721 cm^{-1} (IWB) and 1728 cm^{-1} (IRB). The bands from 1593 to 1490 cm^{-1}, weaker in intensity, could be assigned to different C-H vibration modes from the aromatic ring and the bands located at 1423 and 1378 cm^{-1} may correspond to the scissoring and rocking vibration modes of the alkyl groups. The strong sharp band occurring at 1268 cm^{-1} (IWB) and respectively 1279 cm^{-1} (IRB) is attributed to the twisting vibration mode of CH_2 groups [140], [141].

The bands at 1106 and 1065 cm^{-1} are attributed to –C-O stretching vibrations of the aromatic polyester and the bands from 850 to 729 cm^{-1} could be attributed to the aromatic ring out of plane bending and to the mono-substituted aromatic ring stretch [142].

After UV irradiation, several structural modifications occur. On the protective coating, an overall increase in the intensity of the OH band could be observed, probably due to the formation

of several polar compounds (alcohols, hydroperoxides) by chain scission promoted by the 254 nm UV radiation. The formation of those polar compounds determines the overall increase of the moisture content of the composites, as determined from the intensity increase of the band at 1603 cm^{-1} as well as an increase in the methylene blue adsorbed amount. An increase in the intensity of the band at 845 cm^{-1} ascribed to the inorganic filler could be due to the overall structural modifications of the coating, namely the quantitative reduction of the organic component and/or the modification of the IR absorption coefficient of the material.

The highest relative intensity modifications of the IR absorption bands occur in the case of the white coating, in good agreement with the colour image analysis based on the adsorbed MB amount (figure 4.13.a and table 4.7.) and the higher ratio between the polar and the dispersive components of the surface energy (γ^p/γ^d) (figure 4.13.b) [142].

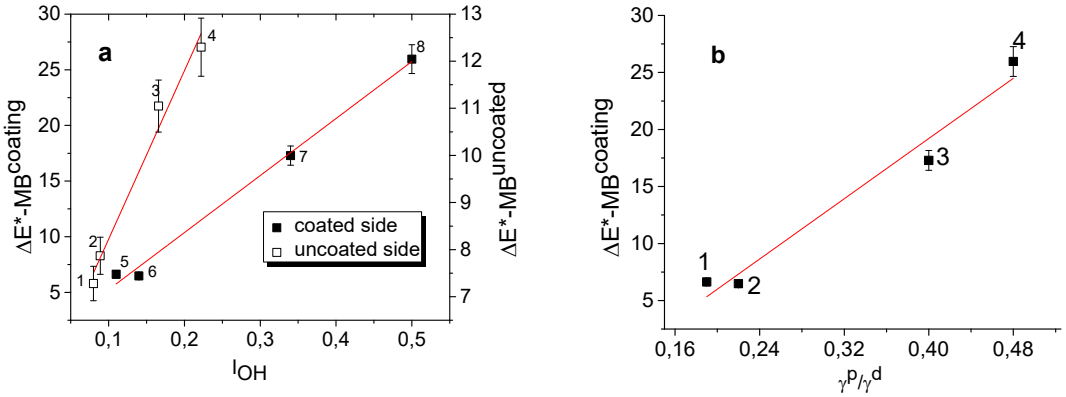

Figure 4.13. Correlation between total colour modification for the composites stained with MB and (a): I_{OH}; (b): surface energy; 1: UVB-RF; 2: UVB-WF; 3: UVF-RF; 4: UVF-WF; 5: UVF-RB; 6: UVF-WB; 7: UVB-RB; 8: UVB-WB [154]

When irradiating the samples on the unprotected side, it could be noted that several modifications occur on the coating, mainly in increasing the ratio (IOH) between the absorption intensity corresponding to the OH groups (I3445–3451) and the absorption intensity of the band at centred 2900 cm^{-1} (I2900).

On the uncoated side, the UV irradiation determines the increase in the polarity of the surface, as determined from the higher relative increase of the intensity corresponding to the OH absorption bands at 3445–3451 cm^{-1} and 1610 cm^{-1}, attributed to the free-adsorbed water. The increase is more pronounced in the case of the white-coated composites. Also, a 3.4% increase of the carbonyl absorption band intensity reported to the band centred at 2900 cm^{-1} could be noted in the case of the UVB-WB sample, in comparison with the initial sample, which could be due to the supplementary oxidation of the material, promoted by chain scission and/or oxidation of the terminal part of the crosslinked resin.

In the case of the UVB-RB sample, minimal increase of OH and carbonyl absorption intensity could be observed (1.3–2%) in comparison with the IRB sample, reported to the band centred at 2900 cm^{-1}. Minimal modifications of the aforementioned absorption intensities occur in the case of the FTIR spectra of the UVF-RB composite, due to the higher UV-screening efficiency of the red protective coating, in comparison with the white coating.

As it can be seen from table 4.8., a linear dependence of ΔE* of the OH band relative intensity and of the γ^p/γ^d ratio for the MB-stained composites exists. Related to this aspect, the sensitivity of the coloristic method is higher for the uncoated side of the GFR-PCs, with respect to the increase of IOH, as demonstrated from the higher slope of the linear dependence in this case (table 4.7.).

Table 4.8. Fitting parameters for the linear dependence between ΔE^* and I_{OH}, respectively γ^p/γ^d [154]

Correlation type	Samples analysis position	Dependence: y = a + b·x		
		a	b	R^2
FTIR-Coloristic	Coated side	4.64	35.76	0.960
	Uncoated side	0.13	51.22	0.997
Surface energy-Coloristic	Coated side	2.11	66.00	0.973

This could be due to the higher amount of adsorbed methylene blue on the uncoated side, correlated with the higher surface roughness and chemical modifications that occur on this side. As the values of the contact angles (and hence the surface energy) is significantly influenced by surface roughness, so the dependence of ΔE^* of the γ^p/γ^d ratio has been discussed only for the coated side. The coating is more resistant to UV degradation, as demonstrated from the lower values of the surface energies ratio.

4.3. Considerations about the composite materials obtained from calcite dust and recycled polyolefins

Since the lifetime of a product depends on the usage and of the stabilising system used, it may be noted that it is possible to stabilise polyolefins so that they maintain their mechanical properties for a large period of time. Calcite mining and process industry represent one of the most promising business areas of the mining sector, with a mean growth in the world production of approximately 6% per year in the 2005-2015 period. Non-hydrated calcium carbonate in crystalline form (calcite) constitutes a base material, of metamorphic or sedimentary origins, frequently used in the construction industry, either as such (marble) or as an admixture with other types of silicate-based minerals (as in the composition of cement pastes and clinkers) [143], [144]. Taking into account that generally, only about 30% of calcite material is effectively used, the rest being discarded as chips, dust or slurry in the cutting, polishing, processing and grinding processes, with detrimental effect on the population health, flora and fauna, new efficient ways of calcite secondary raw material utilization are needed. Nowadays, only about 40% of the total amount of calcite wastes (100 billion tons/year) is being efficiently recycled, by their inclusion in cementitious materials, bricks or as filler in ceramic or polymer matrix composites [145].

The majority of the studies from the reference literature have indicated the use of amorphous calcium carbonate as filler for PO composites, while crystalline calcium carbonate (such as that resulted as waste from marble processing industry) has been used on a lower extent in obtaining composites with virgin PO matrix, as it can be seen from the dynamics of the number of publications in the domain, on a 10 years' span (figure 4.14, source: Scopus database).

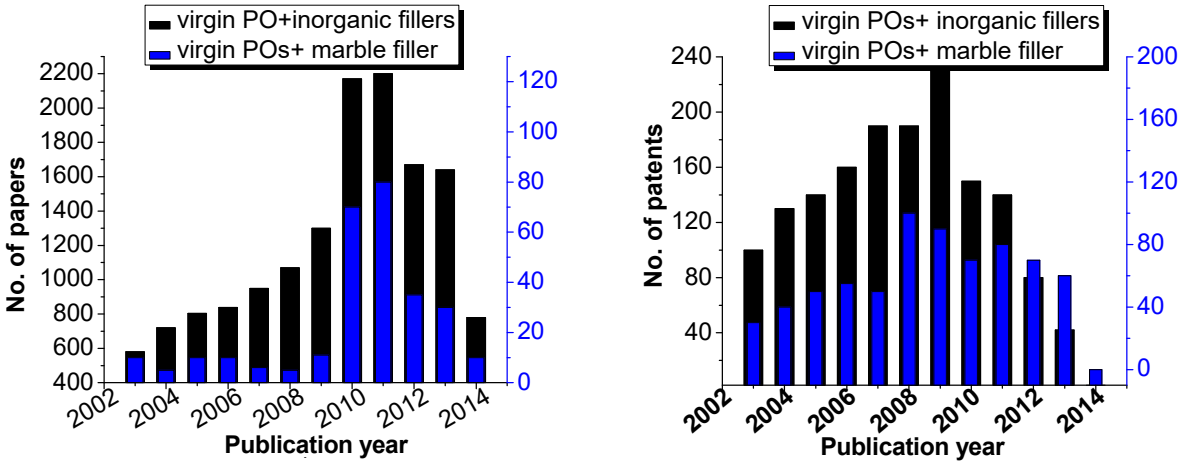

Figure 4.14. Number of publications dynamics in the domain of PO composites and inorganic fillers (10 years' span) [155]

By analysing the reference literature, it could be observed that there are few studies concerning the obtaining of composites with recycled polyolefin matrix and crystalline marble powder. Due to the recycled polyolefins (POw) lower both molecular mass and crystallinity, these materials could be actually more compatible with marble, in comparison to the virgin polyolefins. Using marble as filler presents some elements of difficulty. Firstly, the limited compatibility of the crystalline filler with the thermoplastic polymer matrix, as well as its tendency to agglomerate leads to the obtaining of brittle and low-wear resistance composite materials. Secondly, a high dispersion of the crystalline inorganic filler in the molten polymer is necessary.

Calcite powder is highly abrasive and determines the wear of the raw-material processing equipment [96], [97]. In order to limit the abrasivity of the calcite powder, the particles are ground at a diameter smaller than 5μm and are treated at the surface with tensioactive compounds, in order to improve their dispersion and their compatibility with the thermoplastic polymeric matrix [98], [99].

Traditionally, stearic acid, calcium stearates, fluoro-alkoxysilanes or amino-alkoxysilanes are added in a weight ratio of 5%, reported to the calcite [96]. Recent studies employ the use of nano-sized calcite particles of 40-50 nm diameter and additives in a weight ratio of 8% reported to the calcite [99], [146].

Table 4.9. highlights some recent research in the domain of calcite and polyolefin composites obtaining, in terms of matrix filler and additives characteristics and ratios, as well as of the operational parameters used.

Table 4.9. Operational parameters for calcite-PO composites (reference literature study) [155]

Matrix characteristics	Filler characteristics	Compatibilizer	Operational parameters	References
PP, ρ=0.9 g/cm^3; MFI= 11 g/10 min at 190°C	Marble dust; d_{ap}=2.7-2.95 g/cm^3, 25% ratio reported to PP	Sodium palmitate at 1.3 and 5% loading reported to the filler	Twin screw extruder, v_{mix} = 50 rpm; t_{mix}=25 min; T_{mix}= 200 °C	[97]
PP homopolimer, F41 type	Marble dust, 0-10% ratio reported to PP	Oleic acid at 7% loading reported to the filler	Twin screw extruder, v_{mix} = 60 rpm; t_{mix} =25 min; T_{mix}= 180-240 °C	[147]
PP, ρ=0.91 g/cm^3; MFI= 2.5g/10 min	Marble dust, 20% ratio reported to PP	Stearic acid as coating agent for	Twin screw extruder, v_{mix} = 60 rpm;	[148]

at 230°C		marble (8%) and p-tertbutyl aluminium benzoate	t_{mix} =15 min; T_{mix}= 180-200 °C	
PP homopolimer F401 type, propylene-ethylene copolymer K8003 type	Marble dust, 10-15% ratio reported to PP	γ-aminopropyl-triethoxysilane 25% in acetone	Twin screw extruder, v_{mix} = 140 rpm; t_{mix} =45 min; T_{mix}= 180-200 °C	[99]
PP block-copolymer, ρ=0.91 g/cm^3; MFI= 2.16g/10 min at 230°C	Marble dust, 5-15% ratio reported to PP	Maleic anhydride-grafted PP, X1343 type, 2-4% loading reported to the matrix	Twin screw extruder, v_{mix} = 200 rpm; t_{mix} =45 min; T_{mix}= 230 °C	[98]
PP block-copolymer, ρ=0.91 g/cm^3; MFI= 2.22g/10 min at 230°C	Marble dust, 25-35% ratio reported to PP	γ-aminopropyl-fluoroethoxysilane 15% in toluene	Twin screw extruder, v_{mix} = 180 rpm; t_{mix} =35 min; T_{mix}= 220 °C	[99]
PP homopolimer F401 type	Marble dust; D= 20 μm at 10% ratio reported to PP	Calcium neoalkoxyzirconate (NZ12L)	Twin screw extruder, v_{mix} = 250 rpm; t_{mix} =35 min; T_{mix}= 200 °C	[96]

As it can be seen from table 4.8., the majority of the studies cited in the reference literature make use of fatty acids salts as coating agents and compatibilizer between calcite and polyolefins. Several authors reported however that calcium carbonate actually catalyses the decomposition of the fatty acid at temperatures above 150°C, thus leading to composites with poor mechanical properties [149].

Alkoxysilanes and fluoroalkoxysilanes are generally regarded as efficient compatibilizer between PO and calcite, but they have the disadvantage of being economically inefficient due to their high price, and also possess an environmental risk, due to their dissolution in volatile organic solvents [99], [146].

Further research is still needed in order to find an efficient and ecologic compatibilizer between PO and calcite, with low specific consumption, optimum interfacial adhesion between the components and improved chemical and thermal stability.

4.4. Conclusions

The study **Investigation on the friction coefficient of the composite materials obtained from plastics wastes and cellulosic fibres** reveals that the use of polyolefinic waste fractions separated from municipal solid waste polymers, as such, as a matrix for fibre composites can successfully replace polypropylene and its fibre composites in applications involving friction processes.

The study **Glass fibres reinforced polyester composites degradation monitoring by surface analysis** has been aimed at demonstrating the usefulness of a colorimetric method based on CIELab colour space parameters analysis by photographic image analysis in assessing the surface modifications that occur in different types of E-glass fibre-reinforced ortophtalic polyester composites submitted to accelerate artificial UV-ageing. In order to test the general applicability of the proposed method, two composites with different acryl-based coatings, of red and white colours have been used. The innovative approach of the study is to enhance the colour modifications that occur on the surface of the composite by adsorption of an ionic dye, namely methylene blue. The total colour modifications promoted by the adsorption of this dye on the

surface of the composite has been found to be directly proportional to the relative intensity of the OH band, calculated from the FTIR spectra of the samples and also with the ratio between the polar and the dispersive component of the surface energy, and are with 5–50% higher than in the case of the modifications corresponding to the non-treated surface. Owing to the direct proportionality between the total colour modification parameter and the polarity of the analysed surface, the proposed method can assess the degradation degree of a composite material easier, faster and cheaper than the traditional ones.

The increasing worldwide demand for plastic products and crystalline inorganic raw material-based construction materials has led to the constant build-up of wastes in the environment, with detrimental effects on the biosphere. Even if recent regulations enforce more efficient disposal methods for wastes, still a lot of effort has to be made in the domain of polyolefins and calcite wastes recycling, through obtaining composite materials with calcite as filler. Several bottlenecks are to be addressed, such as the limited compatibility between the polymer and the filler, due to their profound dissimilar chemical nature, the high tendency of calcite powder to agglomerate, coupled with its high abrasivity, which leads to an increased equipment wear and specific energy consumption. An ecologic and efficient compatibilizer, with high thermal and chemical stability could lead to the obtaining of high-value materials, with optimal mechanical properties and improved stability, thus leading to an efficient waste valorisation technique and a sustainable society development.

Chapter 5

POLYMERS MOULDING

This chapter presents two applications of polymer flow inside mould in order to study the influence of shape on the technological and stress results.

First application study the influence of shape on the material consumption, part deformation and injection time [150]. The software used for this study was COSMOSXpress.

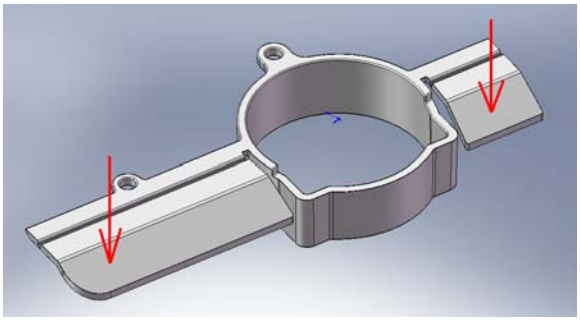

a)

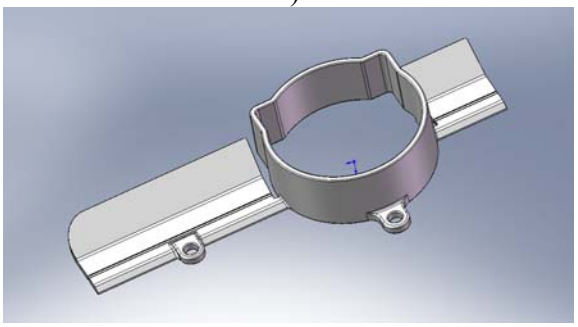

b)

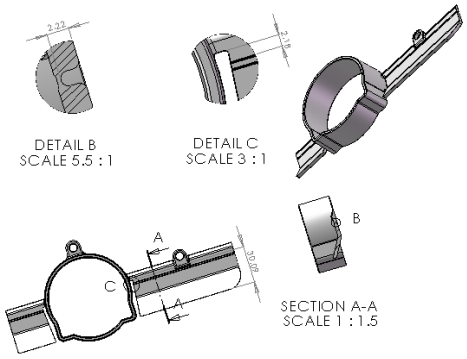

c)

Figure 5.1. 3D model of original part design for articulated flange: front view with loaded side brackets (a), rear view (b) and details (c) [150]

The materials of the part used in this study were PA 66, popular in every major market using thermoplastic materials. Due of its excellent balance of strength, ductility and heat resistance, PA 66 is an outstanding candidate for metal replacement applications.

The requirements are the tubular inner diameter and the limitation of the bigger bracket deformation under 10 N bending force limited to 4 mm. For original articulated flange the volume is 28.2567 cm^3 at a filling time 0.79s. The maximum bending deflection is 26mm. Figure 5.2 presents the deformation and the filling time for the original articulated flange.

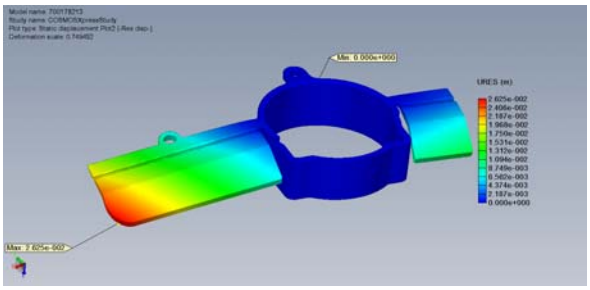

a)

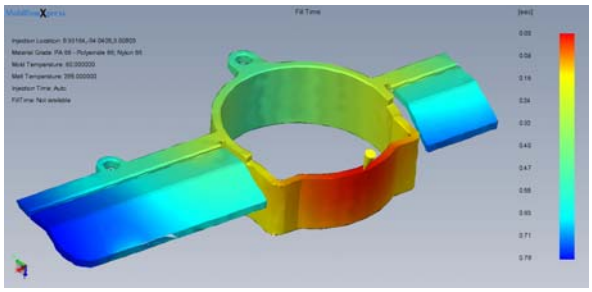

b)

Figure 5.2. Deformation (a) and filling time (b) for the original articulated flange [150]

The first design change of original articulated flange was for detail C and consists in channel shortening from 30.09 mm to 27.74 mm (2.18 mm dimension was removed). For this first change the volume was 28.3001 cm^3 at 0.8s filling time (figure 5.3). The deformation bending under the loading force was 21 mm. Therefore, the growth of the raw material volume was 0.15%, of the filling time 1.26%, obtaining a decrease of the arrow bending with 19.23%.

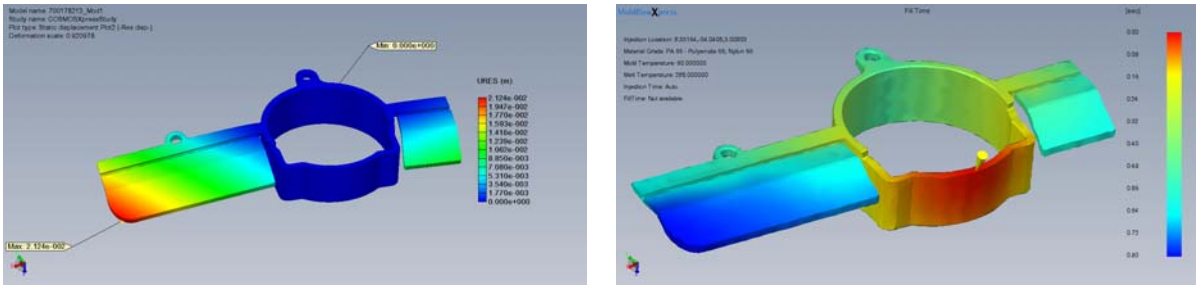

a) b)

Figure 5.3. Deformation (a) and filling time (b) for articulated flange with change 1 [150]

The second design change was removing the channel (2.22 mm); also the channel length decrease from 27.74 to 24.18 mm. For the part with the second modification the volume is 28.7312 cm^3 for 3.08s filling time having the bending of 10.5 mm. Therefore, the growth of raw material was 1.67%, of filling time 289.87% obtaining a decrease of the bending deformation of 59.61%. Deformation and filling injection time are presented in figure 5.4.

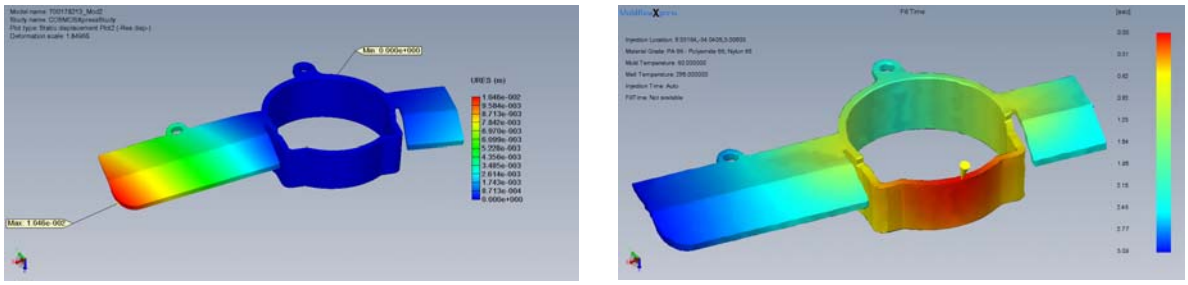

a) b)

Figure 5.4. Deformation (a) and filling time (b) for articulated flange with change 2 [150]

The third change is represented by adding two symmetrical ribs located underneath the two brackets. The part drawing is presented in figure 5.5. For the part with the third change the volume was 28.9124 cm^3 and the filling time was 1.51 s with 5.8 mm bending (figure 5.7). Therefore the growth of the row material volume was 2.32%, of the filling time 91.13% and the decrease of the deformation was 77.69%.

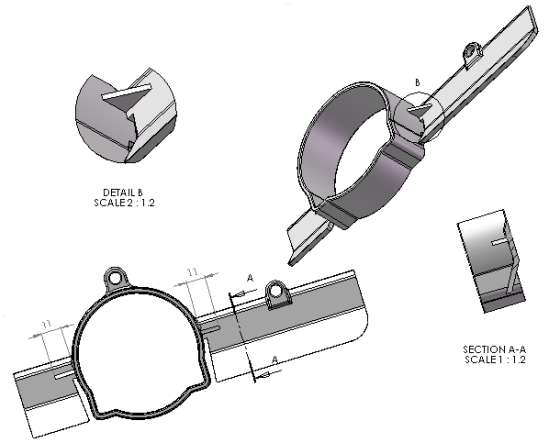

Figure 5.5. Articulated flange drawing with change 3 (adding two identical ribs underneath the two brackets) [150]

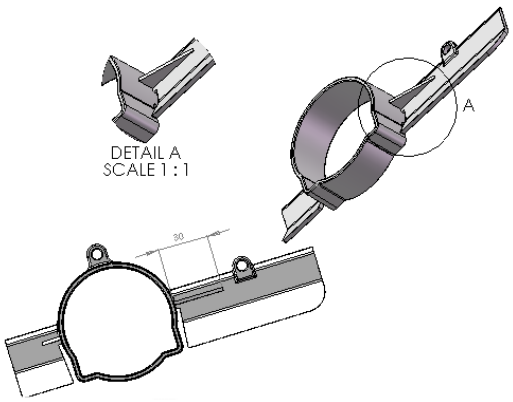

Figure 5.6. Articulated flange drawing with change 4 (replacement of the rib situated under the long bracket with another one bigger) [150]

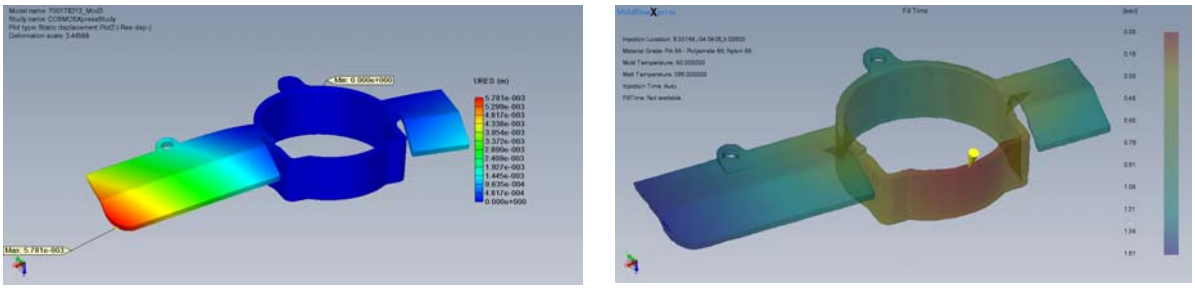

a) b)

Figure 5.7. Deformation (a) and filling time (b) for articulated flange with change 5 [150]

Although the deformation value is close to the desired value the change must continue. The fourth change is the replacement of the rib situated under the long bracket with another one bigger. The part drawing is presented in figure 5.6. For the part with the fourth change the volume was 29.1013 cm^3 and the filling time was 0.9 s with 3.857 mm bending (figure 5.8). Therefore the growth of the row material volume was 2.98%, of the filling time 13.92% and the decrease of the deformation was 85.16%.

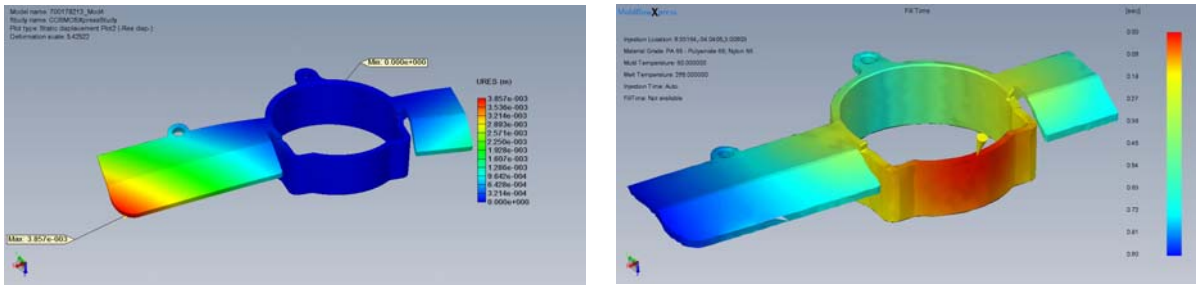

a) b)

Figure 5.8. Deformation (a) and filling time (b) for articulated flange with change 5 [150]

To achieve the goals of the study, there were made successive changes in the part configuration, especially in the stress concentrators' areas. Although the filling time was affected with nearly 14% and the raw material consumption was increased with almost 3%, the bending deformation was substantially decreased, the part fulfilling the imposed conditions.

Second application study the influence of shape on the mouldability and strength. The commercial software that simulate the mould filling, start with 3D modelling part, meshing, selecting the moulding process, selecting the material and setting of injection location. [151]. After analysis, the obtained values are for the filling time, pressure, velocity average, orientation at core, freezing time, bulk temperature, weld lines and air traps (Moldflow, 2002).

Using the Automatic Injection Time check box, the analysis will find the injection time which gives the lowest injection pressure (figure 5.9). The variation of injection pressure against injection time has two influences:

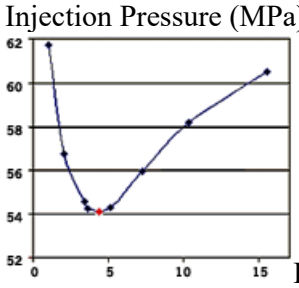

Figure 5.9. Injection pressure vs. injection time [151]

- as the injection time increases from zero, the pressure required to force the molten plastic through the part decreases;
- as the injection time increases, another factor affects the curve; as the flow rate of the molten plastic decreases, its temperature also decreases. The explanation is due to the fact that as the flow slow down, the frictional heating decreases. The decrease in polymer temperature also increases the viscosity, requiring more pressure to fill the part.

The study was done using ABS polymer, with excellent surface appearance, strength, stiffness, toughness, and chemical resistance. This kind of polymer is used for interior trim in automotive industry, computer case, other electronics and appliances.

The main goal in selecting polymer injection locations is to ensure that all flow paths in the model fill at the same time (balanced flow paths). The positioning of injection locations plays an important role in the effects of material orientation on deformation of the parts. In some cases, changing the injection location position is the only way of controlling orientation effects to produce a satisfactory design. The essence of a good position is to avoid problems associated with over packing, such as variation in shrinkage and product sticking in the cavity.

These results show the flow path of the polymer through the part by plotting contours which join regions filling at the same time. These contours are displayed in a range of colours from red, to indicate the first region to fill, through blue to indicate the last region to fill. A short shot is a part of the model that did not fill and will be displayed as translucent. By plotting these contours in sequence time, the given impression is of plastic actually flowing into the mould [152], [153].

The study was done on the simple part, a luggage cover (480x380x40 mm, thickness 2mm), considered initially as flat shell, adding successively ribs in different directions. There are analysed the filling time (s) and von Misses stresses (MPa).

Figure 5.9. shows the flat luggage cover, without any filling problems (4.48s filling time, figure 5.9.b), is not strong enough at any pressure applied in the middle of the part. The material consumption is small, the mould is cheaper, easy to fill (software message: “your part can be easily filled using the current injection locations”), but no resistance at the 100N loading in the middle of the upper wall, resulting a big deformation.

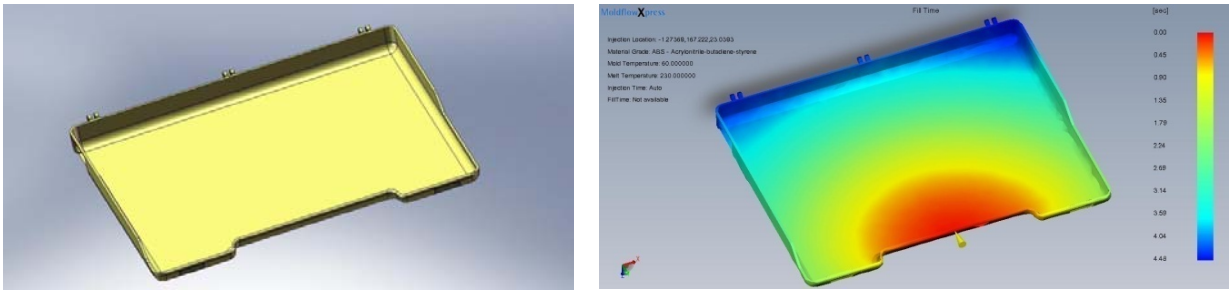

a) b)

Figure 5.9. Flat luggage cover (a) and flow simulation of flat luggage cover (b) [151]

Figure 5.10 shows luggage cover with 1.5 mm ribs on the flow direction (longitudinal). Filling was improved (4.16s), also the mechanical characteristics of the part ($\sigma=2.15\cdot10^5$ Pa). As it was calculated, the increasing of the material consumption compared with the design of figure 2 is 11.49%. The mould price increase, fewer than 5%.

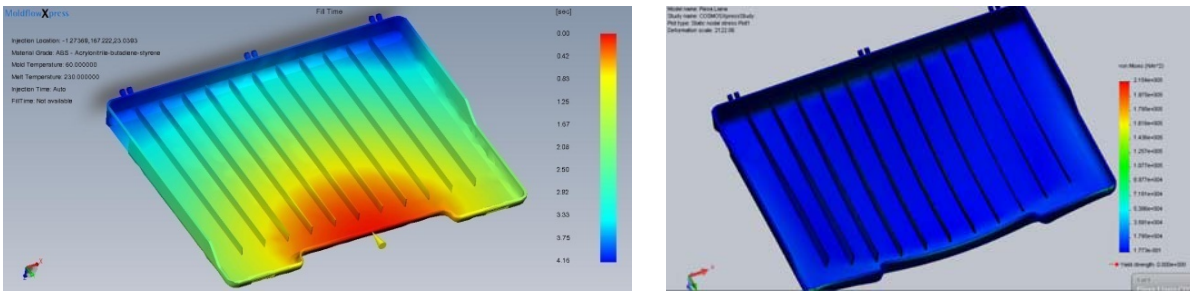

a) b)

Figure 5.10. Luggage cover with longitudinal ribs (a) and flow simulation (b) [151]

In figure 5.11 there are added some ribs on the radial direction in order to improve the stress behaviour of the part ($\sigma=1.88\cdot10^5$ Pa). The part is much stronger, but the tool cost is increasing, the injection cost is increasing and the filling problems appear, all flow reports starting to be negative. The material consumption increases by comparison with the precedent situation with 8.2%. The mould price increase with other few percent against the previous version.

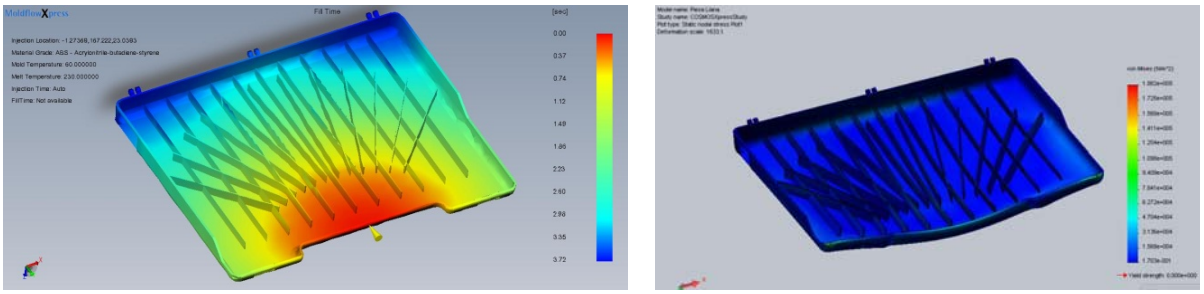

a) b)

Figure 5.11. Luggage cover with longitudinal and radial (a) and flow simulation (b) [151]

In the last case studied there are added also transversal ribs. The part toughness increases ($\sigma=5.1\cdot10^4$ Pa), but the filling problems persist. The material consumption increases with 27.8%.

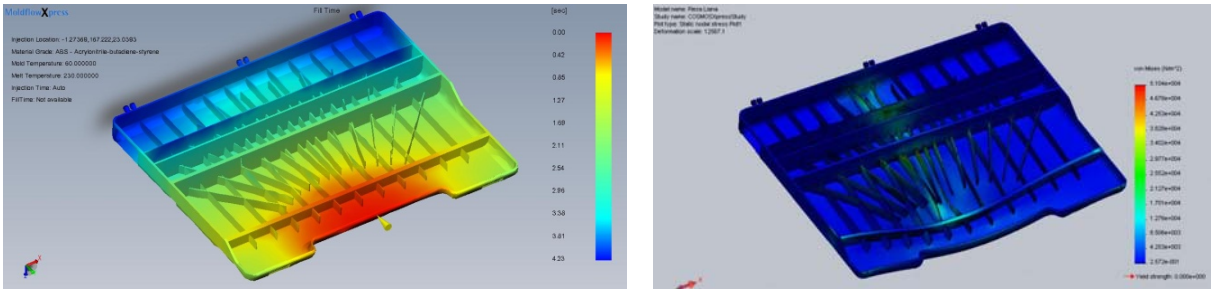

a) b)

Figure 5.12. Luggage cover with longitudinal, radial and transversal ribs (a) and flow simulation (b) [151]

This F.E.A. study emphasizes the relation between the thickness values, shapes, and ribs design. Depending on these, it was chosen the technology for the mould design and machining. The best compromise is the part design with longitudinal ribs, that still keeping a good balance between the material costs, tooling cost, filling time and stress behaviour.

B. EVOLUTION AND CAREER DEVELOPMENT PLANS

The career evolution is seen on two concurrent levels, filling one another, with synergic effects, one of them covering academic activities, and the other dedicated to research, both of them in the field of materials science and engineering.

Proposals for further research are based on the two subjects related to materials engineering, especially materials for environmental protection, introduced in the first five chapters:

- new materials for environmental protection with photocatalytic properties;
- composite materials from secondary raw materials.

New materials for environmental protection

This direction will investigate materials containing different nanoparticles, known for their activity against organic pollutants from waste waters. These nanoparticles can be immobilized in different building materials, which will be used in the depollution systems.

Papers submitted:

Photoactive polymer-cement composites for tannins removal from waste waters

Photoactive glazed polymer-cement composite

Photoactive polymer-cement composites for tannins removal from waste waters

TiO_2 nano-particles exhibit remarkable photocatalytic activity against organic pollutant from waste waters [158,164] but their separation from liquid media after photocatalytic process is a very difficult task.

The immobilization of TiO_2 on different supports could be a good solution to simplify cleaning stage after photocatalysis [165]. In this paper, two types of photoactive polymer-cement composites named macro-defect free cements (MDF) have been obtained both by embedding TiO_2 nanoparticles (Degussa P25) into the composite matrix and by photocatalyst deposition on the composite surface by dip-coating method (in two types of recipe).

Composites surface has been characterized by SEM and XRD and photocatalytic efficiency was determined against tannins from waste waters coming from woodworking industry. Tannins concentration was monitored by VIS-spectrophotometry, using Folin-Ciocalteu method.

All specimens evidenced photocatalytic activity. The process efficiency is dependent on the light wave length and of irradiation duration. The best results have been obtained when MDF containing embedded TiO_2 nano-particles was exposed to 254 nm light (92% after 6 h). Under higher wave length light irradiation (365 nm), the photocatalytic efficiency decreased at 48.2% for MDF containing embedded TiO_2 and at 39.85% for MDF, coated with TiO_2 film.

The obtained results are promising both from environmental protection point of view, taking into account the persistence of tannins in waste waters and the difficulties of their elimination by using classic methods and from the point of view of MDF properties improvement, taking into account its very large range of applications.

Research will be continued using ZnO and ZnO nano-powders with coupling.

Photoactive glazed polymer-cement composite

Heterogeneous photocatalysis is a surface process implying most commonly, a solid photocatalyst (a semiconductor) able to produce, under irradiation with energy equal or greater than its band gap, an electron-hole pair which can promote oxidation-reduction reactions involving the liquid or gaseous compounds from the contact media.

It was demonstrated that photocatalysis is very efficient in many processes related with the life standards in our society such as water and air quality (by advanced depollution of waste water, drinking water, and atmosphere), health maintaining (by bactericidal and self-sterilizing processes), clean energy sources use (photovoltaics, hydrogen production and solar cells), keeping aesthetic of buildings, bridges, tunnels and roads (by self-cleaning and antifogging processes) as well as ensuring a pleasant and healthy climate in cities (by elimination of the urban heat island by using superhydrophilic surfaces that may improve the heat transfer in liquid–vapor-phase transition) [158-160].

The most used photocatalyst is TiO_2 that is characterized by high stability, easy activation in ambient conditions, high catalytic longevity and reliability, non-toxicity, low costing and high availability. Being a surface process, photocatalysis using TiO_2 nano-powders is the most efficient, due to the very high contact surface of photocatalyst with the environment. However, recent findings concerning of adverse biological effects of metal oxide nanoparticles suggest a need to post-process for a minimal environmental release of TiO_2 after the application [161-163]. To overcome this drawback, immobilization of TiO_2 nano-powder on different supports became nowadays an important scientific issue.

The aim of the study is to obtain a new photoactive, water resistant material, by coating a high mechanical resistant macro defect free polymer-cement composite with a photoactive glaze obtained by mixing a commercial silicabased enamel with TiO_2 nano-powder. Silica based enamel was chosen as binder for TiO_2 to the MDF (Macro defect free cements) composite support, both to avoid the self-degrading of organic binders containing photocatalists under UV irradiation and to obtain a protective water and scratch resistant coat for MDF. The composite specimens were coated with photo-active pastes by brushing and then submitted to thermal treatment in an electric oven, at 1050° C for 30 minutes. Three groups of samples were used for testing. Group A contains samples immersed in methylene blue solution and submitted to UV irradiation aiming to monitor their photoactivity, group B containing initial samples, as reference for properties monitoring and group C containing samples immersed in methylene blue solution and kept in dark to monitor the adsorption process.

Efficiency of photocatalytic activity of this material was tested against methylene blue aqueous solution (4.4 mg/L). Influence of the photocatalyst concentration in the glaze paste, of contact time and wave length of the UV radiation on the photocatalysis process was studied. Surface of glazed material was characterized by optic microscopy, scratch test, SEM, XRD, and EDS. The paper is submitted for publication.

The opportunity to use solar energy, which is environmentally friendly, encourages the submission of a grant within the SFERA international projects (Solar Facilities for the European Research Area), with the purpose to use the heat treatment technique in MSSF (Medium Size Solar Furnaces) solar reactors which operate with 2m vertical axis parabolas, available at the PROMES-CNRS facility at Font-Romeu – Odeillo, France. The title of the project was *Improvement of MDF cements properties through metallic oxide coating using solar energy, Acronym SOL4COAT.* The mobility has taken place in September 2016.

Using solar energy in this process is a challenging issue; the main objective was to obtain coated MDF cements with improved properties: higher water resistance, good mechanical strength and photocatalytic activity, applicable both in waste water depollution and in air purification as well as a self-cleaning material with antimicrobial capacity.

Surface characterization analyzes are ongoing and the results will be compared with those obtained with a classical heat treatment furnace in the laboratory.

Research will be also extended to ZnO nano-powders on polymer-cement composite.

Composite materials from secondary raw materials

Composite plastic materials offer many advantages including design freedom, weight reduction, corrosion resistance, cost reduction, and production of complex aerodynamic and noise reduction devices.

Paper submitted:

Thermal and thermorheologic characterization of different polyolefin waste fractions

Due to recent EU environmental regulations regarding the biodegradability issues of polyolefins and the increasing in the recycling rate for this type of materials, thermorheologic parameters determination for plastic wastes is even more important than in the case of virgin polymers, because in this case the actual values of MFR (melt flow rate) is affected by the presence of polymeric impurities (due to inefficient separation), additives (dyes, plasticizers, stabilizers) or surfactants left over from the washing step of the waste material.

In this paper, the melt flow rate under different temperatures and piston loadings have been used to assess the rheologic and thermal behavior of two types of waste polyolefin materials, namely a fraction rich in HDPE and one with a high content in PP.

Two polyolefin-rich fractions consisting of household plastic wastes, provided by Rom Waste Solutions S.A., Bucharest, have been used in this study, namely a high-density polyethylene (HDPE)-rich fraction and a PP-rich fraction. The differential scanning calorimetry (DSC) thermograms of the two waste fractions have been recorded in the -160….500 °C domains with a NETZSCH DSC 200F3 instrument at 10 °C/min heating/cooling rate to determine the glass transition temperatures for the waste fractions components. MFR measurements have been performed with a Zwick Roel MflowC plastometer with standard die dimensions.

The proposed methodology, based on melt flow rate determination, aids in a better understanding of thermoplastic polymer melts through dies, phenomenon encountered in all extrusion processes. The decreasing of the melt viscosity as a function of temperature aids in improving the material flow and in obtaining a more uniform extrudate (filament), therefore supplementary information regarding the processing could be obtained.

Applicative research for new industrial products and technologies

Technical assistance activities for industrial companies from the central part of Romania and from abroad will be continued based on solid partnership relations.

The contract *Studies concerning the real time monitoring of laser welding/cutting process* with Technische Universiteit Delft and Reukema Blocq & Maneschijn BV, started in 2015 is in progress. We develop new possibilities of cutting and welding processes and the monitoring in real time.

Collaboration with the industrial company Rom Waste Solutions S.A., Bucharest is the contract *Determination of thermal and thermo-rheological behaviour of polyolefin waste as well as the density,* started in 2016 and in progress now. Among the company's objectives is the recycling of polymers waste, especially polyolefins (polypropylene and polyethylene). Since the characterization of polyolefins has been a subject studied over the years and presented in the research papers above, the company has requested support in the characterization of

polypropylene and polyethylene, as well as research on the obtaining of composite materials from recycled polyolefins and dust marble. Most research in this field relates to the use of amorphous calcium carbonate. But the company wants to use marble in a crystalline state. Studies will start in the coming period.

Concerning the academic activity, I will continue the collaboration with my colleagues from the universities Technische Universiteit Delft, Nederland and Las Palmas de Gran Canaria University, Spain, an old collaboration, started in 2005. I will collaborate with my colleagues from Romanian universities and from Research Centres too, to find new opportunities.

Together with the teachers from Delft we started a MOOC which is a European Course of Recycling. The recycling boom brings a need for the training of tens of thousands of students, engineers, managers and policy officers in the EU, and, in time, many more from the BRIC countries. The aim of the *European Course in Recycling* is to address this group of new entrants in the field with a low-cost, high-quality, flexible and interactive multimedia distant learning course which takes advantage of the unique knowledge base in technology and innovation, industry network, reputation and laboratory facilities of leading European universities in the field of recycling. The course is an initiative of the Delft Resources and Recycling chair. The concept of the course is to provide students from universities (particularly seeking minor programmes), engineers in industry as well as governmental/policy officers with a flexible and up-to-date course, designed by leading professors in the field. The course will allow participants to quickly acquire a professional level of understanding about selected subjects in recycling: technology, economics, social or policy-related issues. The combined course material represents about 3 months' full-time study (equivalent to 20 ECTS). The students interact with the multimedia course materials for a designated period of time without any intervention of tutors.

I will continue to add new knowledge by accessing Erasmus Program with partner universities from EU.

All the new knowledge and all the experience that I will rich each year through exchanges with teachers and specialists in the field of Materials Engineering I will processed and I will transmit to the students, on their own terms.

I will design new laboratory practise according to the results obtained in my research area and based on the existing equipment.

The themes of future research will be given to the students in collaboration with industry to find their applicability.

REFERENCES

[1] Plastics the facts, 2016, http://www.plasticseurope.org/documents/document/20161014113313-plastics_the_facts_2016_final_version.pdf

[2] Andrady A.L., Plastics and the environment, John Wiley & Sons, Inc., Hoboken, New Jersey, 2003.

[3] Plastics the facts, 2014, http://www.plasticseurope.org/Document/plastics-the-facts-2014.aspx

[4] Zhuo C., Levendis Y.A., Upcycling waste plastics into carbon nanomaterials: A review, J Appl Polym Sci 131(4), DOI:10.1002/app.39931, 2014.

[5] Brandrup J., Bittner M., Michaeli W., Menges G., (Eds.). Recycling and recovery of plastics, New York, NY: Hanser, 1996.

[6] Ambrose C.A., Hooper R., Potter A.K., Singh M.M., Diversion from landfills: quality products from valuable plastics. Resour Conserv Recy 36(4):2002, 309-318.

[7] Dodbiba G, Takahashi K, Sadaki J, Fujita T. The recycling of plastic wastes from discarded TV sets: comparing energy recovery with mechanical recycling in the context of life cycle assessment, J Clean Prod 16(4):2008, 458-470.

[8] Cavalieri F., Padella F., Development of composite materials by mechanochemical treatment of post-consumer plastic waste, Waste Manage 22(8):2002, 913-916.

[9] Aguado J., Serrano D.P., San Miguel G., Castro M.C., Madrid S., Feedstock recycling of polyethylene in a two" step thermo"catalytic reaction system, Eselvier, J. Anal. Appl. Pyrolysis, nr.79/2007, 415-423.

[10] Părpăriță E., Teză de doctorat, Academia Română-Institutul de chimie Macromoleculară 'P. Poni" Iaşi, 2014.

[11] Achilias D.S., Roupakias C., Megalokonomos P., Lappas A.A., Antonakou E.V., Chemical recycling of plastic wastes made from polyethylene (LDPE and HDPE) and polypropylene (PP), Journal of Hazardous Materials, 149/2007, pag. 536-542.

[12] Breault R.W., Gasification Processes Old and New: A Basic Review of the Major Technologies. Energies 3:2010, 216-240.

[13] Chhiti Y., Salvador S., Commandre J.M, Broust F., Couhert C. Wood Bio-Oil Noncatalytic Gasification: Influence of Temperature, Dilution by an Alcohol and Ash Content, Energ Fuel 25:2011, 345-351.

[14] Williams E.A., Williams P.T., The pyrolysis of individual plastics and plastic mixture in a fixed bed reactor, J Chem Tech Biotechnol 70:1997, 9-20.

[15] Diaz R., Warith M., Life-cycle assessment of municipal solid wastes: Development of the WASTED model, Waste Manage 26:2006, 886-901.

[16] Magnetic Sorting and Ultrasound Sensor Technologies for Production of High Purity Secondary Polyolefins from Waste, acronym W2Plastics, project number 212782, topic: ENV-2007-3.1.3-02: New technologies for waste sorting.

[17] Baltes L., Draghici C., Manea C., Ceausescu D., Tierean M., Trends in Selective Collection of the Household Waste, Environmental Engineering and Management

Journal, July/August 2009, Vol.8, No. 4, 985-991.

[18] http://www.gdrc.org/uem/waste/waste.html

[19] Garces C., Lafuente A., Pedraja, M., Rivera P., Urban Waste Recycling Behavior, Antecedents of Participation in a Selective Collection Program, Environmental Management, 30, 2002, 378–390.

[20] Guidelines for Municipal Solid Waste Management in the Mediterranean Region, 8. Waste collection II.mixed/source separate collection.

[21] Turcitu Badalan A., A Romanian produce 5 kilos of household waste weekly, The Thought Newspaper; 2008.

[22] Ghita S., Packaging management and waste Packaging management-selective collection, Water Management and Environmental Ministry, Bucharest November; 2006.

[23] Ghita S., Packaging management and waste Packaging management in Romania, Environmental and Sustainable Development Ministry, Bucharest October 1; 2008.

[24] Al-Salem S.M., Lettieri P., Baeyens J., Recycling and recovery routes of plastic solid waste (PSW): A review, Waste Management, 29, 2009, 2625-2643.

[25] Ashori A., Nourbakhsh A., Characteristics of wood–fiber plastic composites made of recycled materials, Waste Management, 29, 2009, 1291-1295.

[26] Goodship V., Introducing to Plastics Recycling, Rapra Technology Ltd., Shawbury, United Kingdom, 2007.

[27] Hamad K., Kaseem M., Deri F., Recycling of waste from polymer materials: An overview of the recent works, Polymer Degradation and Stability, 98, 2013, 2801-2812.

[28] Vidal R., Martínez P., Garraín D. Life cycle assessment of composite materials made of recycled thermoplastics combined with rice husks and cotton linters. Int J Life Cycle Assess 14:2009, 73–82.

[29] Lagaron J.M., Ocio M.J., Lopez-Rubio A., Antimicrobial Packaging Polymers. A General Introduction, In: Antimicrobial Polymers, Lagaron J.M., Ocio M.J., Lopez-Rubio A. (Eds.), First Edition, John Wiley & Sons, Inc., New Jersey, 2012, 1-23.

[30] Patachia S., Moldovan A., Tierean M., Baltes L., Composition Determination of the Romanian Municipal Plastics Wastes, The 26th International Conference on Solid Waste Technology and Management, March 27 – 30, 2011, Philadelphia, U.S.A., Journal of Solid Waste Technology and Management, ISSN 1091-8043, 940-951.

[31] Patachia F.S.C., Catana Damian L.N., Tierean M., Baltes L., Microbial Safety of Plastic Materials Obtained from Wastes, Environmental Engineering and Management Journal, 14(2015), 6, 2015, 1303-1312.

[32] Walters R.N., Hackett S.M., Lyon R.E., Heats of combustion of high temperature polymers, http://large.stanford.edu/publications/coal/references/docs/hoc.pdf

[33] Kittle P.A., Alternate daily cover materials and subtitle D-the selection technique, Rusmar Incorporated West Chester, PA, 1993, http://www.aquafoam.com/papers/selection.pdf

[34] http://www.kedel.co.uk

[35] Crompton T.R., Polymer Reference Book, Rapra Technology Ltd., Shawbury, United Kingdom, 2006.

[36] Mohammed-Ziegler I., Oszlanczi A., Somfai B., Horvolgyi, Z., Paszli I., Holmgren A.,

Forsling W., Surface free energy of natural and surface-modified tropical and European wood species, adhesive, Journal of Adhesion Science and Technology, 18, 2004, 687-713.

[37] Owens D., Wendt R., Estimation of the Surface Free Energy of Polymers, J. Appl. Polym. Sci 13:1969, 1741-1747.

[38] Rabel W., Einige Aspekte der Benetzungstheorie und ihre Anwendung auf die Untersuchung und Veränderung der Oberflächeneigenschaften von Polymeren, Farbe und Lack 77,10:1971, 997-1005.

[39] Kaelble D.H., Dispersion-Polar Surface Tension Properties of Organic Solids, J. Adhesion 2:1970, 66-81.

[40] Castell P., Wouters M., With G., Fischer H., Huijs F., Surface modification of poly(propylene) by photoinitiators: Improvement of adhesion and wettability, Journal of Applied Polymer Science, 92, 2004, 2341-2350.

[41] Rudawska A., Zajchowski S., Surface free energy of polymer/wood composites, Polimery, 52, 2007, 453-455.

[42] Katsikogianni M., Missirlis Y.F., Concise review of mechanisms of bacterial adhesion to biomaterials and of techniques used in estimating bacteria-material interactions, European Cells and Materials, 8, 2004, 37-57.

[43] Sivakumar P.M., Iyer G., Natesan L., Doble M., 3- Hydroxy-4 methoxychalcone as a potential antibacterial coating on polymeric biomaterials, Applied Surface Science, 256, 2010, 6018–6024.

[44] Pavia D.L, Lampman G.M., Kriz G.S., Introduction to Spectroscopy. A Guide for Students of Organic Chemistry, 2nd edition, Saunders College Publishing, Philadelphia, USA, 1996.

[45] Gardette M., Perthue A., Gardette J. L., Janecska T., Földes E., Pukánszky B., Therias S., Photo- and thermal-oxidation of polyethylene: Comparison of mechanisms and influence of unsaturation content, Polymer Degradation and Stability, 98, 2013, 2383–2390.

[46] Bonilla M.A., Fernández-García M., Polymeric Materials with Antimicrobial Activity, Progress Polymer Science, 37, 2012, 281-339.

[47] Costiuc L., Popa V., Serban A., Lunguleasa A., Tierean M.H., Investigation on heat of combustion of waste materials, Proceedings of the International Conference on Urban Sustainability, Cultural Sustainability, Green Development Green Structures and Clean Cars, Malta, September 15-17, 2010, 165-168.

[48] Costiuc L., Lunguleasa A., Improving measurement accuracy of biomass heat of combustion using an oxigen bomb calorimeter, Bulletin of the Transilvania University of Brasov, vol.2(51)-2009, 467-474.

[49] European Committee for Standardization, Solid recovered fuels - Methods for the determination of calorific value, DD CEN/TS 15400:2006, 2006.

[50] Costiuc L., Patachia S., Baltes L., Tierean M., Investigation on Energy Density of Plastic Waste Materials, The 26th International Conference on Solid Waste Technology and Management, March 27 – 30, 2011, Philadelphia, U.S.A., Journal of Solid Waste Technology and Management, 930-939.

[51] Walters R.N., Hackett S.M., Lyon R.E., Heats of combustion of high temperature polymers, http://large.stanford.edu/publications/coal/references/docs/hoc.pdf

[52] Gent M.R., Menendez M., Toraño J., Isidro D., Torno S., Cylinder cyclone (LARCODEMS) density media separation of plastic wastes, Waste Management, 29, 2009, 1819–1827.

[53] Shent H., Pugh R.J., Forssberg E., A review of plastics waste recycling and the flotation of plastics, Resource Conservation Recycling, 25(2), 1999, 85–109.

[54] Bezati F., Froelich D., Massardier V., Maris E., Addition of tracers into the polypropylene in view of automatic sorting of plastic wastes using X-ray fluorescence spectrometry, Waste Management, 30, 2010, 591–596.

[55] Carvalho M.T., Ferreira C., Portela A., Santos J.T., Application of fluidization to separate packaging waste plastics, Waste Management, 29, 2009, 1138–1143.

[56] Yoshida M., Nakatsukasa S., Nanba M., Gotoh K., Zushi T., Kubo Y., Oshitani J., Decrease of Cl contents in waste plastics using a gas-solid fluidized bed separator, Advanced Powder Technologies, 21, 2010, 69–74.

[57] Bakker E.J., Rem P.C., Fraunholcz N., A novel method to separate polyolefin's from shredder residue based on inverse magnetic density separation, Proc. IdentiPlast Conference Brussels, Concert Noble, 1, 2007.

[58] Bakker E.J., Rem P.C., Hartmann D., Bakker G.J., Magnetic density separation, Environmental Science and Technology, Houston, 12, 2007.

[59] Bakker E.J., Rem P.C., Fraunholcz N., Upgrading mixed polyolefin waste with magnetic density separation, Waste Management, 29, 2009, 1712-1717.

[60] Rem P., Solaria V., Di Maio F., High-purity products from plastic waste: The W2Plastics project, Environmental Engineering and Management Journal, 8, 2009, 963-966.

[61] Di Maio F., Rem P.C., Hu B., Serranti S., Bonifazi G., The W2Plastics Project: Exploring the limits of polymer separation, Open Waste Management Journal, 3, 2010, 91-99.

[62] Rem, P., Di Maio, F., Hu, B., Houzeaux, G., Baltes, L., Tierean, M., Magnetic fluid equipment for sorting of secondary polyolefins from waste, Environmental Engineering and Management Journal, 12, 2013, 951-958.

[63] Serranti S., Bonifazi G., Post-consumer polyolefins (PP-PE) recognition by combined spectroscopic sensing techniques, Open Waste Management Journal, 3, 2010, 36-46.

[64] Vajna B., Palásti K., Bodzay B., Toldy A., Patachia S., Buican R., Croitoru C., Tierean M., Complex Analysis of Car Shredder Light Fraction, Open Waste Management Journal, 3, 2010, 46-55.

[65] Hu B., Fraunholz N., Rem P., Wetting Technologies for High-Accuracy Sink-Float Separations in Water-Based Media, Open Waste Management Journal, 3, 2010, 71-80.

[66] Hu B., van Beek K., Bosman A., Rem P.C., Bakker E.J., Di Maio F., Magnetization Control of Magnetic Liquids for Sink-Float Separations, Open Waste Management Journal, 3, 2010, 81-89.

[67] Bakker E.J., Berkhout A.J., Hartmann L., Rem P.C., Turning Magnetic Density Separation into Green Business Using the Cyclic Innovation Model, Open Waste Management Journal, 3, 2010, 99-116.

[68] Di Maio F., Rem P.C., Hu B., Fraunholcz N., Serranti S., Bonifazi G., The W2Plastics Project halfway achievements, 26th Int. Conf. on Solid Waste Technology and Management, Philadelphia, PA, U.S.A., March 27 – 30, 2011, 915-929.

[69] Bakker M.C.M., Sanaee S.A., Capabilities of Ultrasound for Monitoring and Quantitative Analysis of Polyolefin Waste Particles in Magnetic Density Separation (MDS), Open Waste Management Journal, 3, 2010, 117-126.

[70] Bonifazi G., Serranti S., New quality control and sorting strategies for polyolefins (PP-PE) recycling, 24th Int. Conf. on Solid Waste Technology and Management, Philadelphia, PA, USA, March 15-18, 2009, 606.

[71] Bonifazi G., Serranti S., Solid Waste Stream On-line Quality Control: New HyperSpectral Imaging Based Devices and Detection Logic Implementation for an Efficient Products Certification, 25th Int. Conf. on Solid Waste Technology and Management, Philadelphia, PA, USA, March 14-17, 2010, 198.

[72] Bonifazi G., Serranti S., Design of an hyperspectral imaging based platform for quality control in the MDS-based recycling process of polyolefins, 26th Int. Conf. on Solid Waste Technology and Management, Philadelphia, PA, U.S.A., March 27 – 30, 2011, 936.

[73] Serranti S., Gargiulo A., Bonifazi G., Characterization of post-consumer polyolefin wastes by hyperspectral imaging for quality control in recycling processes, Waste Management, 31, 2011, 2217-2227.

[74] Serranti S., Gargiulo A., Bonifazi G., The use of hyperspectral imaging for quality control in the MDS-based recycling process of polyolefins, 26th Int. Conf. on Solid Waste Technology and Management, Philadelphia, PA, U.S.A., March 27 – 30, 2011, 952.

[75] Rem P.C., Berkhout S., Peter M., Method and apparatus for separating solid particles based on difference in density, Japanese Patent, No. 167850, 2007.

[76] Houzeaux G., Samaniego C., Calmet H., Aubry R., Vázquez M., Rem P., Simulation of Magnetic Fluid Applied to Plastic Sorting, Open Waste Management Journal, 3, 2010, 127-138.

[77] Tierean, M.H., Baltes, L.S., Rem, P.C, Foris, T. Feasibility study of the production of secondary polyolefins from the plastic wastes using magnetic density separation, Metalurgia International, Special issue vol. XVIII no. 5 (2013), 149-152.

[78] Behrens W., Hawranek P.M., Manual for the Preparation of Industrial Feasibility Studies, UNIDO Publication, ISBN 92-1-106269-1, Vienna, 1991.

[79] Overton R., Feasibility Studies Made Simple, Martin Books Pty Ltd, Boat Harbour, 2007.

[80] Rodney Turner J., Gower Handbook of Project Management, Gower Publishing Limited, R T Pringle and Dr M B Barker, Hampshire, 2007.

[81] Arkansas Small Business Development Center, Business Blueprints: Is Your Business Idea Feasible? University of Arkansas at Little Rock, 2002.

[82] http://www.energy.eu

[83] http://www.plasticsnews.com/resin-pricing/recycled-plastics.html

[84] http://www.recycledplastic.com/plastic-prices/oct-2011-scrap-prices

[85] Ursutiu D., Samoila C., Baltes L.S., Tierean M.H., Vekas L., Jinga V., Labview in ultrasound plastic materials measurement, Journal of Optoelectronics and Advanced Materials, Vol. 15, No. 7- 8, July – August 2013, 750 – 754.

[86] National Instrumensts web page: http://www.ni.com/labview

[87] Bica D., Vékás L., Rasa M., J. Magn. Magn. Mater. 252, 10, 2002.

[88] Bica D., Vékás L., Avdeev M.V., Marinica O., Balasoiu M., Garamus V.M., J. Magn. Magn. Mater. 311, 17, 2007.

[89] Bica D., Vékás L., Avdeev M.V., Balasoiu M., Marinica O., Stoian F.D., Susan-Resiga D., Török G., Rosta L., Prog. Colloid Polym. Sci. 125, 1, 2004.

[90] Mažeika L., Šliteris R., Vladišauskas A., Ultragarsas (Ultrasound), 65(4), 2010.

[91] Jakevièius L., Butkus J., Vladišauskas A., Ultragarsas, Nr.1(58), 2006.

[92] Scalarone D., Lazzari M., Chiantore O., Acrylic protective coatings modified with titanium dioxide nanoparticles: Comparative study of stability under irradiation, Polym Degrad Stabil, 97, 2012, 2136-2142.

[93] Harizi W., Chaki S., Bourse G., Ourak M., Mechanical damage characterization of glass fiber-reinforced polymer laminates by ultrasonic maps, Compos Part B-Eng, 70, 2015, 131-137.

[94] Cecen V., Seki Y., Sarikanat M., Tavman I.H., FTIR and SEM analysis of polyester- and epoxy-based composites manufactured by VARTM process, J Appl Polym Sci, 108, 2008, 2163-2170.

[95] Ferreira J.M., Errajhi O.A.Z., Richardson M.O.W., Thermogravimetric analysis of aluminised E-glass fibre reinforced unsaturated polyester composites, Polym Test, 25, 2006, 1091-109.

[96] Özen I., Şimşek S., Vital importance of moisture level in all stages of processing from calcium carbonate coating through polyethylene/calcium carbonate compounding to film generation, Powder Technology, Vol 270 (5), 2015, 320-328.

[97] Pradittham A., Charitngam N., Puttajan S., Atong D., Pechyen C., Surface modified $CaCO_3$ by palmitic acid as nucleating agents for polypropylene film: mechanical, thermal and physical properties, Energy Procedia Vol 56, 2014, 264 – 273.

[98] Rungruang P., Grady B.P., Supaphol P., Surface-modified calcium carbonate particles by admicellar polymerization to be used as filler for isotactic polypropylene, Colloids and Surfaces A: Physicochem. Eng. Aspects Vol. 275, 2006, 114–125.

[99] Tang Z., Cheng G., Cheng Y., Yu X., Wang H., Characteristics evaluation of calcium carbonate particles modified by surface functionalization, Advanced Powder Technology Vol 25, 2014, 1618–1623.

[100] Baltes L.S., Tierean M.H., Patachia S., Investigation on the friction coefficient of the composite materials obtained from plastics wastes and cellulosic fibres, Journal of Optoelectronics and Advanced Materials, Vol. 15, No. 7- 8, July – August 2013, 785 – 790.

[101] Rymuza Z., Tribology of Anti-Friction Polymers, WNT, Warszawa, 1986.

[102] Yamaguchi Y., Tribology of Plastic Materials, Tribology Series, Vol. 16, Elsevier, New York, 1990.

[103] Uetz H., Wiedemeyer J., Tribologie der Polymere, Carl Hanser Verlag, München-Vienna, 1985.

[104] Rymuza Z., Tribology of Polymers, Archives of Civil and Mechanical Engineering, Elsevier, Vll(4), 177, 2007.

[105] Georgescu C., Studies and research on developments of superficial layer parameters in friction and wear processes of composite materials with polybutylene terephthalate

matrix, PhD thesis, Dunarea de Jos University, Galati, Romania, 2012.

[106] Evans D.C., Lancaster J.K., The Wear of Polymers, Treatise on Materials Science and Technology, Vol. 13, Wear, Academic Press inc., New York, 1979.

[107] Tomescu L., Tarău I., Georgescu C., Research on composites surfaces with PTFE and glass fiber matrix, after sliding in water using Taguchi method, Intern. Conf., Moderns technologies, quality and restructuring, Chişinău, Moldavia, Vol. II, 2001, 468.

[108] Dasari A., Yu Z.Z., Mai Y.W., Fundamental aspects and recent progress on wear/scratch damage in polymer nanocomposites, Materials Science and Engineering, Vol. 63, 31, 2009.

[109] Rîpă M., Deleanu L., Damage in tribosystems, Zigotto Press, Galaţi, 2008.

[110] Myshkin N.K., Kovalev A.V., Adhesion and Friction of Polymers, Polymer Tribology, Imperial College Press, London, 3, 2009.

[111] Pouzada A.S., Ferreira E.C., Pontes A.J., Friction properties of moulding thermoplastics, Polymer Testing, Science Direct 25, 1017, 2006.

[112] Quaglini V., Dubini P., Friction of Polymers Sliding on Smooth Surfaces, Advances in Tribology, Article ID 178943, 1, 2011.

[113] Bahadur S., The development of transfer layers and their role in polymer tribology, Wear, vol. 245, no. 1-2, 92, 2000.

[114] Quaglini V., Dubini P., Ferroni D., Poggi C., Influence of counterface roughness on friction properties of engineering plastics for bearing applications, Materials and Design, vol. 30, no. 5, 1650, 2009.

[115] Jiang H., Browning R., Fincher J., Gasbarro A., Jones S., Sue H.J., Influence of surface roughness and contact load on friction coefficient and scratch behaviour of thermoplastic olefins, Applied Surface Science 254, 4494, 2008.

[116] Moldovan A., Composites materials based on polyolefins and cellulose fibres from secondary raw materials, PhD thesis, Transilvania University of Brasov, Romania, 2012.

[117] Pothan L.A., Luyt A.S., Thomas S., Polyolefin/natural fiber composites in polyolefin composites, John Wiley & Sons Inc., 2008.

[118] Rowell R.M., Challenges in Biomass–Thermoplastic Composites, Journal of Polymers and the Environment, Vol.15, 229–235, 2007.

[119] Bobancu S., Cozma R., Instrument for measuring friction characteristics in a plane coupling, Ninth World Congress on the Theory of Machines and Mechanisms, vol. 4, Milano, Italy, 1995, 2935.

[120] Udroiu R., Mihail L.A., Experimental determination of surface roughness of parts obtained by rapid prototyping, Recent Advances in Circuits, Systems, Electronics, Control and Signal processing, Proc. 8-th WSEAS International Conference on Circuits, systems, electronics, control & signal processing, 2009, 283.

[121] Moldovan A., Patachia S., Vasile C., Darie R., Manaila E., Tierean M., Natural Fibres/Polyolefins Composites (I) UV and Electron Beam Irradiation, J. Biobased Mater. Bioenergy 7, 58, 2013.

[122] Patachia S., Croitoru C., Friedrich C., Effect of UV exposure on the surface chemistry of wood veneers treated with ionic liquids, Appl. Surf. Sci. 258, 2012, 6723–6729.

[123] Croitoru C., Patachia S., Doroftei F., Parparita E., Vasile C., Ionic liquids influence on the surface properties of electron beam irradiated wood, Appl. Surf. Sci. 314, 2014, 956–966.

[124] Dobritoiu R., Patachia S., A study of dyes sorption on biobased cryogels, Appl.Surf. Sci. 285, 2013, 56–64.

[125] Papancea A., Patachia S., Characterization of dyes loaded PVA based hydrogels through CIELAB method, Environ. Eng. Manage. J. 14 (2), 2015, 361–371.

[126] Correia J.R., Cabral-Fonseca S., Branco F.A., Ferreira J.G., Eusébio M.I., Rodrigues M.P., Durability of pultred glass-fiber-reinforced polyester profiles forstructural applications, Mech. Compos. Mater. 42/4, 2006, 325–338.

[127] Chirkst D.E., Krasotkin I.S., Cheremisina O.V., Streletskaya M.I., Ivanov M.V., Determination of the surface area of minerals by sorption of methylene blueand thermal desorption of argon, Russ. J. Appl. Chem. 76, 2003, 663–665.

[128] Nunes C.A., Guerreiro M.C., Estimation of surface area and pore volume of acti-vated carbons by methylene blue and iodine numbers, Quim Nova 34, 2011, 472-476.

[129] Painting K., Kirsop B., A quick method for estimating the percentage of viablecells in a yeast population, using methylene-blue staining, World J. Microbiol.Biotechnol. 6, 1990, 346–347.

[130] Harari A., Sippel R.S., Goldstein R., Aziz S., Shen W., Gosnell J., Duh Q.Y., Clark O.H., Successful localization of recurrent thyroid cancer in reoperative necksurgery using ultrasound-guided methylene blue dye injection, J. Am. Coll. Surg. 215, 2012, 555–561.

[131] Moulzakis D.E., Zoga H., Galiotis C., Accelerated environmental ageing study of polyester/glass fiber reinforced composites (GFRPCs), Compos. Part B – Eng. 39, 2008, 467–475.

[132] Gu H., Degradation of glass fibre/polyester composites after ultraviolet radiation, Mater. Design 29, 2008, 1476–1479.

[133] Errajhi O.A.Z., Osborne J.R.F., Richardson M.O.W., Dhakal H.N., Water absorption characteristics of aluminised E-glass fibre reinforced unsaturated polyester composites, Compos. Struct. 71, 2005, 333–336.

[134] Panek M., Reinprecht L., Colour stability and surface defects of naturally aged wood treated with transparent paints for exterior constructions, Wood Res. –Slovakia 59, 2014, 421–429.

[135] Sirocic A.P., Hrnjak-Murgic Z., Jelencic J., The surface energy as an indicator of miscibility of SAN/EDPM polymer blends, J. Adhes. Sci. Technol. 27, 2013, 2615–2628.

[136] Miyazaki H., Teranishi Y., Ota T., Fabrication of UV-opaque and visible-transparent composite film, Sol. Energ. Mater. Sol. C. 90/16, 2006, 2640–2646.

[137] Kang D.J., Han D.H., Kang D.P., Fabrication and characterization of photocurable inorganic–organic hybrid materials using organically modified colloidal-silica nanoparticles and acryl resin, J. Non-Cryst. Solids 355, 2009, 397–402.

[138] Simionescu C.I., Popa A.A., Comanita E., Ionescu L., Poly(methyl metacrylate) macroazoinitiator – synthesis, characterization and its behavior in blockcopolymerization, Rev. Roum. Chim. 38, 1993,1027–1030.

[139] Rot K., Huskic M., Makarovic M., Mlakar T.L., Zigon M., Interfacial effects in glass fibre composites as a function of unsaturated polyester resin composition, Compos. Part A –

Appl. Sci. 32, 2001, 511–516.

[140] Varga C., Miskolczi N., Bartha L., Lipoczi G., Improving the mechanical properties of glass fibre reinforced polyester composites by modification of fibre surface, Mater. Design 31, 2010, 185–193.

[141] Isa M.T., Ahmed A.S., Aderemi B.O., Taib R.M., Mohammed-Dabo I.A., Effect of fiber type and combinations on the mechanical, physical and thermal stability properties of polyester hybrid composites, Compos. Part B – Eng. 52, 2013, 217–223.

[142] Moulzakis D.E., Zoga H., Galiotis C., Accelerated environmental ageing study of polyester/glass fiber reinforced composites (GFRPCs), Compos. Part B – Eng. 39, 2008, 467–475.

[143] Alyamac K.E., Ince R., A preliminary concrete mix design for SCC with marble powders, Construction and Building Materials Vol 23, 2009, 1201–1210.

[144] Leong Y.W., Abu Bakar M.B., Ishak Z.A.M., Ariffin A., Pukanszky B., Comparison of the mechanical properties and interfacial interactions between talc, kaolin, and calcium carbonate filled polypropylene composites, Journal of Applied Polymer Science Vol 91 (5), 2004), 3315-3326.

[145] Gahleitner M., Grein C., Bernreitner K., Synergistic mechanical effects of calcite micro- and nanoparticles and β-nucleation in polypropylene copolymers, European Polymer Journal (2012) Vol 48 (1) 2012, 49-59.

[146] Tanniru M., Misra R.D.K., Reduced susceptibility to stress whitening during tensile deformation of calcium carbonate-reinforced high density polyethylene composites, Materials Science and Engineering A, Vol 424, 2006, 53–70.

[147] Baoqing S., Jipeng L., Zhixu W., Effect of Oleic Acid-modified Nano-$CaCO_3$ on the Crystallization Behavior and Mechanical Properties of Polypropylene, Chinese J. Chem. Eng. Vol 14(6), 2006, 814-818.

[148] Bellayer S., Tavard E., Duquesne S., Piechaczyk A., Bourbigot S., Mechanism of intumescence of a polyethylene/calcium carbonate/stearic acid system, Polymer Degradation and Stability Vol 94, 2009, 797–803.

[149] Vasile C., Boborodea C., Sabliovschi M., Moroi G., Caraculacu A., The Copolymerization of the Pyrolysis Products of Polyethylene with Styrene, Acta Polym Vol 37(7), 1986, 419-422.

[150] Balteş L.S., Study concerning part and injection molding die design, Metalurgia International, vol. 16/5, 2011,166-170.

[151] Baltes L., Ţierean M., Influence of the part shape on the polymer flow inside mold an overall strength, Annals of DAAAM for 2009 & Proceedings of the 20th International DAAAM Symposium, ISBN 978-3-901509-70-4, ISSN 1726-9679, pp 553, Editor B. Katalinic, Published by DAAAM International, Vienna, Austria 2009, 1107-1108.

[152] Bar-Meir G., Fundamentals of Die Casting Design, http://artikel software.com/file/dieCasting.pdf, 2000, Accesed on: 2009-06-27.

[153] Tres P.A., Designing Plastic Parts for Assembly, ISBN 1-56990-350-6, Carl Hanser Verlag Munich, Germany, 2006.

[154] Croitoru C., Patachia S., Papancea A., Baltes L., Tierean M., Glass fibres reinforced polyester composites degradation monitoring by surface analysis, Applied Surface

Science, 358, 2015, 518-524.

[155] Croitoru C., Giubega A., Patachia S., Baltes L., Pascu A., Roata I., Tierean M., State of the Art in Calcite and Polyolefins Recycling, Bulletin of the Transilvania University of Braşov, Series I, Vol. 9 (58) No. 1 - 2016, 35-40.

[156] https://ec.europa.eu/programmes/horizon2020/en/h2020-section/waste

[157] ttp://s3platform.jrc.ec.europa.eu/documents/20182/89682/ Proposals_for_Smart_specialization_Lithuania.pdf/62c77005-c818-47bd-afba-6add66413a80

[158] Fujishima A., Zhang X., Tryk D.A., TiO_2 photocatalysis and related surface phenomena, Surf Sci Rep 63, 2008, 515-582.

[159] Chen J., Poon C., Photocatalytic construction and building materials: From fundamentals to applications, Build Environ 44, 2009, 1899–1906.

[160] Vučetić S.B., Rudić O.L., Markov S.L., Bera O.J., Vidaković A.M., Sever Skapin A.S., Ranogajec J.G., Antifungal efficiency assessment of the TiO_2 coating on façade paints, Environ Sci Pollut Res 21, 2014, 11228–11237.

[161] Canesi L., Ciacci C., Balbi T., Interactive effects of nanoparticles with other contaminants in aquatic organisms: Friend or foe? Mar Environ Res 111, 2015, 128-134.

[162] Xia B., Zhu L., Han Q., Sun X., Chen B., Qu K., Effects of TiO_2 nanoparticles at predicted environmental relevant concentration on the marine scallop Chlamys farreri: An integrated biomarker approach, Environ Toxicol Phar 50, 2017, 128–135.

[163] Jimeno-Romero A., Oron M., Cajaraville M. P., Soto M., Marigómez I., Nanoparticle size and combined toxicity of TiO_2 and DSLS (surfactant) contribute to lysosomal responses in digestive cells of mussels exposed to TiO_2 nanoparticles, Nanotoxicology 10(8), 2016, 1168-1176.

[164] Ba-Abbad M.M., Kadhum H.A.A., Mohamad A.B., Takriff M.S., Sopian K., Synthesis and Catalytic Activity of TiO_2 Nanoparticles for Photochemical Oxidation of Concentrated Chlorophenols under Direct Solar Radiation, International Journal of Electrochemical Science, 7(6), 2012, 4871-4888.

[165] Sopyan I., Hafizah N., Jamal P., Immobilization of TiO_2 with cement: Photocatalyic degradation of phenol and its kinetic study, Indian Journal of Chemical Technology, Vol. 18, July 2011, 263-270.